

ACTA GEO TECHNICA SLOVENICA

2011/1

D. peila et al.

THE BEHAVIOUR OF A TWO-COMPONENT BACK-FILLING GROUT USED IN A TUNNEL-BORING MACHINE

M. U. pavlič & B. praznik

DETECTING KARSTIC ZONES DURING HIGHWAY CONSTRUCTION USING GROUND-PENETRATING RADAR

N. Laredj et al.

A COUPLED THERMO-HYDRO-MECHANICAL MODEL OF EXPANSIVE CLAYS SUBJECTED TO HEATING AND HYDRATATION

M. kamalzare & R. ziaie-moayed

INFLUENCE OF GEOSYNTHETIC REINFORCEMENT ON THE SHEAR STRENGTH CHARACTERISTICS OF TWO-LAYER SUB-GRADE

D. boumezerane et al.

FUZZY-SETS DECISION-SUPPORT SYSTEM FOR GEOTECHNICAL SITE SOUNDINGS

B. ćosić et al.

GEO-INFORMATION TECHNOLOGY FOR DISASTER RISK ASSESSMENT



ustanovitelji **founders**

Univerza v Mariboru, Fakulteta za gradbeništvo
University of Maribor, Faculty of Civil Engineering

Univerza v Ljubljani, Fakulteta za gradbeništvo in geodezijo
University of Ljubljana, Faculty of Civil and Geodetic Engineering

Univerza v Ljubljani, Naravoslovnotehniška fakulteta
University of Ljubljana, Faculty of Natural Sciences and Engineering

Slovensko geotehniško društvo
Slovenian Geotechnical Society

Društvo za podzemne in geotehniške konstrukcije
Society for Underground and Geotechnical Constructions

izdajatelj **publisher**

Univerza v Mariboru, Fakulteta za gradbeništvo
University of Maribor, Faculty of Civil Engineering

odgovorni urednik **editor-in-chief**

Ludvik Trauner
University of Maribor

uredniki **co-editors**

Bojana Dolinar
University of Maribor

Borut Macuh
University of Maribor

Stanislav Škrabl
University of Maribor

Helena Vrecl Kojc
University of Maribor

Bojan Žlender
University of Maribor

posvetovalni uredniki **advisory editors**

Darinka Battelino
University of Trieste

Heinz Brandl
Vienna University of Technology

Chandrakant. S. Desai
University of Arizona

Pedro Seco e Pinto
National Laboratory of Civil Engineering

lektor **proof-reader**

Paul McGuiness

naklada **circulation**

500 izvodov - issues

tisk **print**

Tercia tisk d.o.o. Ptuj

Revija redno izhaja dvakrat letno. Članki v reviji so recenzirani s strani priznanih mednarodnih strokovnjakov. Baze podatkov v katerih je revija indeksirana: SCIE - Science Citation Index Expanded, JCR - Journal Citation Reports / Science Edition, ICONDA - The international Construction database, GeoRef. Pri financiranju revije sodeluje Javna agencija za knjigo Republike Slovenije.

uredniški odbor **editorial board**

József Farkas
Budapest University of Technology and Economics

Theodoros Hatzigogos
Aristotle University of Thessaloniki

Rolf Katzenbach
Technical University Darmstadt

Nasser Khalili
The University of New South Wales, Sydney

Zlatko Langof
University of Sarajevo

Jakob Likar
University of Ljubljana

Janko Logar
University of Ljubljana

Bojan Majes
University of Ljubljana

Milan Maksimović
University of Belgrade

Borut Petkovšek
Slovenian National Building and Civil Engineering Institute

Mihael Ribičič
University of Ljubljana

César Sagasetta
University of Cantabria

Patrick Selvadurai
McGill University

Stephan Semprich
University of Technology Graz

Devendra Narain Singh
Indian Institute of Technology, Bombay

Abdul-Hamid Soubra
University of Nantes

Küchi Suzuki
Saitama University

Antun Szavits-Nossan
University of Zagreb

Ivan Vaniček
Czech Technical University in Prague

Jianhua Yin
The Hong Kong Polytechnic University

naslov uredništva **address**

ACTA GEOTECHNICA SLOVENICA
Univerza v Mariboru, Fakulteta za gradbeništvo
Smetanova ulica 17, 2000 Maribor, Slovenija
Telefon / Telephone: +386 (0)2 22 94 300
Faks / Fax: +386 (0)2 25 24 179
E-pošta / E-mail: ags@uni-mb.si

spletni naslov **web address**

<http://www.fg.uni-mb.si/journal-ags/>

The journal is published twice a year. Papers are peer reviewed by renowned international experts. Indexation data bases of the journal: SCIE - Science Citation Index Expanded, JCR - Journal Citation Reports / Science Edition, ICONDA - The international Construction database, GeoRef. Financially supported also by Slovenian Book Agency.

VSEBINA

2	Ludvik Trauner UVODNIK
4	daniele peila in drugi LASTNOSTI DVOKOMPONENTNEGA UTRAJEVALNEGA MATERIALA PRI VATANJU PREDORA S TBM
15	matevž u. pavlič in uroš praznik DEFINIRANJE KRAŠKIH CON PRI GRADNJI AVTOCESTE Z UPORABO GEORADARJA
28	nadia laredj in drugi ZDRUŽEN TERMO-HIDRO-MEHANIČNI MODEL NABREKLJIVIH GLIN, PODVRAŽENIH SEGREVANJU IN HIDRACIJI
38	mehrad kamalzare in reza ziaie-moayed VPLIV GEOSINTETIČNEGA ARMIRANJA NA STRIŽNO TRDNOST DVOSLOJNIH TAL
50	djamladdine bouzemerane in drugi SISTEM MEHKE MNOŽICE ZA ODLOČANJE PRI GEOTEHNIČNEM NAČRTOVANJU
64	borđe cosić in drugi GEO-INFORMACIJSKA TEHNOLOGIJA ZA OCENO TVEGANOSTI NESREČ
76	NAVODILA AVTORJEM

CONTENTS

Ludvik Trauner EDITORIAL	3
daniele peila et al. THE BEHAVIOUR OF A TWO-COMPONENT BACK- FILLING GROUT USED IN A TUNNEL-BORING MACHINE	5
matevž u. pavlič and uroš praznik DETECTING KARSTIC ZONES DURING HIGHWAY CONSTRUCTION USING GROUND-PENETRATING RADAR	16
nadia laredj et al. A COUPLED THERMO-HYDRO-MECHANICAL MODEL OF EXPANSIVE CLAYS SUBJECTED TO HEATING AND HYDRATATION	29
mehrad kamalzare and reza ziaie-moayed INFLUENCE OF GEOSYNTHETIC REINFORCEMENT ON THE SHEAR STRENGTH CHARACTERISTICS OF TWO-LAYER SUB-GRADE	39
djamladdine bouzemerane et al. FUZZY-SETS DECISION-SUPPORT SYSTEM FOR GEOTECHNICAL SITE SOUNDINGS	51
borđe cosić et al. GEO-INFORMATION TECHNOLOGY FOR DISASTER RISK ASSESSMENT	65
INSTRUCTIONS FOR AUTHORS	77

UVODNIK

Z veseljem sporočamo, da so se uredniškemu odboru mednarodne znanstvene revije Acta Geotechnica Slovenica (AGS) pridružili novi trije člani in sicer prof. dr. Devendra Narain Singh (Indian Institute of Technology, Bombay), prof. dr. Jianhua Yin (The Hong Kong Polytechnic University) in prof. dr. Nasser Khalili (The University of New South Wales, Sydney). Z njihovo pomočjo bo AGS postala še bolj prepoznavna in uporabna revija v široki geotehnični stroki. Za njihovo aktivno sodelovanje pri objavljanju visoko kvalitetnih člankov se jim zahvaljujemo.

Pričujoča številka AGS prinaša šest zanimivih člankov.

Avtorji prvega prispevka Luca Borio, Daniele Peila in Sebastiano Pelizza obravnavajo enega od najpomembnejših postopkov pri uporabi mehanizirane metode izkopa predora, to je takojšnje polnjenje praznega prostora, ki se ustvari za segmentno oblogo na koncu stroja za vrtnanje polnega profila (TBM). V pričujočem prispevku so analizirani različni sistemi takšnega načina vtiskanja malte, še posebej pa je predstavljen dvokomponentni sistem skupaj z rezultati in analizi laboratorijskih preizkusov.

Matevž U. Pavlič in Blaž Praznik opisujeta georadarske meritve, ki so se izvajale za detekcijo podpovršinskih kraških pojavov ob izgradnji nacionalne avtoceste v jugo-vzhodnem delu Slovenije. Predvidena trasa avtoceste je locirana večinoma v dinarskem krasu z veliko gostoto kraških pojavov, ki so vidni že na površju. Preiskave z georadarjem so bile izbrane zaradi ekstremno heterogene narave kraškega terena, kjer konvencionalne metode preiskovanja ne pridejo v poštev.

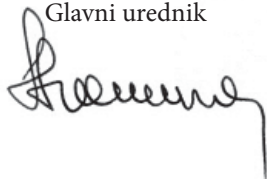
Tretji članek avtorjev Laredj Nadia, Missoum Hanifi, Bendani Karim in Maliki Mustapha prikazuje numerično formulacijo združenega termo-hidro-mehanskega procesa v nenasičeni nabrekli glini, posebej v kompaktnem bentonitu z dodajanjem tekočine v več fazah. Predstavljen model se lahko uporabi pri dvodimenzionalnih problemih z različnimi začetnimi in robnimi pogoji.

Mehrad Kamalzare in Reza Ziaie-Moayed prikazujeta rezultate testov strižne trdnosti, izvedenih na nearmiranih in armiranih vzorcih zemljin z različnimi geosintetikami. Rezultati so pokazali, da lahko vključevanje teh materialov poveča ali zmanjša parametre strižne trdnosti vmesne ploskve med dvema plastema tal v odvisnosti od značilnosti geosintetike.

Djamalddine Boumezerane, Smaïn Belkacemi in Bojan Žlender so v prispevku predstavili sistem mehkega sklepanja (Fuzzy Inference System), ki omogoča, da se na podlagi razpoložljivih kvalitativnih in kvantitativnih informacij oceni število raziskovalnih točk, potrebnih za ustrezen opis terena. Iz predstavljenih primerov je razvidno, da se lahko sistem mehkega sklepanja uporablja kot sistematično orodje za pomoč pri odločanju za inženirje, ki se ukvarjajo s terenskimi raziskavami.

Šesti članek, ki so ga prispevali Đorđe Ćosić, Srđan Popov, Dušan Sakulski in Ana Pavlović prikazuje metodo ocenjevanja tveganja, ki vsebuje poleg tveganj tudi parametre kot so ranljivost, izpostavljenost in varnost. Vsebuje tudi okoljske in družbene komponente nevarnosti.

Ludvik Trauner
Glavni urednik



EDITORIAL

We would like to announce that the Editorial Board of the scientific journal Acta Geotechnica Slovenica (AGS) has three new members: Prof. Dr. Devendra Narain Singh (Indian Institute of Technology, Bombay), Prof. Dr. Jianhua Yin (The Hong Kong Polytechnic University) and Prof. Dr. Nasser Khalili (The University of New South Wales, Sydney). With their help, AGS will become an even more recognized and useful journal in the broad geotechnical field. We would like to express our thanks for their active cooperation in publishing high-quality articles.

This issue of AGS brings together six interesting articles.

The authors of the first contribution, Luca Borio, Daniele Peila and Sebastiano Pelizza, deal with one of the most important procedures during the mechanized method of tunnel excavation, i.e., the instantaneous filling of the annulus that is created behind the segment lining at the end of the tail during the TBM advance. In their article, different systems of such grout back-filling are analyzed. In particular, a two-component system injection is presented together with the results and analyses of laboratory tests.

Matevž U. Pavlič and Blaž Praznik describe ground-penetrating radar measurements that were carried out for the purpose of detecting subsurface karstic features during the construction of the national highway in the south-eastern part of Slovenia. The expected highway route is located mostly in the dinaric karstic region with a high density of karstic features visible on the surface. The ground-penetrating radar method was chosen because of the heterogeneous nature of the karst, where conventional research methods are not suitable.

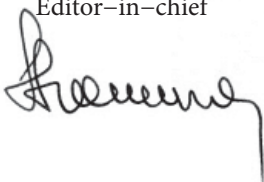
The third article, by Laredj Nadia, Missoum Hanifi, Bendani Karim and Maliki Mustapha, presents a numerical formulation for coupled thermo-hydro-mechanical processes in unsaturated expansive clays, especially in compacted bentonite, with a multiphase fluid flow. The implied model is applicable to two-dimensional problems with various initial and boundary conditions.

Mehrad Kamalzare and Reza Ziaie-Moayed present their test results of shear strength, performed on unreinforced and reinforced samples with different geosynthetics. The results show that the inclusion of these materials can increase or decrease the shear-strength parameters of the interface of two-layered soils.

In their paper, Djamalddine Boumezerane, Smaïn Belkacemi and Bojan Žlender introduce a fuzzy-sets decision-support system that allows an estimation of the research points needed for the necessary characterization of a site, based on qualitative and quantitative information. The cases presented show that a Fuzzy Inference System can be used as a systematic decision-support tool for engineers dealing with site characterizations.

The sixth article by Đorđe Ćosić, Srđan Popov, Dušan Sakulski and Ana Pavlović shows a risk-assessment method that includes, apart from hazards, parameters such as vulnerability, exposure and safety. It also involves the environmental and social components of risk management.

Ludvik Trauner
Editor-in-chief



LASTNOSTI DVOKOMPONENTNEGA UTRJEVALNEGA MATERIALA PRI VRTANJU PREDORA S TBM

DANIELE PEILA, LUCA BORIO IN SEBASTIANO PELIZZA

o avtorjih

Daniele Peila
Politecnico di Torino,
Department of Environment, Land and Geo-engineering
Corso Duca degli Abruzzi 24, 10129 Torino, Italija
E-pošta: daniele.peila@polito.it

vodilni avtor

Luca Borio
Politecnico di Torino,
Department of Environment, Land and Geo-engineering
Corso Duca degli Abruzzi 24, 10129 Torino, Italija
E-pošta: luca.borio@polito.it

Sebastiano Pelizza
Politecnico di Torino,
Department of Environment, Land and Geo-engineering
Corso Duca degli Abruzzi 24, 10129 Torino, Italija
E-pošta: sebastiano.pelizza@polito.it

izvleček

Eden od najpomembnejših postopkov pri uporabi mehanizirane metode izkopa predora je takojšnje polnjenje praznega prostora, ki se ustvari za segmentno oblogo na koncu stroja za vrtanje polnega profila (TBM). Njegov glavni cilj je zmanjšati usedanje površine nad predorom, ki ga povzroča rezanje hribine s TBM. Da bi natančno dosegli cilje, morata simultani sistem polnjenja z zadnje strani z vtiskanjem utrjevalnega materiala zadovoljiti tehnične, operacijske in izvedbene zahteve. Predstavljen dvokomponentni sistem vtiskanja utrjevalnega materiala v pšraksi postopoma zamenjuje uporabo tradicionalne malte. V pričujočem prispevku so analizirani različni sistemi takšnega načina vtiskanja malte, še posebej pa je predstavljen dvokomponentni sistem skupaj z rezultati in analizami laboratorijskih preizkusov.

ključne besede

vrtanje, mehanizirano vrtanje, polnjenje segmentov, usedanje, polnjenje malte z zadnje strani

THE BEHAVIOUR OF A TWO-COMPONENT BACK-FILLING GROUT USED IN A TUNNEL-BORING MACHINE

DANIELE PEILA, LUCA BORIO and SEBASTIANO PELIZZA

about the authors

Daniele Peila
Politecnico di Torino,
Department of Environment, Land and Geo-engineering
Corso Duca degli Abruzzi 24, 10129 Torino, Italy
E-mail: daniele.peila@polito.it

corresponding author

Luca Borio
Politecnico di Torino,
Department of Environment, Land and Geo-engineering
Corso Duca degli Abruzzi 24, 10129 Torino, Italy
E-mail: luca.borio@polito.it

Sebastiano Pelizza
Politecnico di Torino,
Department of Environment, Land and Geo-engineering
Corso Duca degli Abruzzi 24, 10129 Torino, Italy
E-mail: sebastiano.pelizza@polito.it

abstract

The instantaneous filling of the annulus that is created behind the segment lining at the end of the tail during the TBM advance is an operation of paramount importance. Its main goal is to minimize the surface settlements due to any over-excavation generated by the passage of the TBM. To correctly achieve the goals, a simultaneous back-filling system and the injected material should satisfy the technical, operational and performance characteristics. A two-component system injection for the back-filling is progressively substituting the use of traditional mortars. In this paper different systems of back-filling grout and in particular the two-component system are analyzed and the results of laboratory tests are presented and discussed.

keywords

tunneling, mechanized tunneling, segment lining, settlements, back-fill grouting

1 INTRODUCTION

Full-face shield machines have shown an ever increasing number of applications thanks to their ability to

minimize and control surface subsidence when a tunnel is excavated with a low overburden. The excavation using these machines is made by a rotating cutter-head fitted with pick or disk cutters or a combination of both, while the face stability is guaranteed by the pressure in the bulk chamber, behind the cutter head, obtained or with a bentonite slurry (Slurry Shield and Hydroshield) or with conditioned soil [10 and 11] (Earth Pressure Balance Shields). The tunnel is then supported by a segmental lining that is installed continuously during the advance of the machine and this works as the final lining too. To permit the advance of the machine and of the shield, and for technological reasons, the excavation diameter is usually bigger than the external diameter of the final lining due to the overcutting necessary to permit the advancing of the shield, to the conicity of the shield itself and to the thickness of the shield (Fig. 1). For these reasons, around the lining there is an open space that must be continuously filled during the machine's advance.

The instantaneous filling of this "annulus", which is created behind the segment lining at the end of the shield tail, is an operation of paramount importance for the correct mechanized tunnelling procedure, particularly in an urban area. Its main goal is to minimize surface settlements due to any over-excavation generated by the passage of the TBM [4, 6, 7, 10]. Furthermore, the back-filling operation has to [2, 3, 4, 5, 8, 11, 12]:

- lock the segmental lining into position, avoiding movement owing to both segmental self-weight and the thrust forces, hoop stresses, generated by the TBM;
- bear the loads transmitted by the TBM back-up weight;
- ensure a uniform, homogeneous and immediate contact between the ground and the lining;
- avoid puncture loads by ensuring the application of symmetrical and homogeneous loading along the lining;
- complement the waterproofing of the tunnel with the concrete lining and gasketry (i.e., if the lining has cracks due to a wrong installation, back-fill grout should help to mitigate any water inflow).

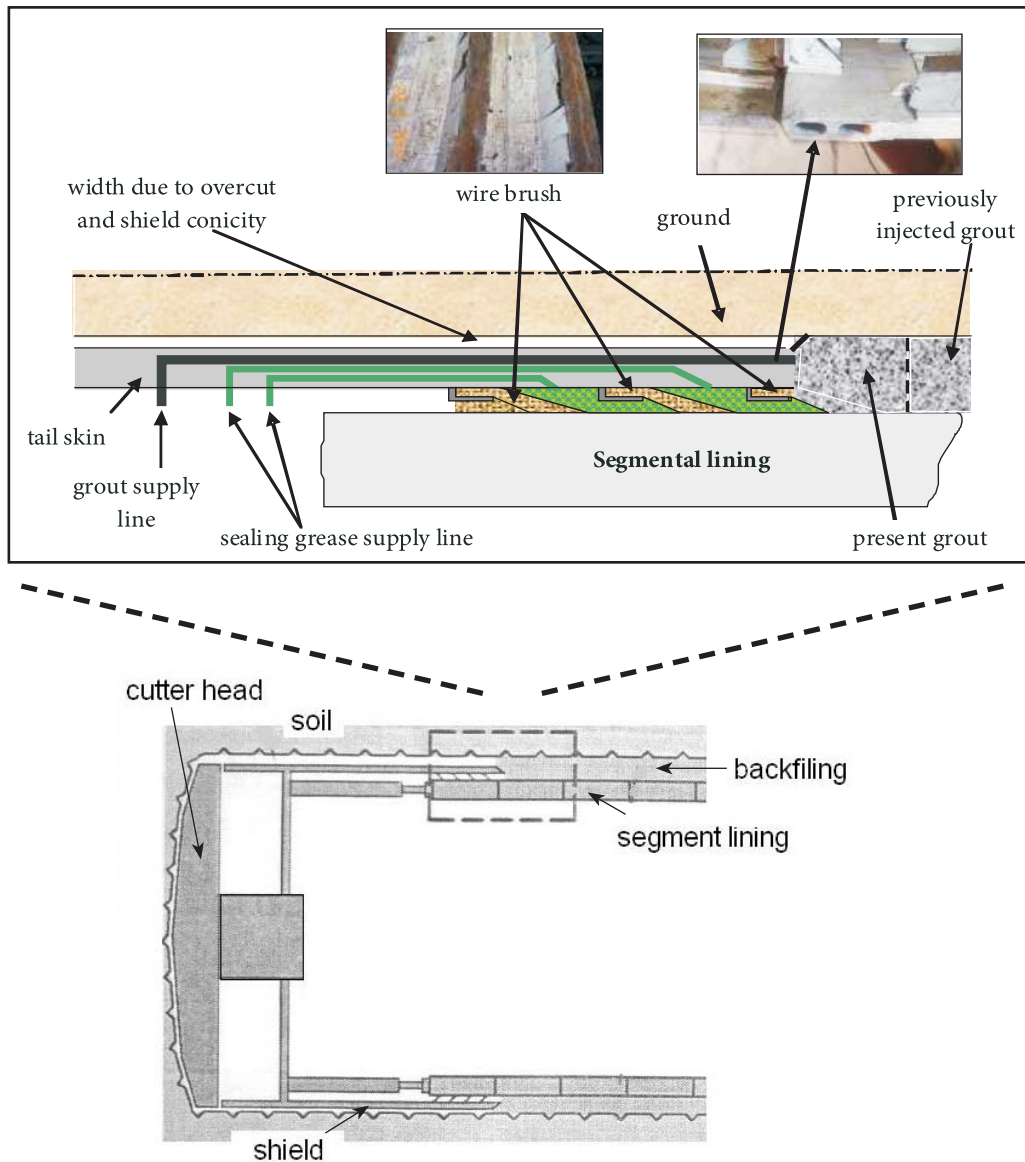


Figure 1. Scheme of the grouting through the tailskin.

To correctly achieve of all the above-mentioned goals, the simultaneous back-filling system and the injected material should satisfy the following technical, operational and performance characteristics:

- the back-filling has to be ideally instantaneous in order to avoid the presence of voids in the “annulus” while advancing with the TBM. For this reason, the back-filling is typically carried out through pipes located in the TBM’s tail skin;
- the “annulus” must be regularly and completely filled so that the lining is regularly linked to the surrounding ground (the system becomes monolithic);
- the reliability of the system must be guaranteed in terms of the transportability of the mix. The grout must therefore be designed in order to avoid choking of the injection pipes and the pumps’ segregation and bleeding in association with the time the grout is being transported and the distance from the batching to the injection;
- the injected material has to gel very quickly after injection (which is carried out progressively with the “annulus” generation) but without choking the injection pipes and nozzles (especially the ones for the accelerator admixture). The injection must always be carried out until either the maximum pressure is

achieved, which depends on the TBM face pressure, or the theoretical volume;

- the injection can be re-started and integrated with any previously injected material at any time;
- the injected material should be homogeneous with respect to the physical characteristics and mechanical behaviour throughout the “annulus”;
- the injected material must be impossible to wash out with the ground water.

Back-filling requires that the longitudinal injection pressure should be higher than the pressure at the excavation face and it should be homogeneous during the whole injection process.

From the perspective of the structural design of the segmental lining these injections can actually be considered as a radial hydrostatic pressure, which acts simultaneously on the support structure and on the ground in opposite directions. This effect is very important because when the ring exits from the shield, during the machine advancement, it must be blocked in the ground by the backfilling. The backfilling material acts in order to completely fill the ring void and to give an external load to the segmental lining ring that “encloses” it and tends to limit or better eliminate any asymmetry of the load with a reduction of the bending moments and compress the ground at the boundary, thus eliminating any type of void that could have been created. The injected material, when passing from fluid to solid, should maintain the achieved static equilibrium; therefore, it should not be reduced in volume nor pressure-filtered into the ground.

2 TYPE OF MATERIAL FOR BACK-FILLING

The injected materials can have different characteristics and they are of different types and require different equipment, as summarized in Table 1, following the classification proposed by Thewes and Budach [8], following the scheme proposed by EFNARC [3]. Generally speaking, the three main types of injected materials can be divided into inert mixes, cement mixes and two-component mixes. The main properties of these mixes are reported in the following.

2.1 INERT MIX

The inert mix is based on the sand transported in water with other constituents, such as filler, fly ash, etc. In the rock mass it is possible to use a simple mix of sand and gravel (pea gravel) just to fill the annulus void. Generally speaking, it is a cheap system. The absence of cement

avoids the risk of clogging the pipes due to any premature setting [3, 5].

The sand has to be properly selected/graded and mixed: size and type anomalies significantly increase the possibility of an irregular and heterogeneous filling, leading to pipe clogging.

As the sand cannot pump readily, it is needed to inject behind the tailskin through the segments. Typically, this is carried out through either 1 or 2 propriety grout sockets that are cast into the segments. This has a counter effect of possibly adding to potential weak points from a waterproofing perspective.

The setting is very retarded (or it never occurs) and the final strength is very low (even when it is not important to achieve any such strength). The inert mix is often chosen by French designers and contractors, as briefly described by the Working Group n.4 of the AFTES [1]: “The control of the injected material and of its hardening during the production and injection are really complex, and the progressive renunciation of the cement mix is in favour of products with a postponed grip (the pozzolanic reaction) and poor compression strength. This product is injected directly and continuously throughout the pipes that are placed in the thickness of the tail behind the last ring in the annular space, directly behind this one”.

2.2 CEMENTITIOUS MIX

The cementitious mix is made up of water, cement, bentonite and the chemical admixtures necessary to modify the water/binder ratio and the initial and final setting times. It is an active mix with a very high fluidity. It has to be easily pumpable, and is usually retarded (some hours) to avoid the risks of choking the pipes during transportation and injection.

The presence of cement helps in the development of mechanical strength, which can reach high values (15-20 MPa at 28 days, even if it is not really necessary for good back-filling). Also, this type of mix is very negatively influenced by variations in its ingredients, which can lead to the pipes choking. This mix should be injected as near to the face as possible to provide quick support to the segmental ring. Injection through the tailskin into the “annulus” can cause serious problems with choking.

Thewes and Budach [8] and EFNARC [3] have described these types of mixes in reduced active systems. Reduced active systems have a fraction of cement, usually varying between 50 kg/m³ and 100 kg/m³, while only in active systems does the binder component develop full hydration with a cement content of over 200 kg/m³.

2.3 TWO-COMPONENT MIX

The two-component mix is typically a super fluid grout, stabilized in order to guarantee its workability for a long time (from batching, to transport and injection), to which an accelerator admixture is added at the injection point into the “annulus”. The mix gels a few seconds after the addition of the accelerator (normally 10-12 seconds, during which the TBM advances approximately 10-15 mm). The gel exhibits a thixotropic consistency and starts developing mechanical strength almost instantaneously (weak but sufficient for the purpose: 50 kPa at 1 hour is typical).

This system is injected under pressure throughout the “annulus” and is able to penetrate into any voids that are present. Also, it can penetrate into the surrounding ground (depending on its permeability).

Furthermore, the retarding agent has a plasticizing effect and is able to inhibit the mix from setting, thereby guaranteeing its workability up to 72 hours after batching: this facilitates stockpiling grout in the mixer-containers that are bigger than the theoretical volume of material to be injected for every ring. This is useful for avoiding one of the most common mistakes, i.e., batching and stockpiling only the theoretical amount and not more. If eventually a bigger void is found that needs to be filled

in, you would leave the crown unsupported for too long, so leading to potentially serious consequences.

The addition of the accelerator admixture to the fluid mortar leads to an almost immediate gel formation, which starts developing mechanical strength. Such gels are homogeneous and therefore avoid the point loading of the segments.

The constituents of the two-component back-fill grout are sourced from “industrial” production and so should be perfectly controlled: this guarantees its regularity, with obvious advantages in the constancy of the fresh and hardened mixes. No constituent should exhibit variable characteristics (such as sand might).

By using a proper mix-design and specifically designed equipment the risks of choking can be minimized. Some problems could arise with the nozzle of the accelerator line choking: this can normally be attributed to an improper cleaning regime or simple wear and tear of the injection outlet mechanism.

The bentonite significantly increases the homogeneity and impermeability of the hardened mix. Furthermore, it minimises the bleeding, helps in achieving the thixotropic consistency when the flow stops because the “annulus” is full and so helps in the gelling process, conferring higher impermeability to the system (less than 10^{-8} m/s).

Table 1. Field of application of various backfilling technologies (redrawn from [8]).

Material	Application range		Backfilling system		Required equipment				Specific/remarks
	Hard rock	soil	A	B	a	b	c*	d	
Mortar active system	•	•	•	•	•				Conventional mortar, stiffness behaviour depends on using of additives
Mortar reduced active system	•	•		•	•				stiffness behaviour depends on using of additives
Mortar inert system		•		•	•				stiffness behaviour depends on using of additives
Two-component grout		•	•	•		○	•		stiffness behaviour just after mixing
Deforming mortar	•		•				•		Only usable in hard rock (material under development)
Pea gravel	•		•					•	Often used in hard rock, increased bedding by using mortar at the bottom, normally lower modulus of deformation and lower properties of embedment than for an active mortar

Key:

• : applicable - ○ : limited applicability

A: Backfilling through the grout holes in the lining segments, B: Backfilling through the tailskin-

a: piston pump; b: peristaltic pump; c*: progressive cavity pump; d: pressurized air

In an Italian subway-station excavation we can see, once the “dummy” segments have been removed, the presence of the “annulus” filled with the gel. The photograph allows us to see the presence of the back-fill under the invert segments (Fig. 2) that demonstrates the complete filling of the voids.

3 TWO-COMPONENTS MIX: EXAMPLES OF APPLICATIONS

Here are some significant examples of tunnelling projects in different countries where the two-component system was and is currently being used for the back-filling operation.

3.1 METRO LINE C – ROME (ITALY)

The Metro Line C is currently under construction in Rome. Two EPB machines (6.7m diameter) finished excavating the first part of the line (approx. 4km), while the other two have just started. In the first part of the line, the ground where the machines were excavating was a low-permeable, stable “pozzolana”, but later the TBMs will drive into a permeable and soft ground. Although the first project dealt with the injection of a traditional cementitious grout for the back-filling operation, the chosen method was finally a two-component system. The first component is an ultra-fluid mortar, with the following characteristics:

- it is stable and does not present any separation between the water and the solid contents, despite

the very high water/binder ratio. This is important to avoid problems of clogging in the injection lines, even during long breaks, and to allow the transportation of the mortar, even for long distances;

- it is able to guarantee the workability for at least 72 hours from its batching. Immediately before its injection, the mortar is admixed with an accelerator, which leads to an almost immediate creation of the thixotropic gel. The gel is able to fill in completely the annular space around the concrete lining (as proved by the several core samples extracted through the segments) and to improve the waterproofing features of the tunnel (the permeability coefficient of the hardened material is comparable that of a clay). The ingredients of the two-component mix are reported in Table 2.

Table 2. Two-component mix adopted in Metro C Line in Rome (values per m³ of hardened material).

Water	770-820 kg
Bentonite	30-60 kg
Cement	310-350 kg
Retarding agent by Mapei	3-7 l
Accelerator admixture by Mapei	50-100 l

The right dosage of each ingredient depends on several factors, such as the desired pumpability: for example, in those machines where the mix is pumped from the batching plant directly to the TBM, the material must have great pumpability properties and the bleeding must be minimised; therefore, the percentage of bentonite is increased.

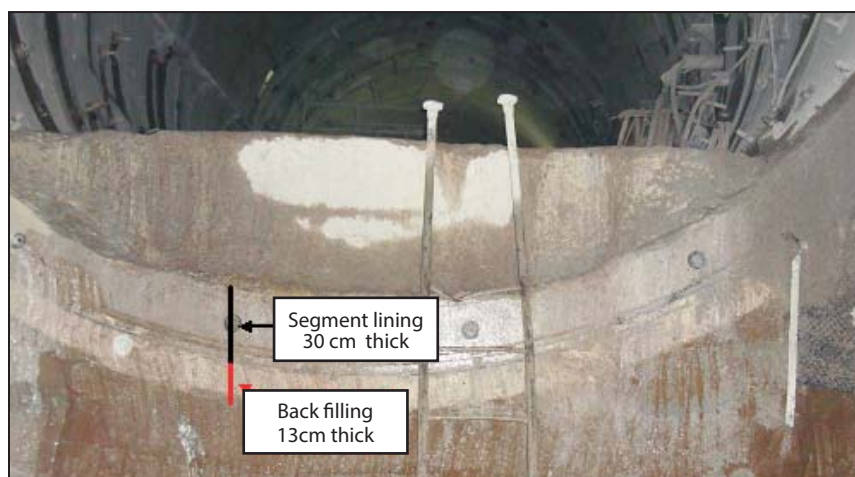


Figure 2. Example of backfilling in a metro tunnel in Italy (Prof. Pelizza’s picture archive).

The project requirements about the development of mechanical strengths only deal with the very early and early stages (up to 24 hours), which means when the TBM tail passes over and the back-filling material comes into contact with the surrounding ground.

For longer stages, the requirements only regard the durability of the hardened material (ensured by the natural humidity of the ground) and its impermeability.

3.2 ORAKI MAIN SEWER HOBSON DIVERSION (OMSHD) – AUCKLAND (NEW ZEALAND)

This project concerns the excavation of a 4.3-m-diameter Mixed-face Shield. The average productions were 114 metres of bored and lined tunnel per week. The project requirements were particularly high in terms of the mechanical strengths to be achieved, even at long stages. In particular, the two-component material had to achieve: 0.1 MPa at 30 minutes and 5 MPa at 28 days.

The only way to achieve such great values was to use an amount of cement that was higher than typically used (480 kg per cubic metre of hardened material). At the same time, the grout was not pumpable enough with such an amount of cement and the addition of a super-plasticizer admixture was necessary (Table 3).

Such a mix guaranteed proper pumpability and stability properties to the fresh grout and was able to achieve average values of compressive strength at 28 days from batching of 5.1 MPa.

Table 3. Two-component mix adopted in Oraki Main Sewer Hobson Diversion (OMSHD) – Auckland (values per m³ of hardened material).

Water	730 kg
Bentonite	30kg
Cement	480 kg
Retarding agent by Mapei	1 l
Super-plasticizer by Mapei	5 l
Accelerator admixture by Mapei	50 l

It is important to underline that such a high compressive-strength request is not strictly necessary for a proper back-filling, as already mentioned. In fact, the back-filling material cannot have structural tasks at long stages, when all the external loads (ground, water) are supported by the segmental lining. The two-component mortar should just act as an “interface” between the surrounding ground and concrete, in order to homogeneously discharge the pressures on the lining.

3.3 METRO LINE IN SOFIA (BULGARIA)

This project concerns the construction of two 3.47-km - long parallel tunnels, which were completed at the beginning of 2009 and were excavated by an EPB machine with a diameter of 5.82 m.

The alluvium ground where the tunnel was bored was subject to many and frequent geological and geotechnical variations. The composition of the material used to fill the annular voids behind the segmental lining is summarized in Table 4 [9].

Table 4. Two component mix adopted in the metro line of Sofia (values per m³ of hardened material).

Water	795 kg
Bentonite	25 kg
Cement	290 kg
Retarding agent by Mapei	2.5 l
Accelerator admixture by Mapei	74 l

Such a material was able to gel in approximately 12 seconds and to achieve 0.03 MPa of compressive strength at 1 hours and 1.5 MPa at 24 hours.

Nothing was requested in terms of the mechanical behaviour for longer stages. The injection ratio was varying, depending mainly on the infiltration of material into the surrounding ground: the average values were 120-130% of the theoretical volumes.

3.4 METRO LINE 1 IN BRESCIA (ITALY)

The project concerns the construction of a metro-line tunnel in alluvial ground with a tunnel diameter of 9.15m, excavated by an EPB machine. The composition of the two-component mix used is summarized in Table 5.

Table 5. Two-component mix adopted in the metro line of Brescia (values per m³ of hardened material).

Water	816 kg
Bentonite	42 kg
Cement	315 kg
Retarding agent	3 l
Accelerator admixture	60 l

3.5 LTA BORED TUNNEL CONTRACTS - SINGAPORE

Another important reference, regarding the use of the two-component mix, is the construction of the LTA

Bored Tunnel in Singapore, which included approximately 20 Lots for a total of more than 50 km of tunnels. In every Lot, the use of the traditional cementitious grout was substituted by the injection of an ultra-fluid grout able to gel in a few seconds of the injection and to completely fill in all the annular space around the segmental ring.

The use of such a material was successful in all the tunnels, which were bored with different types of TBMs (EPB, Slurry Shields), manufactured by different suppliers, and in different geological conditions (clay, alluvium ground, fluvial deposits, granite, gravel, etc.).

This also proves the flexibility of the two-component back-filling and its adaptability to very different and changing conditions of boring.

3.6 CONCLUSIONS OBTAINED FROM CASE HISTORIES

All the mentioned examples prove that the current tendency is to privilege the back-filling of ultra-fluid two-component mixes, activated with an accelerator and able to generate a thixotropic gel in a few seconds. This system avoids all negative aspects correlated with the use of traditional cementitious grouts and is able to achieve all the technical requests demanded for the back-filling of injected material.

All these examples prove the efficacy of back-filling using ultra-fluid two-component mixes, activated with an accelerator. The fluid is able to penetrate into the earth and annulus, subsequently generating a thixotropic gel in a few seconds.

4 PERFORMANCE ANALYSIS OF THE TWO-COMPONENT SYSTEM

4.1 CREATION OF AN ANNULAR UNCOMPRESSIBLE BUBBLE

As the injected material for the two-component system is an ultra-fluid liquid which, thanks to the addition of an accelerator admixture just before its injection, obtains a thixotropic consistency in a few seconds, and as it is made up of a huge amount of water (approximately 800 litres per cubic metre of material), it is without doubt an incompressible fluid, just like water.

The consequence is that the annulus void that is created, after the TBM tail-skin passage, has to be considered as

a closed annular bubble that is filled, instant per instant, with an incompressible fluid.

Therefore, every movement of the surrounding ground that tends to enter in the bubble or any movement of the concrete lining which tends to reduce the bubble volume, instantaneously leads to the creation of another reaction-pressure in the ball, uniform along all the volume and above all the surfaces of the volume, which avoids any type of deformation.

Therefore, the incompressible ball of gel confines perfectly and completely everywhere the concrete rings already installed and the new concrete ring that has to be installed.

In order that this can be effectively real, it is necessary that the following conditions are met:

- the injected material must remain incompressible;
- the fluid cannot escape from the bubble:
 - it cannot permeate through the surrounding ground (this is avoided by the underground water that exerts a hydrostatic pressure on the injected material).
 - it cannot escape through the space between the tail and the excavation profile, that is avoided by a correct balance between the tunnel face pressure and the injection pressure (which must be approx. 0.2 bar higher, not more);
- if the surrounding ground in bad condition tends to close towards the bubble, it cannot be allowed to move with excessive pressures, otherwise the pressure needed to advance the machine would increase too much. This has to be balanced and controlled with the right equilibrium between the pressure in the excavation chamber and the injection pressure. This can be aided by lubrication of the extrados of the tailskin with a bentonite slurry. It is suggested that the bentonite slurry injection takes place exactly where the tail is blocked and weighs on the ground, which means behind the invert of the lining and in the final part of the tail;
- the segment ring just installed cannot have deformations (in general, without ovalization) due to its own weight, which could lead to an anomalous installation of the rings or a too low pressure on the upper segments;
- the gel cannot be leached by the underground water.

It is evident from the above reasons that it is necessary to inject a fluid that does not harden instantaneously, but that becomes a gel quickly and progressively without avoiding the formation of an incompressible ball at constant volume.

The long-term mechanical strength of the back-fill material does not have any meaning, because it does not give any structural contribution to bearing the hydrostatic and geostatic loads (these are completely supported by the concrete lining), but the gel has to be as homogeneous as possible in order to mitigate the external loads (a closed ball!).

To achieve this goal it is doubtless necessary that the gel cannot decompose after its injection: its durability must guarantee that the incompressible annular ball is kept permanently.

Therefore, all the attention should be paid to the behaviour of the injected material at early stages (from the first seconds to some hours), which includes the injection and installation of some segment rings. It is evident that the existence of a closed incompressible ball is the most efficient and important factor.

4.2 DURABILITY

The durability of the gel that totally fills the annular bubble is guaranteed in the normal humidity conditions of the ground (even more when the tunnel is drilled under the water table). During the construction of many Metro Lines in Singapore the authors understand that since the two-component system has started to be used, more than ten years ago, there has only been a positive indication of the grout's durability. A comprehensive proof of the behaviour for the future does not exist, but the gel must have two features that indicate its durability:

- the undeformability: this parameter immediately appears as the most significant, as the gel is made up principally of water. If the water is not lost (due to evaporation or filtration), the material will remain stable. It is, therefore, essential that the hosting ground keeps its natural humidity;
- the technical impermeability of the ground (10^{-8} m/sec). This is the physical parameter that favours the creation of the situation described above.

Both the mentioned characteristics can be measured in the laboratory and can be assumed as indicators of durability.

4.3 CONSISTENCY AND COMPRESSION STRENGTH OF THE HARDENED MIX

The first important consideration deriving from what has been written above is that, when a super-fluid two-component mix is used, the early-stages mechanical

strengths are more important than the latter stages: in fact, the concrete lining, not the back-filling, must bear all the hydrostatic and geostatic pressures.

In the example of the Sofia Metro Line, it is clear from the table that the requested data are 0.03 MPa at 1 hour and 1.5 MPa at 24 hours and nothing is said about longer stages.

This position appears to be absolutely correct because it is in the first hours (8 rather than 24 when the TBM advances regularly) that the gel must fill every void in the “annulus” (and eventually in the surrounding ground) and protect the segment lining. This is carried out thanks to the high fluidity of the injected material and its quick gel creation. Furthermore, the gel must block the ring in its projected position (avoiding the formation of point loads) and at the same time avoid the last installed rings deforming due to the TBM thrust and cutting-wheel rotation.

It is of paramount importance that the mix creates a gel after a few seconds and so an incompressible closed ball is generated: therefore, the gel creation must be tested (at 0.5 and 8 hours stages the measures of mechanical strengths are suitable, for example, with a pocket penetrometer). The rationale of the half hour can be adjusted to suit the time taken to build one ring should be long enough for the grout to achieve sufficient strength to avoid floating around in the grout.

Measures above the 24 hours are only suitable for checking that the gel does not decompose, but increases its strength in order to allow the extraction of cores through the segments, useful to directly check the effective total filling of the “annulus”.

It is without doubt that a measure of the compressive strengths on cores extracted in situ (even if the coring partially disturbs the samples) is the most reliable and significant, because the material is injected into the “annulus” at pressure and there remains in environmentally natural conditions.

5 TESTS ON THE TWO-COMPONENT BACK-FILLING GROUT MIX

In the following the results of a series of tests regarding the physical and mechanical behaviour of a two-component injection grout for filling the annular voids behind the segmental lining during mechanized tunnelling with EPB machines are presented, showing how this mix works properly for the mechanized tunnelling purposes.



Figure 3. Phases of preparation of the hardened grout samples.

The tests were carried out both on a fresh and on a hardened mix. The technical procedure (Fig. 3) that was used to obtain the samples of hardened material is:

- 10 litres of fresh and ultra-fluid grout were prepared in a bucket;
- the right amount of accelerator admixture was added and mixed to the grout for some seconds to properly distribute the accelerator in the whole grout volume;
- when the material starts hardening, the mixing is stopped;

while the mix quantities are reported in Table 6.

Table 6. Two-component mix adopted for the tests.

Component	Average quantities [kg/m ³]
Water	796
Bentonite	35
Cement type IV/B-P 32.5 R	350
MAPEQUICK CBS SYSTEM 1	6.4
MAPEQUICK CBS SYSTEM 2	84.8

5.1 TESTS ON FRESH GROUT

To check the suitability of the fresh grout for the EPB tunneling procedure, the following tests were carried out:

- bleeding test (ASTM C940). This test is carried out by leaving undisturbed 500 ml of mix for three hours and after measuring the percentage of water separation. This value for a good mix should not exceed 3%;
- Marsh cone test (ASTM C185). The test makes it possible to evaluate the fluidity and viscosity of the mix. It is carried out using a standardized cone (Fig. 4) and measuring the time request by 1000 ml of mix to flow. The optimal value for the tunneling purposes should be about 30-45 s;
- hardening time evaluation. This test was carried out by mixing 500 ml of grout and 48 g of accelerator. The hardening time is fixed when the mix is no longer workable (Fig. 5).

These tests make it possible to evaluate whether the mix can be easily and safely pumped through the tail



Figure 4. Execution of Marsh cone test.



Figure 5. Grout mix after hardening.

skin and also provide the maximum time while the not accelerated mix remains stable without separation of the solid phase (mainly cement grains). The obtained results are reported in Table 7, showing the good behavior of the studied mix.

Table 7. Results of the bleeding tests on different samples.

Sample	Time since the grout was prepared [h]	Bleeding value [%]	Marsh cone time [s]	Hardening time [s]
A	0	3	33	12
B	12	2	32	12
C	24	2	32	13.5

5.2 TESTS ON HARDENED GROUT MIX

After seven days from the mix preparation, the sample was cored (\varnothing 54 mm, diameter/height ratio=1) and the uniaxial compressive strength of the grout mix was measured at different curing times, keeping the samples under soil with its natural humidity. From Figure 6, where all the results are summarized, it is possible to see how the grout mix hardens in time and that it reaches values greater than 4.5 MPa.

To study the effect of the curing condition it is possible to compare the samples that were maintained inside a soil with its natural humidity and those that were maintained in the open air.



Figure 7. Example of two samples cured under natural soil and two cured in the open air. The difference in behaviour is clear.

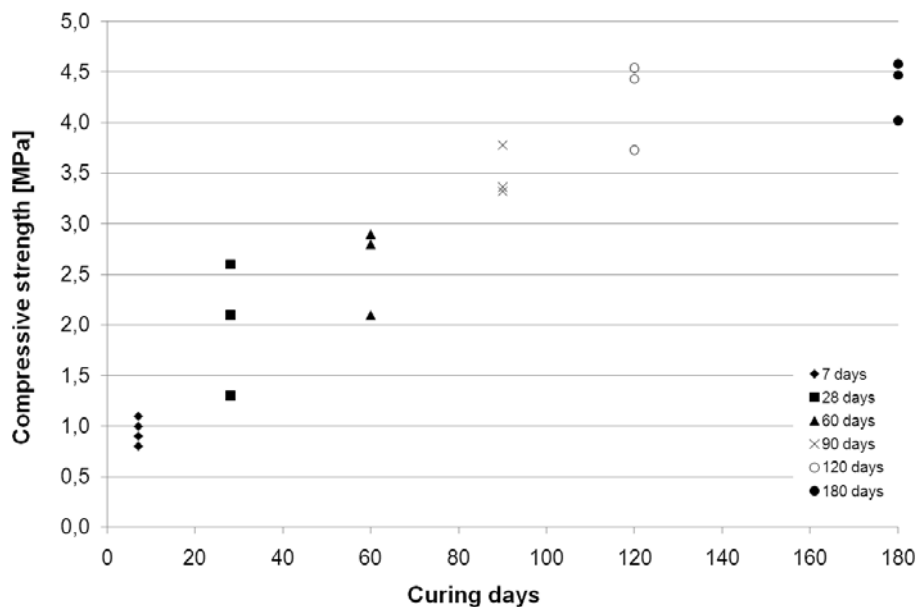


Figure 6. Uniaxial compressive strength of the two-component tested mix.

From the photographs it is clear, the great difference of behaviour: if the sample loses its natural water it then loses its mechanical properties.

6 CONCLUSIONS

The two-component system injection for back-filling while excavating with shielded TBMs is progressively substituting the traditional use of cementitious mortars for two main reasons: it reduces the risks of choking pipes and pumps (typical when pumping cementitious systems) and guarantees a complete filling at the pressure of all the annular voids created after the TBM tail passage, thus avoiding the surrounding movements. The main features of such a material are: super-fluid initial consistency, the creation of a gel after a few seconds from the injection, compressive strengths from approx. 0.1 to 1 MPa at early stages.

Effectively, the goal of the back-filling is carried out in the first minutes after its injection; therefore, it is important to focus attention on the last 2-3 installed rings, and not more.

Consequently, also according to international methods, it is important to verify that the mix actually makes a gel quickly, in order to confine homogeneously the segment ring.

As it is impossible to verify the event inside the “annulus”, it is necessary to simulate that by preparing samples in the laboratory, with which it is possible to determine the consistency achieved by the gel in the first hours and later. The latter stages are meaningless, because the gel’s mechanical strength does not influence the structural behaviour of the tunnel lining if the “annulus” is actually completely filled in.

ACKNOWLEDGMENTS

The author thanks MAPEI UTT and Dott. Dal Negro, Eng. Schulkins and Eng. Boscaro for the useful suggestions. The research was partly conducted with the financial support of DITAG – Politecnico di Torino.

REFERENCES

- [1] AFTES, (French National Tunnelling Association), Choosing mechanized tunnelling techniques (2005) Paris.

- [2] Bappler, K. (2008). Entwicklung eines Zweikomponenten-Verpresssystems für Ringspaltverpressung beim Schildvortrieb, Taschenbuch für den Tunnelbau 2008, Verlag Gluckauf GmbH, Essen, 263-304.
- [3] EFNARC (2005). Specification and guidelines for the use of specialist products for Mechanized Tunnelling (TBM) in Soft Ground and Hard Rock www.efnarc.org.
- [4] Guglielmetti, V., Mahtab A. and Xu, S. (2007) Mechanised tunnelling in urban area, Taylor & Francis, London.
- [5] Japan Society for Civil Engineering (2006). Standard Specification for tunneling, JSCE ed., Tokyo.
- [6] Maidl, B., Herrenknecht, M. and Anheuser, L. (1995). Mechanised Shield Tunnelling, Ernst&Sohn, Berlin.
- [7] Pelizza, S., Peila, D., Borio, L., Dal Negro, E., Schulkins R. and Boscaro, A. (2010). Analysis of the Performance of Two Component Back-filling Grout in Tunnel Boring Machines Operating under Face Pressure, *Proceedings of ITA-AITES World Tunnel Congress 2010: “Tunnel vision towards 2020”*, Vancouver, 14-20 May 2010.
- [8] Thewes M., and Budach C. (2009). Grouting of the annular gap in shield tunnelling – An important factor for minimisation of settlements and production performance, *Proceedings of the ITA-AITES World Tunnel Congress 2009 “Safe Tunnelling for the City and Environment”*, Budapest, 23-28 May 2009.
- [9] Tomoya, I., Toshihiko, A., Mitsufumi, Y., and Stoyan, B. (2009). Excavation management with use of shield machine in rapidly changing soil condition, *Proceedings of the ITA-AITES World Tunnel Congress 2009 “Safe Tunnelling for the City and Environment”*, Budapest, 23-28 May 2009.
- [10] Vinai, R., Oggeri C. and Peila D. (2007). Soil conditioning of sand for EPB applications: A laboratory research, *Tunnelling and Underground Space Technology*, 23, No.3, 308-317
- [11] Vinai, R., Borio, L., Peila, D., Oggeri, C. and Pelizza S. (2008). Soil conditioning for EPBMs, *Tunnels and Tunnelling International*, December, 25-27.
- [12] Wittke, W., Erichsen, C. and Gattermann, J. (2006). Stability Analysis and Design for Mechanized Tunnelling, WBI, Felsbau GmbH, Aachen.

DEFINIRANJE KRAŠKIH CON PRI GRADNJI AVTOCESTE Z UPORABO GEORADARJA

MATEVŽ U. PAVLIČ IN BLAŽ PRAZNIK

o avtorjih

vodilni avtor

Matevž U. Pavlič
Building and Civil Engineering Institute ZRMK d.o.o.
Dimičeva 12, 1000 Ljubljana, Slovenija
E-pošta: matevz.pavlic@gi-zrmk.si

Blaž Praznik
Building and Civil Engineering Institute ZRMK d.o.o.
Dimičeva 12, 1000 Ljubljana, Slovenija
E-pošta: blaz.praznik@gi-zrmk.si

izvleček

Georadarske meritve so bile izvajane za detekcijo pod površinskih kraških pojavov ob izgradnji nacionalne avtoceste v jugo-vzhodnem delu Slovenije. Predvidena trasa avtoceste je locirana večinoma v dinarskem krasu z veliko gostoto kraških pojavov, ki so vidni že na površju. Preiskave z georadarjem so bile izvedene v vseh območjih, kjer so bili projektirani globoki vkopi v kraški apnenec, z namenom detekcije ter karakterizacije kraških pojavov. Preiskave z georadarjem so bile izbrane zaradi ekstremno heterogene narave kraškega terena, kjer konvencionalne metode preiskovanja ne pridejo v poštev oziroma so finančno preveč zahtevne. Ena glavnih prednosti preiskav z georadarjem je, čeprav je globina penetracije omejena na nekaj metrov, ločljivost ter preiskanost terena, saj lahko v idealnih pogojih zagotovimo ločljivost nekaj centimetrov na celotnem kontinuiranem profilu. Zaradi dejavnikov, ki omejujejo globinski doseg preiskav z georadarjem, so bile preiskave izvajane istočasno z samo gradnjo avtoceste. Preiskave smo na podlagi preučitve korelacij med dosegom ter ločljivostjo izvajali z 2000 MHz oddajno – sprejemno zaščiteno anteno po cestnem telesu pred polaganjem asfaltne sloja. Iz 2D radarski profilov (radargrame) smo skonstruirali 3D modele površja, kjer so bile označene močnejše EM anomalije. Različni razmaki med posameznimi 2D profili so bili testirani z namenom ugotovitve optimalne finančno – časovne kombinacije, ki je še vedno zagotavljala potrebno ločljivost. Pridobljeni rezultati so bili kalibrirani ter testirani s testnim vrtanjem. Vrtanje je bilo izvajano dvakrat, in sicer, prvič za kalibracijo georadarskih anomalij z radargramov z dejanskimi kraškimi pojavi na terenu ter drugič za preverjanje rezultatov. Skupno je bilo izvrtanih več kot 30 vrtin na predhodno določenih lokacijah. Podatki s testnega vrtanja so se izkazali kot zelo dobri, saj so bile ugotovljene anomalije v veliki večini (nad 95%) posledica uklonov med apnencem in prazninami oziroma apnencem ter glinenimi žepi.

Vrtanje testnih vrtin se je izkazalo kot zelo primerno orodje za kalibracijo georadarskih anomalij zajetih na radargramih. Tak pristop se je izkazal, kot zelo natančen pri interpretiranju georadarskih anomalij kraških pojavov, 77% anomalij je bilo po kalibracijskem vrtanju pravilno interpretiranih kot jama oziroma glineni žep, 23% napačno interpretiranih pa so bili interpretirani kot glineni žep namesto praznine ali obratno.

Istočasna preiskava z georadarjem ter gradnjo avtoceste se je izkazala kot zelo uspešna, saj je tako (po odstranitvi glinenih slojev) razmerje med globinskim dosegom ter ločljivostjo optimalno.

ključne besede

Kras, georadar, geotehnika, jame, kraški pojavi, detekcija

DETECTING KARSTIC ZONES DURING HIGHWAY CONSTRUCTION USING GROUND-PENETRATING RADAR

MATEVŽ U. PAVLIČ and BLAŽ PRAZNIK

about the authors

corresponding author

Matevž U. Pavlič
Building and Civil Engineering Institute ZRMK d.o.o.
Dimičeva 12, 1000 Ljubljana, Slovenia
E-mail: matevz.pavlic@gi-zrmk.si

Blaž Praznik
Building and Civil Engineering Institute ZRMK d.o.o.
Dimičeva 12, 1000 Ljubljana, Slovenia
E-mail: blaz.praznik@gi-zrmk.si

abstract

Ground-penetrating radar (GPR) has been applied to determine the subsurface karstic features during the construction of the national highway in the south-eastern part of Slovenia. The highway construction is situated mostly in the dinaric karstic region with a high density of karstic features visible on the surface. Ground-penetrating radar prospecting was done in all areas where a slope was cut into the limestone bedrock. The main purpose of the survey was to map potentially hazardous zones in the highway subsurface and to detect and characterize the karst. The ground-penetrating radar method was used because of the heterogeneous nature of the karst. With its high degree of karstification and geological diversity all conventional methods failed. One of GPR's main advantages is that, while the penetration depth is limited to several meters, the obtained resolution can be on the scale of centimeters and the measured profile is continuous. Because of the ground-penetrating radar's limitations with respect to depth, the range surveying was done simultaneously with the road construction using 200-MHz bistatic antenna on the level of the highway plane. All the 2D radargrams were constructed in 3D models where the measurements were made in raster with 2 meters between a single GPR profile. This two-meters spacing was determined as the optimal value in which only a minimal resolution-price tradeoff was made. The gathered results were tested and compared to experimental drillings and excavations so that any anomalies and

reflections were calibrated.

The drilling was conducted twice, first to calibrate the radargram reflections and secondly to check and confirm the calibration success. Altogether, over 30 boreholes were drilled at various previously selected locations. The data obtained from the drilling proved to be very helpful with the calibration since anomalies found during the drilling were almost exclusively (over 95%) a result of the propagation of radar waves from the limestone to an air void or from the limestone to a clay pocket.

Drilling test boreholes proved to be a very useful tool for the calibration of the GPR anomalies recorded in 2D radargrams. Such a process showed a near 100 % accuracy with respect to interpreting the subsurface features, with 77% correctly interpreted as caves or clay pockets and 23% wrongly interpreted, where the interpretation was a void but it was indeed partly a clay-filled and partly an air-filled void. The completed survey also showed simultaneous surveying with GPR and road construction is a very efficient and economical way to predict various karstic features and the density of the karstic forms.

keywords

karst, ground-penetrating radar, geotechnics, cavities detection

1 INTRODUCTION

More than half of Slovenia is karst. With the construction of the national highway, a lot of stability problems emerged where constructions was being made on the karstic surface. In previous years a collapse of the highway's structure has occurred because of cavities under the surface of the road. A large hole emerged in the middle of the fast lane, causing great danger to anyone included in the traffic. Fortunately, however, no one was hurt. Since then karstologists have been included in the planning and construction of national highways ([4],

[5], [13], [6], [7], [8], [18]). During one of the highway constructions in the south-western part of Slovenia the largest cave was found, measuring 460 meters in length and 70 meters in depth [9]. Ground-penetrating radar was first used in Slovenia to survey highways constructed over a karstic terrain in 2003, between Unec and Postojna, with the goal to create a map of potentially hazardous areas ([14], [15]). Komel and Pavlič [10] showed the results of a GPR survey on a karstic surface near Sežana, which was done with the same goal of determining the cavities and other karstic features. The results of various ground-penetrating surveys in the past over the karstic surface have shown that this method is very successful at determining karstic features and potentially hazardous zones in the karstic subsurface. For that and many other reasons (mostly economic) investors decided that during the construction of the final highway part, Pluska–Hrastje, which is largely situated in a dinaric karst (also called Dolenjski kras), all the parts of the highway where slope cuttings were planned, were surveyed for cavities and other karstic features that could potentially undermine the stability of the road. The ground-penetrating radar method was used as the main surveying technique over intervals where the slope was cut in the karstic limestone. Altogether, more than 50 km of 2D ground-penetrating radar profiles (radargrams) were taken over a length of approximately 3600 meters of highway. Radargrams were taken in raster (rectangular) patterns with 5 or 11 radargrams

constructing each raster. These radargrams were ultimately used to construct a 3D model of the GPR anomalies. This article describes various karstic and geological features that were found during the survey.

2 STUDY AREA

The survey area is located in the south-eastern part of Slovenia (Figure 1), where a missing part of the national highway A2 is being constructed. An area over which roughly 15 kilometers of highway is planned is situated on Jurassic limestone with some small percentage of dolomite. Because of the relatively large presence of ground water, this area was developed as dinaric karst, also known as Dolenjski kras.

Ground-penetrating radar was used simultaneously with the construction of the highway because of the noticeable silty and clayey sediment cover over the limestone and the karstic nature of the terrain. The studied area is densely covered with surface karstic features, such as karren, uvalas and also with underground features, such as sinkholes and caves. There were a few registered karstic caves in this area (determined by the speleologists) and a few more were found during the geological mapping of the terrain. Highway A2 is situated in the slopes of hills above the town of Trebnje and planned so that significant slope cuttings will be made in the

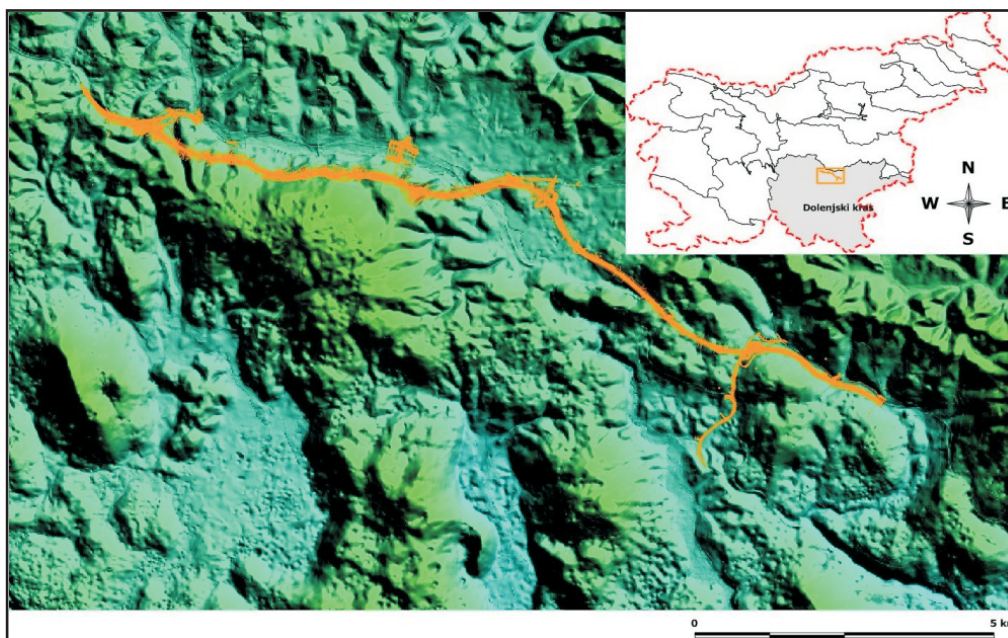


Figure 1. Location of the construction site of the last part of highway A2 Karavanke–Obrežje.

limestone bedrock and epikarstic zone above. The limestone terrain, when the highway's deep slope cuttings (the slope was cut up to 40 meters in limestone bedrock) were constructed, was surveyed with ground-penetrating radar to determine possible voids and other karstic features under the planned road.

3 GROUND-PENETRATING RADAR BASICS

Ground-Penetrating Radar (GPR) is a geophysical imaging technique used for subsurface exploration and monitoring. It is widely used within the forensic, engineering, geological, mining and archeological communities. GPR provides an almost ideal technique for karstic surface evaluation, especially if the upper clayey and silty cover is removed.

In general, GPR is a non-destructive technique that emits a short pulse of electromagnetic energy, which is radiated into the subsurface. When this pulse strikes an interface between layers of materials with different electrical properties, part of the wave reflects back to the surface where the reflection is detected, and the remaining energy continues through the medium. GPR evaluates the reflection of electromagnetic waves at the interface between two different dielectric materials. Two electrical properties are of great importance to a GRP survey. The first is the electrical conductivity (σ) and the second is the electrical permittivity, also known as the dielectric constant. Electrical conductivity is the ability of a material to conduct electric current. The water content and the porosity can have a large impact on the conductivity values (1) [3].

$$\sigma = n(1-s)\sqrt{\sigma_a} + ns\sqrt{\sigma_w} + (1-n)\sqrt{\sigma_s}; \quad (1)$$

In the above equation σ , σ_a , σ_w , and σ_s represent the overall conductivity, the conductivity of the air, the conductivity of the water and the conductivity of the soil particles. n is a porosity factor and s is the degree of saturation.

The other important factor for the propagation of radar waves into the subsurface is a dimensionless constant called the relative dielectric constant (ϵ), which is the capacity of media to store a charge when an electric field is applied [3]. The relative dielectric constant (ϵ) of a non-metallic medium is a function of three different materials within the medium – solid, fluid and gas [2]. If a material is dielectrically homogeneous, then the wave reflections will indicate a single thick layer. The reflection coefficient (2) can be analyzed and sometimes used

to distinguish between the types of medium from which the electromagnetic waves are reflecting.

$$r = \left[\frac{\sqrt{\epsilon_2} - \sqrt{\epsilon_1}}{\sqrt{\epsilon_2} + \sqrt{\epsilon_1}} \right]; \quad (2)$$

Equation for the reflection coefficient r [1], where ϵ_1 is the dielectric constant of the first medium and ϵ_2 is the dielectric constant of the second medium.

The problem with ground-penetrating radar is that it is in general a contrast method, meaning that the reflections that we obtain during requisition are merely reflections between the different electric properties of a medium. There is no way of knowing which exact medium the amplitude of the reflections belongs to. In theory, you can get the same reflection coefficients from materials, e.g., where $\epsilon_1=9$ and $\epsilon_2=1$ or where $\epsilon_1=36$ and $\epsilon_2=4$. In both cases the reflection coefficient is $r = -0.5$. The dielectric constant is inversely proportional to the velocity of the propagation of radar waves through a medium. The dependency of the reflection coefficient (r) on the dielectric constant (ϵ) is shown in Figure 2 (a). The velocity of the radar waves' propagation through different media is shown in Figure 2 (b).

The signal polarity (whether the reflection coefficient is positive or negative when it passes from one medium to another) can also provide valuable information about the subsurface material. Signal polarity is a function of the dielectric constants between two media [2]. Figure 3 shows the oscillation of a radar wave as it passes through different materials. From the signal polarity we can assume relative changes in the dielectric constants of the media.

The karstic formations in the survey mainly consist of karstic high-plasticity clay, voids and karstic limestone rocks in which the electric constant is roughly 24, 1 and 12, respectively (the values were obtained during an analysis of the reflections' hyperbolas). Water poses a big problem in analyzing the reflection coefficient and its polarity because it changes the electric properties of the medium drastically (it changes the conductivity of the medium). Typical values for the electric properties of different media are presented by Daniels [16].

For a successful GRP survey a compromise between the required range (depth) and the ability to resolve one feature from another (resolution) has to be made. Both range and resolution are functions of the GPR antenna and the electromagnetic properties of media. The higher the antenna frequency, the smaller the range of EM waves' penetration.

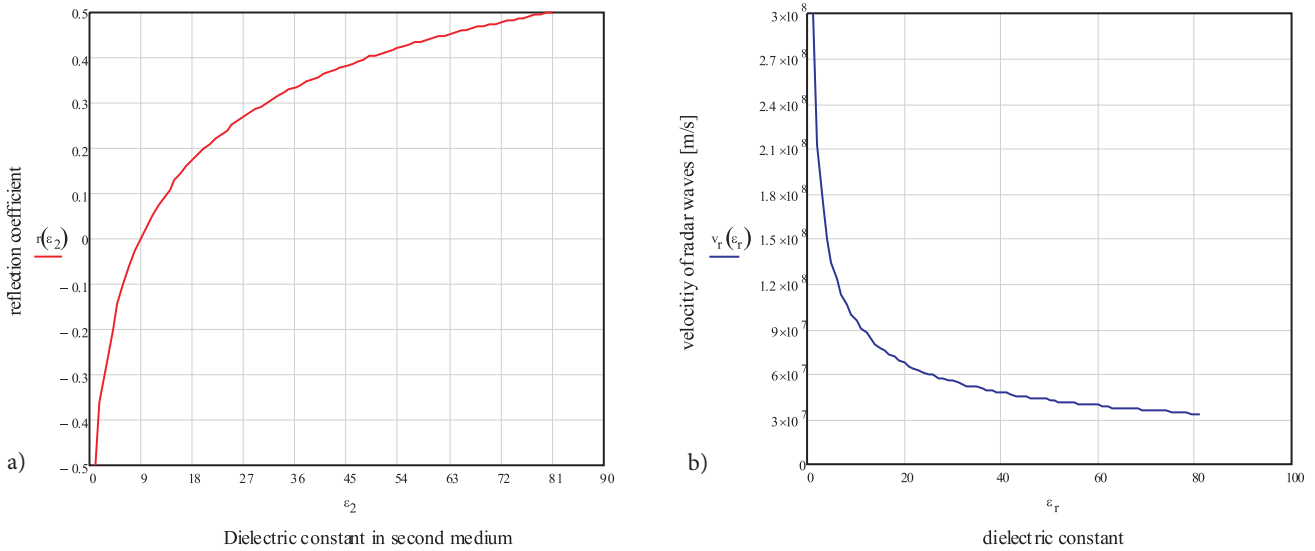


Figure 2. a) Dependence of the reflection coefficient (r) on the dielectric constant (ϵ) of the materials. In the figures $\epsilon_1=9$ and ϵ_2 range from 1 (in air) to 81 (in high mineral soil containing water), b) The velocity of the radar wave's propagation (m/s) in relation to different dielectric constants ϵ .

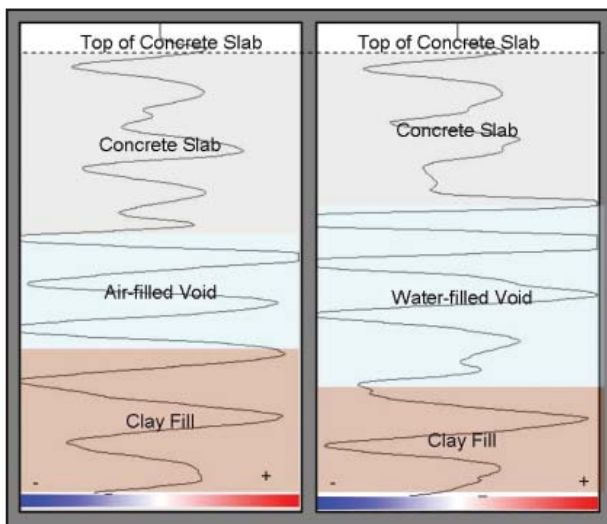


Figure 3. Different signal polarities of the GPR signal as it passes through media [2].

With the GPR equipment used, bistatic shielded antennas (bistatic – transmitter and receiver in one antenna) were employed, which send a signal in an ellipsoidal, cone-shaped pattern into the ground. If unshielded antennas were to be used, the GPR emits a signal in 3D space, so more noise is recorded.

Two different resolutions (horizontal and vertical) are of great importance in the GPR survey and are a function of the choice of the antenna and the media. Figure 4 (a)

shows the relation between the horizontal resolution and the depth for various frequency antennas. The horizontal resolution varies with depth and can be roughly estimated from the radius of the first Fresnel zone [17] (3).

$$H_r = \sqrt{\lambda \cdot d + \frac{1 \cdot \lambda^2}{4}} \quad (3)$$

where λ is the wavelength of the EM waves through the media and d is the depth.

The vertical resolution can be estimated with equation (4) below:

$$V_r = \frac{c}{4 + \nu \cdot \sqrt{\epsilon}} \quad (4)$$

where ν is the central frequency of the antenna and ϵ is the dielectric constant of the media.

The range of penetration is also dependent on the dielectric constant of the media, i.e., if the maximum range for a 200-MHz antenna would be 10 meters in certain media, a 900-MHz antenna would have a range up to 1 meter in the same media. The determination of the velocity is of great importance in order to change the time sections into depth. For that, a hyperbola approximation was used, with which the average velocity for the karstic limestone was determined as $\nu = 8.4\text{cm/nsec}$. Figure 4 (b) shows the hyperbola approximation for determining the velocity of the radar waves' propagation through the media.

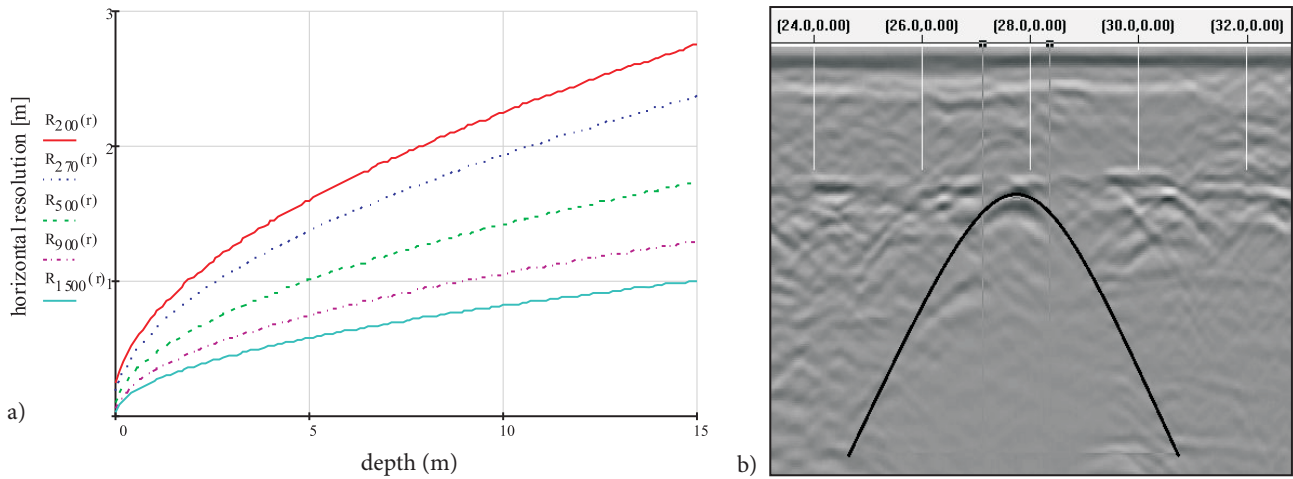


Figure 4. a) Relation between the depth and the resolution for various antennas. b) Hyperbola approximation for a determination of the radar waves' propagation through the media.

4 METHODOLOGY

A ground-penetrating radar survey was conducted simultaneously with the construction of a major highway A2 Karavanke–Obrežje in the sub-section of Pluska–Hrastje. First, major ground work was done to excavate the rock to the final planum of the highway. After that, the GPR survey was conducted in several profiles along the planned road surface (Figure 5).

GSSI's SIR – 3000 system was used with a bistatic shielded antenna to measure over 100 grids in parts where the highway construction was cut in karstic limestone. The acquired profiles in grids, consisting of either 5 or 11 2D profile lines (radargrams), amount to over 50 kilometers in length. These grids were used to construct three-dimensional models for each separate slope cutting in order to see the propagation of the karstic features in space. A study was made where several different variants of the 2D profile line distribu-

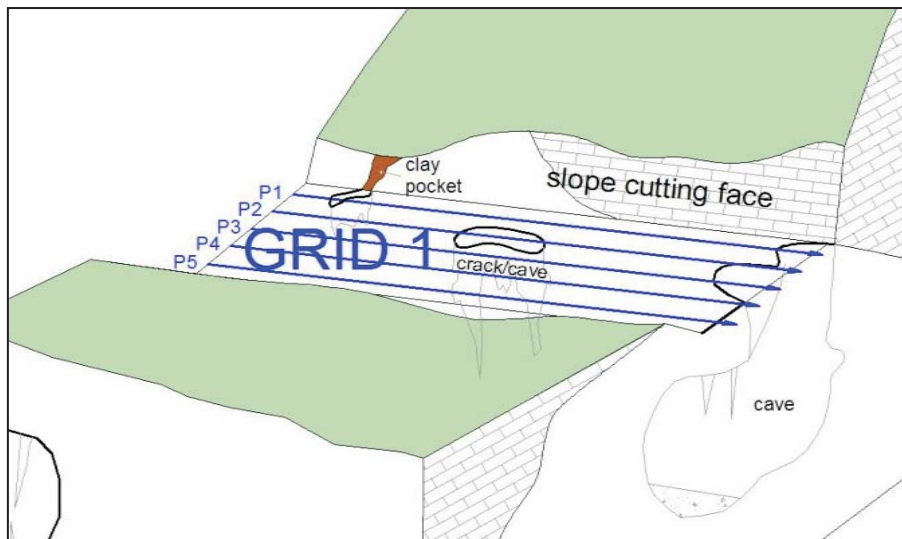


Figure 5. GPR survey in the slope cutting on the planum of highway.

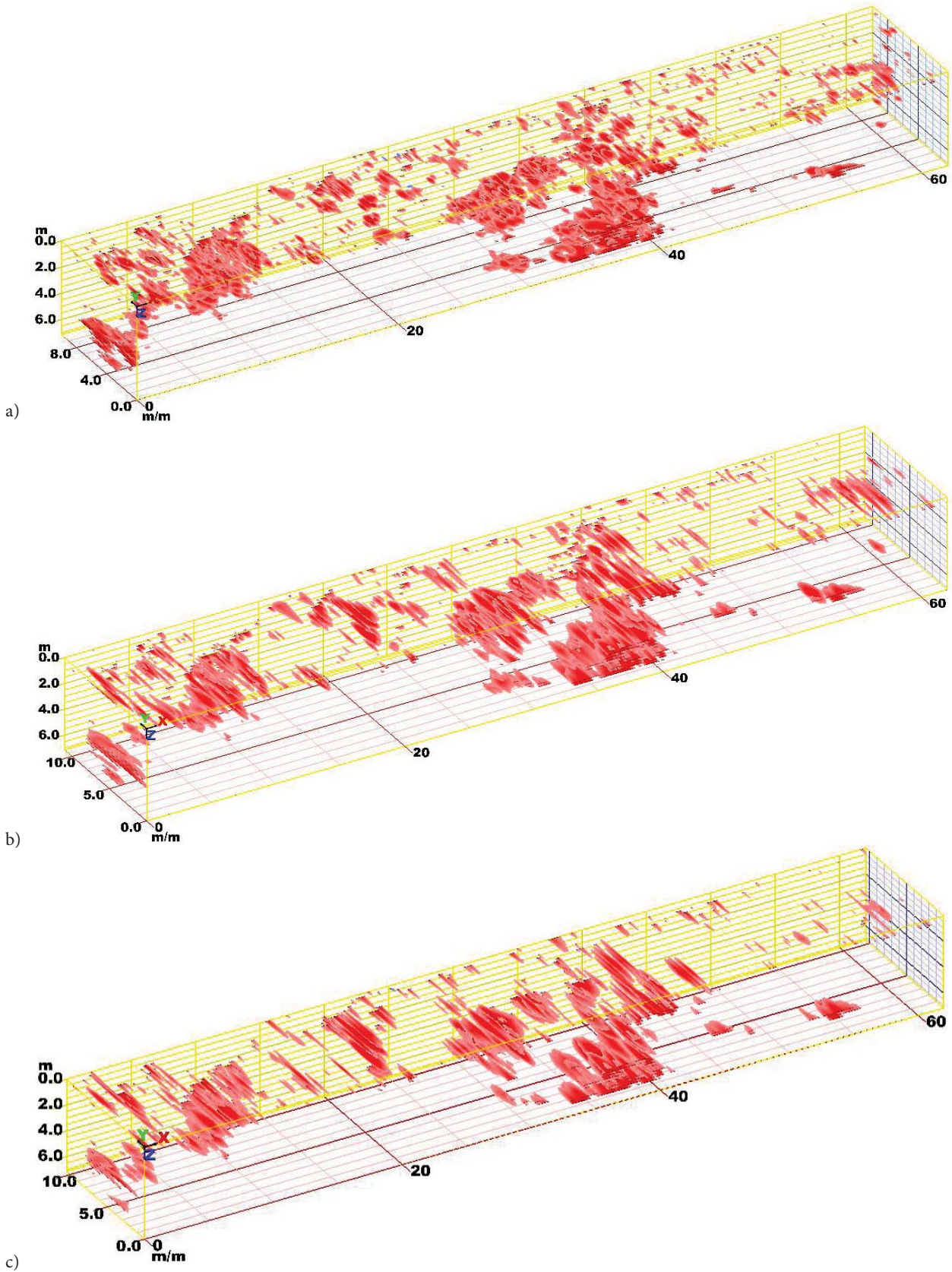


Figure 6. Feature resolution with a) 1 meter spacing between 2D profiles, b) 2.5 meter spacing between profile lines and c) 4 meter spacing between profile lines.

tion in a raster were used in order to sufficiently map all the geotechnical important forms. Figure 6 shows the resolution of 3D models created in the same area with different spacings between the profile lines, where in (a) the spacing between the 2D profile line is 1 meter and in (b) the spacing between the two profile lines is 2.5 meters and in (c) the spacing is 4 meters.

In the conducted survey a 200-MHz antenna was used as a compromise between the resolution and the desired depth for the research. The geotechnical conditions to be met required researching the ground to a depth of around 7 meters under road construction in order to be sure that the stability of the road structure was not compromised. A range of 170 nsec into the subsurface was reached with selected antenna which, with the average dielectric constant of media 12.7, amounted to approximately 7.5 meters of depth. The average dielectric constant was obtained from a hyperbola analysis, which gave a speed for the EM waves of approximately 8.4 cm/nsec. For the distance calibration a GSSI survey wheel was used in order to accurately measure the distance, while simultaneously charging electric pulses into the ground. An electromagnetic pulse was charged every two centimeters in the ground as 50 scans per meter were used. With this set up, a theoretical horizontal resolution by means of the first Fresnel zone gives a value of approximately 1.5 meter [12] [17] at a depth of 6 meters. These values are a mathematical approximation and can vary in real conditions. The horizontal resolution represents the distance at which two different objects with similar electromagnetic properties could be distinguished. The vertical resolution with a 200-MHz antenna used was approximately 10 cm.

As GPR is a contrast method of different reflections between the electromagnetically different media, there is no sure way of knowing that the reflection seen in the radargram is a consequence of dry clay to wet clay or from limestone to wet clay. Assumptions for the type of karstic features below were made based on the analysis of radargrams, "a priori" geological knowledge of the surveyed terrain and the geometrical shapes of the anomalies.

In order to confirm our assumptions, drilling was conducted to confirm whether the recorded reflection occurred on the border between limestone and an empty void or limestone and a clay-filled void. Based on geological knowledge of the terrain and the actual open slope cuttings, different types of media were not expected.

Over 15 boreholes up to 10 meters deep were drilled on several previously decided locations. The data obtained from drilling proved to be very helpful with the calibration since the anomalies found during drilling were almost exclusively (over 95%) a result of the propagation

of radar waves from the limestone to an air void or from limestone to a clay pocket.

After the calibration was complete, several more boreholes were drilled in order to confirm our calibrations of the radar reflections. From 18 interpretations (reflection on a radargram later tested with boreholes) 14 were accurate (which means if the interpretation was a clay pocket, a clay pocket was confirmed with drilling). At the other 4 locations where the interpretations were not completely accurate it was the case where voids were partly filled with clay and partly empty (air filled). The reason why our interpretations were not correct is because the dimensions of the clay part and the void part were smaller than the vertical and/or horizontal resolution.

Drilling proved to be a very helpful tool for the calibration of GPR anomalies recorded in 2D radargrams. Over 77 % of the tested reflections were correctly interpreted as voids or clay pockets and others were combinations of partly clay-filled and partly air-filled voids with small dimensions.

The number of test boreholes needed for successful detections can vary significantly from the type of subsurface in the survey. In our case the geology was karstic limestone with more or less repetitive features throughout the surveyed area. For that reason, very low numbers of boreholes were needed for a successful calibration.

GSSI RADAN 6.6 software was used for the processing of the ground-penetrating radar profiles. The processing flow used included a zero time correction, an infinite impulse response filter (band-pass filter for removing high and low frequencies), stacking, stretching, background removal and Kirchhoff migration for the geometry correction and the time-depth conversion. A topographic correction was not applied to any of the acquired profiles because the surveyed area was almost perfectly horizontal. According to Lehman and Green [11], topographic corrections should be considered in regions with surface gradients that are greater than 10% or the slope angle is higher than 6°.

5 KARSTIC FEATURES REVEALED

During the GPR survey several different karstic and geological features were revealed. Among them, small karstic caves, karstification between sedimentary layers, clayey areas, clay-filled cracks and abysses, water-rinsed (empty) cracks and several different variations of the mentioned forms. The main goal of our survey was to find areas and features that could be potentially hazardous to the stability of the road structure. The different structures found and confirmed with test drilling are shown.

Some examples of different karstic features that were revealed and tested with experimental drilling are shown. After several experimental boreholes, the reflections from the radar signal were better understood. Anomalies where the first reflections were negative were determined as cavities and anomalies, and where the first reflections were positive they were set as clayey and silty areas. These reflections were combined together with a knowledge of the geology of the area to map hazardous areas in each slope cutting.

On the left-hand side of Figure 7, typical anomalies encountered when doing GPR measurements in karst are shown. The anomalies represent two fracture sets oriented at an angle to one another. Because of the stress-strain dynamics, fractures usually evolve in almost perpendicular directions (i.e., a conjugate system). With that and because the fractures are a medium in which water is moving relatively fast, some fractures become wider and partly filled with clay. Areas where both fractures interfere are usually a place where karstic cavities occur. The middle of Figure 7 shows the EM polarities (i.e., the reflection coefficient) diagram of an anomaly where a red vertical line is presented. The first strongest reflection on the diagram is negative, which means that the EM wave progressed from a material with a higher dielectric constant to a material with a lower dielectric constant (as in the case of a limestone-to-air border). The results obtained during the experimental drilling served us as a calibration tool so that we could be certain that the anomaly in question is a cavity. On the right-hand side of Figure 7 we combined the radargram and the 3D anomalies that we obtained from Radan 6.6. The figure shows the propagation of an anomaly through the measured raster.

Figure 8 shows another feature common to karst regions and that is easily identified with GPR prospecting, i.e., delineation due to sedimentary layering. Limestone

layers of different thickness are usually karstified on the contacts. Karstification occurs in different ways. In Figure 8 the first anomaly (the red line and the polarity diagram with index 1) shows a small cavity on the part of the sedimentary layer. The dimension of this cavity is small (smaller than 0.5 m). The polarity diagram with index 2 shows layering with crevasses of small dimensions. All the peaks in the polar diagram with index 2 start towards positive, which means that these karstified crevasses between the layers are filled with clay. A 3D view of such an example is shown in the lower part of Figure 8.

Left side of upper part (index 1) on Figure 8 represents a void (cavity) in between layers, the right part (index 2) is clay filled crevasses between layers. The upper part of the figure represents 2D radargram, the lower a 3D view of the measured raster.

Figure 9 shows a typical cavity signature with negative polarity when the signal crosses from the higher to the lower conductive layer. Strong and parallel horizontal reflections indicate the presence of homogenous media (air) with dimensions of approximately 1 x 1.5 m.

Other karstic and geological features can be seen in Figure 10. The left part of the picture shows an unfiltered (un-migrated) radargram with drafted features in it, while the right part of the figure shows filtered data with the time-depth migration of the same area. The karstic cave is seen in both radargrams with the corresponding scan (red vertical line) showing where the polarity of the reflection is negative. The radargram shows a fairly large upside-down funnel-shaped region with many strong horizontal reflections that start with a negative polarity. The experimental drilling showed that the cavities found in the researched area are usually partially filled with clay. The right part of Figure 10 shows migrated (corrected time depth and geometry) data in which we could assess the anomaly's dimensions. At a depth

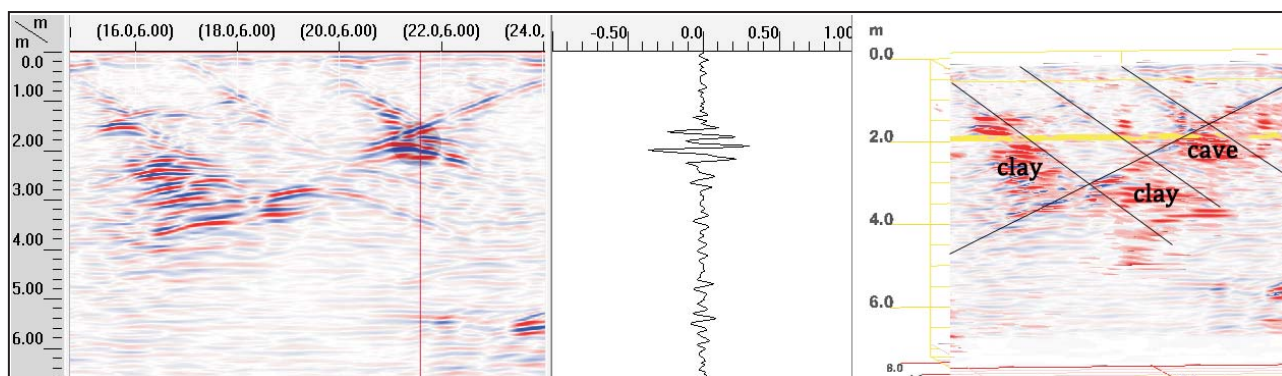


Figure 7. Conjugated system of fractures in limestone with small karstic cavity.

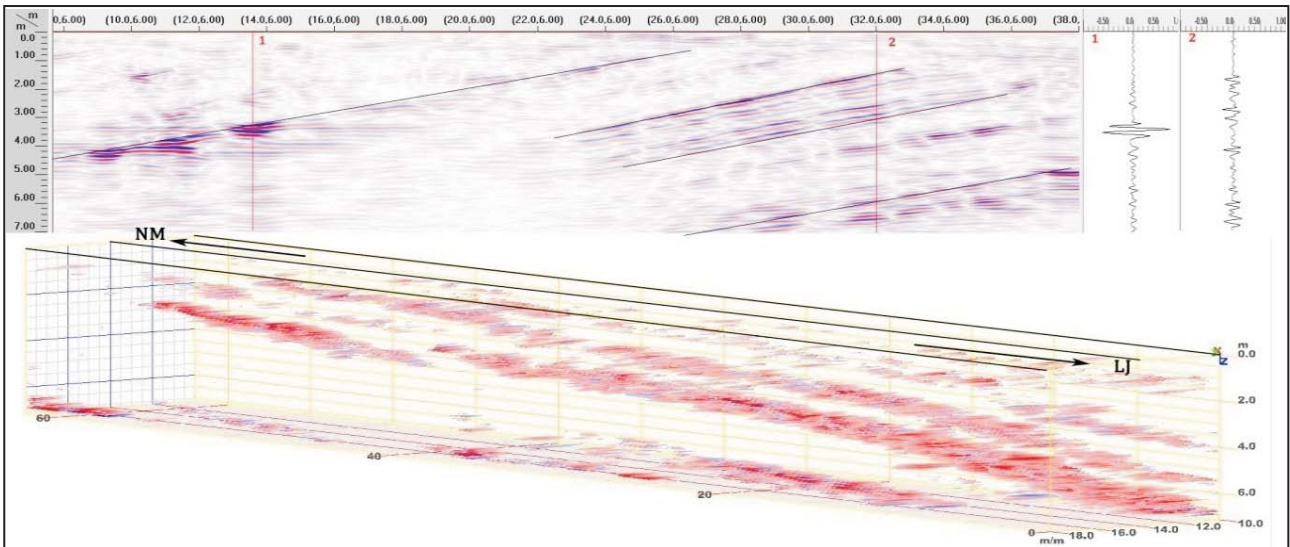


Figure 8. Delineation due to sedimentary layers and karstification of these crevasses.

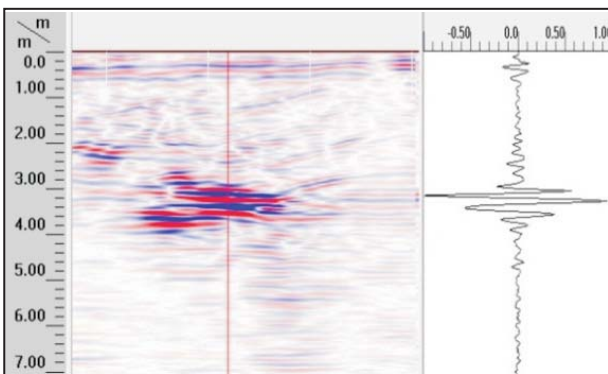


Figure 9. Reflections from a karstic cave of small dimensions at a depth of about 3 meters below the surface.

of approximately 2.2 meters a horizontal anomaly is seen where the water table was recorded (WT). The vertical band on the left side of Figure 10, where strong anomalies occur (electric cable), is due to the ringing effect when the radar signal passes through a highly conductive medium, i.e., an electric cable. The signal gets trapped between two reflectors and is multiplied in the way seen on Figure 10.

Figure 11 shows a strong anomaly where the GPR signal passes from the dry upper gravelly embankment material to the wet karstic clay. This anomaly was confirmed with an on-site excavation to assess the potential danger to the road construction.

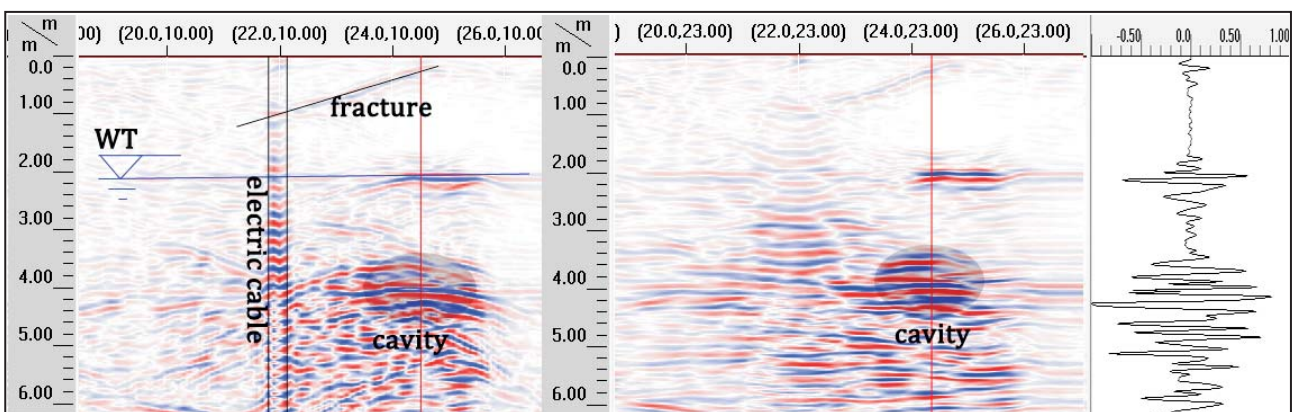


Figure 10. Several karstic and geological features acquired with ground-penetrating radar in the subsurface.

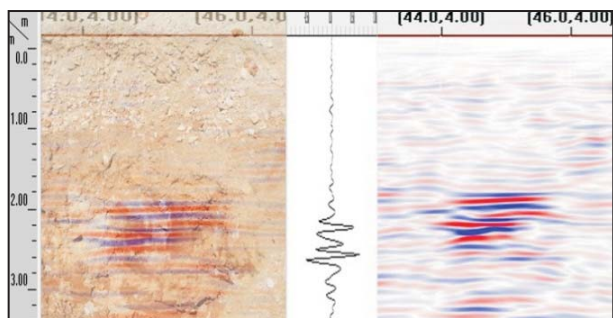


Figure 11. Wet karstic clay reflections.

6 CONCLUSIONS

Ground-penetrating radar proved to be a very effective method for determining the karstic features and other geological phenomena that could undermine the stability of a construction. Nevertheless, a great deal of effort should be made to effectively choose the right equipment and raster for the desired job. The antenna-resolution relation with the electrical properties of the subsurface should be closely studied in order to get the desired results. Also, the distribution of the GPR profiles in the measured raster is very important to effectively map the progression of potentially hazardous karstic features in space.

Initially, the survey was started on a very dense raster (1m between 2D profiles), which was very expensive and time consuming (three hours to record 60 meters of length). After several areas were studied and a study was made using several different distances between the GPR lines, a conclusion was made to increase the distance between the radargrams from 1 meter to 2 meters. This was the optimum distance for a given geology in order to retain the needed resolution and be time effective. Ultimately, the 3D model for each slope cutting was constructed from 2D lines which were geo-referenced to show the GPR anomaly distribution in space.

As GPR is a contrast method of different reflections between the electromagnetically different media, there is no sure way of knowing that a reflection seen in a radargram is a consequence of dry clay to wet clay or from limestone to wet clay. Assumptions for the type of karstic features below were made on the basis of an analysis of radargrams, "a priori" geological knowledge of the surveyed terrain and the geometrical shapes of the anomalies.

Drilling was conducted twice, first to calibrate the radargram reflections and secondly to check and confirm the calibration success. Altogether, over 30 boreholes were

drilled at different previously selected locations. The data obtained from drilling proved to be very helpful with a calibration since the anomalies found during drilling were almost exclusively (over 95%) a result of the propagation of radar waves from limestone to an air void or limestone to a clay pocket.

Drilling proved to be a very helpful tool for the calibration of GPR anomalies recorded in 2D radargrams. Over 77 % of the tested reflections were correctly interpreted as voids or clay pockets and others were combinations of partly clay-filled and partly air-filled voids of small dimensions.

GPR has proven to be a very cost-effective and reliable method for determining karstic features that could compromise the stability of the road. Taking in consideration that almost 100,000 m² of area was surveyed, it is also very time effective as it is almost impossible to survey an area this big with any other field method (boreholes, DPSH, SPT, etc.) to an accuracy obtained with GPR. A quick estimate is: in order to get roughly the same research coverage that a GPR survey offers, around 700 meters of boreholes should be drilled per 60 meters length of highway lane (60 meters in length x 9 meters width). Taking this into account the price ratio is around 1:5 to 1:10 for the GPR survey.

While the GPR method is very effective and it is in some cases possible to accurately predict the type of anomaly, on the other hand, this is not necessarily true in others cases, where the presence of changes in EM anomalies and the GPR reflections in the subsoil can be related to the variation of other physical properties (porosity, density, saturation, etc.).

In the presented article GPR prospecting was used side-by-side with the construction of the road. Even though in such an approach some logistical and operational problems occur, it is the most economical way to research the area. GPR surveying was done together with experimental drilling and excavations to calibrate the obtained reflections. With the side-by-side approach all heavy machinery is available so that experimental drillings or excavations are easily done and affordable.

Even though GPR is a very efficient method for karst surveying, there are some restrictions. One of the biggest restraints is that usually there is a considerable amount of clay soil, which greatly attenuates the GPR waves. One other thing that is common to the karstic world and poses a problem for a successful GPR survey is an uneven surface. In order for a GPR survey to be successful, all these restrictions have to be closely examined and studied so that the optimal equipment and measurement plan can be chosen.

ACKNOWLEDGMENTS

The authors would like to thank the investors DARS and the contractor SCT d.d. for their good cooperation in conducting a survey and helping with all the logistical problems.

REFERENCES

- [1] Daniels, D. J., Ground Penetrating Radar (2nd Edition). Institution of Engineering and Technology. On-line (2010), http://knovel.com/web/portal/browse/display?EXT_KNOVEL_DISPLAY_bookid=1244&VerticalID=0
- [2] Gherig M. D., Morris D. V., Bryant J. T., (2004). Ground penetrating radar for concrete evaluation studies, on-line (2010). http://www.foundation-performance.org/pastpresentations/gehrig_paper_march2004.pdf.
- [3] Kathnage A., (2008)+., SIR 3000 Training notes, Internal reference.
- [4] Knez M., Slabe T. (2004a). Karstology and the opening of caves during motorways construction in the karst region of Slovenia. *Int. J. Speleology*, 31(1/4), p. 159 – 168.
- [5] Knez M., Šebela S. (1994). Novo odkriti kraški pojavi na trasi avtomobilske ceste pri Divači, *Naše jame*, 36/102.
- [6] Knez M., Slabe T. (2001). Karstology and expressway construction. *Proceedings of 14th IRF Road World Congress*, Paris.
- [7] Knez M., Slabe T. (2004b). Highways on karst. In: Gunn J. (ed): *Encyclopedia of caves and karst science*. Fitzroy Dearborn, New York, London, p. 419-420.
- [8] Knez M., Slabe T. (2005). Caves and sinkholes in motorway construction, Slovenia. In: Waltham T F, Bell M, Cullshaw (eds); *Sinkholes and subsidence: karst and cavernous rocks in engineering and construction*. Springer, Berlin, p. 283 – 288.
- [9] Knez M., Slabe T., Šebela S., Grabrovšek F. (2007). The largest cave discovered in a tunnel during motorway construction in Slovenia's classical Karst, *Environmental Geology*, vol. 54, p. 711-718, SpringerLink.
- [10] Komel P., Pavlič M. U., (2008). Uporaba georadarja v geotehniki, geologiji in gradbeništvu ob praktičnih primerih - Ground penetrating radar use in geotechnics, geology and civil engineering on case studies. V: LOGAR, Janko (ur.), PETKOVŠEK, Ana (ur.). *Razprave petega posvetovanja slovenskih geoteknikov, Nova Gorica 2008, Nova Gorica, 12. do 14. junij 2008*. Ljubljana: Slovensko geotehniško društvo, 2008, p. 143-153.
- [11] Lehmann F., Green A. G., (2000). Topographic migration of georadar data: Implications for acquisition and processing. *Geophysics* 65(3): p. 836–848.
- [12] Reynolds J. M. (1997). *An introduction to applied and environmental geophysics*. Wiley, Chichester.
- [13] Šebela S., Mihevc A., (1999). The vulnerability map of karst along highways in Slovenia. In: Beck B F, Petit A J, Herring J G (eds): *Hydrogeology and engineering geology of dolines and karst – 1999. Proceedings of the 7th multidisciplinary conference on dolines and the engineering and environmental impacts on Karst*. A A Balkena, Rotterdam, p. 419 – 422.
- [14] Živanovič M., (2003a). Poročilo o georadarskih meritvah na območju vdorov vozišča na AC odseku Unec – Postojna, internal report GI ZRMK d.o.o.
- [15] Živanovič M., (2003b). Primeri uporabe georadarskih raziskav v različnih kamninah: *Geološki zbornik-razprave, poročila. 16. posvetovanje slovenskih geologov*. Ljubljana: Naravoslovnotehniška fakulteta, Oddelek za geologijo, 2003, p. 181-186.
- [16] Daniels J. D., (2004), *Ground penetrating radar*, 2nd edition, 726p.
- [17] Wikipedia on-line, (2010), http://en.wikipedia.org/wiki/Fresnel_zone
- [18] Knez, M. (ed), Slabe, T. (ed), (2007). *Kraški pojavi razkriti med gradnjo slovenskih avtocest*, (Carso-logica, 7), Ljubljana: Založba ZRC SAZU, p. 250.

ZDRUŽEN TERMO-HIDRO-MEHANIČNI MODEL NABREKLJIVIH GLIN, PODVRŽENIH SEGREVANJU IN HIDRACIJI

NADIA LAREDJ, HANIFI MISSOUM, KARIM BENDANI IN MUSTAPHA MALIKI

o avtorjih

vodilni avtor

Nadia Laredj

Université Abdelhamid Ibn Badis de Mostaganem,
Construction, Transport and Protection of the Environment laboratory
D28 . A5. Rue Benanteur Charef, CP°27000, Mostaganem, Alžirija
E-pošta: nad27000@yahoo.fr

Hanifi Missoum

Université Abdelhamid Ibn Badis de Mostaganem,
Construction, Transport and Protection of the Environment laboratory(LCTPE)
BP°227, Route Belhacel, CP°27000, Mostaganem, Alžirija
E-pošta: hanifimissoum@yahoo.fr

Karim Bendani

Université Abdelhamid Ibn Badis de Mostaganem,
Construction, Transport and Protection of the Environment laboratory(LCTPE)
BP°227, Route Belhacel, CP°27000, Mostaganem, Alžirija
E-pošta: kbendani@yahoo.fr

Mustapha Maliki

Université Abdelhamid Ibn Badis de Mostaganem,
Construction, Transport and Protection of the Environment laboratory(LCTPE)
12. Bâtiment F, Cité Yasmine, zone CIA, CP°27000, Mostaganem, Alžirija
E-pošta: mus27000@yahoo.fr

izvleček

Članek prikazuje numerično formulacijo združenega termo-hidro-mehanskega procesa v nenasičeni nabrekli glini, posebej v kompaktnem bentonitu z dodajanjem tekočine v več fazah. Za model je značilna prisotnost deformabilne trdne snovi, napolnjene s tekočo vodo in zrakom. Predpostavlja se, da na pretoka porne vode in zraka vpliva posplošen Darcyjev zakon.

Vpeljane nelinearne parcialne diferencialne enačbe so popolnoma vezane in jih rešimo z uporabo Galerkin-ega pristopa - utežnih ostankov v prostorski domeni in implicitno integracijsko shemo v časovni domeni. Model smo primerjali z eksperimentalnim preizkusom iz literature, ki vključuje preizkus bentonita v laboratorijskih pogojih. Izračunane relativne napake med eksperimentalnimi in numeričnimi rezultati so 3% za temperaturo in 7% za napetosti. Podan numerični model napoveduje zadovoljive rezultate glede na rezultate eksperimentalnih meritev. Model lahko uporabimo pri dvodimenzionalnih problemih z različnimi začetnimi in robnimi pogoji, v ta model zlahka vključimo nelinearne parametre zemljine.

ključne besede

termo-hidro-mehanski proces, nenasičen betonit, končni element, numerično modeliranje, nabreklije glin

A COUPLED THERMO-HYDRO-MECHANICAL MODEL OF EXPANSIVE CLAYS SUBJECTED TO HEATING AND HYDRATATION

NADIA LAREDJ, HANIFI MISSOUM, KARIM BENDANI AND MUSTAPHA MALIKI

about the authors

corresponding author

Nadia Laredj
Université Abdelhamid Ibn Badis de Mostaganem,
Construction, Transport and Protection of the Environment laboratory
D28 . A5. Rue Benanteur Charef, CP°27000, Mostaganem, Algeria
E-mail: nad27000@yahoo.fr

Hanifi Missoum
Université Abdelhamid Ibn Badis de Mostaganem,
Construction, Transport and Protection of the Environment laboratory
BP°227, Route Belhacel, CP°27000, Mostaganem, Algeria
E-mail: hanifimissoum@yahoo.fr

Karim Bendani
Université Abdelhamid Ibn Badis de Mostaganem,
Construction, Transport and Protection of the Environment laboratory
BP°227, Route Belhacel, CP°27000, Mostaganem, Algeria
E-mail: kbendani@yahoo.fr

Mustapha Maliki
Université Abdelhamid Ibn Badis de Mostaganem,
Construction, Transport and Protection of the Environment laboratory
12. Bâtiment F, Cité Yasmine, zone CIA, CP°27000, Mostaganem, Algeria
E-mail: mus27000@yahoo.fr

abstract

The focus of this work is to provide a numerical formulation for coupled thermo-hydro-mechanical processes in unsaturated expansive clays, especially in compacted bentonite, with a multiphase fluid flow. The model is characterized by the presence of a deformable solid matrix filled with two fluid phases (liquid water and air). In the proposed model, both pore-water and air transfers are assumed to be governed by the generalized Darcy's law. Fully coupled, nonlinear partial differential equations are established and then solved by using a Galerkin weighted residual approach in the space domain and an implicit integrating scheme in the time domain. The model has been validated against an experimental test from the literature, which involves bentonite under laboratory conditions. The calculated relative errors between the experimental and numerical results are 3% for the temperature and 7% for the stresses. Consequently, the developed numerical model predicts satisfactory

results, when compared to the experimental test measures. The model is applicable to two-dimensional problems with various initial and boundary conditions; non linear soil parameters can be easily included in this model.

keywords

thermo-hydro-mechanical process, unsaturated bentonite, finite element, numerical modelling, expansive clays

1 INTRODUCTION

The thermo-hydro-mechanical modelling of a partially saturated soil considered as a multiphase porous medium composed of a deformable solid skeleton and fluid phases filling the pore spaces of the soil is of great interest in widely different fields of engineering. This article specifically focuses on unsaturated swelling clays, which are widely distributed in nature. In agriculture, water adsorption by the clay determines the ability of the soils to transport and supply the water and nutrients. Compacted bentonites play a critical role in various high-level, nuclear-waste isolation scenarios and in barriers for commercial landfills [1, 2]. In engineering and construction the swelling and compaction of clayey soils induce stresses that are very troublesome in the foundations and structures of buildings. The engineering behaviour of unsaturated soil has been the subject of numerous experimental and theoretical investigations [3-8].

In recent years, the coupled thermo-hydro-mechanical behaviour in porous media has been a subject of great importance in many engineering disciplines. Many mathematical models in the literature were proposed for fully saturated conditions [9-12], whereas few numerical approaches have been reported regarding the partially saturated porous materials [13-18]. These models are generally based on typical simplifying assumptions, such as the rigid soil skeleton (no solid deformation) [19],

the static gas phase (no gas flow) [14, 16, 17, 20] and the quasi-static condition [14, 16, 17, 20], which are in contrast to the physics of the problem in many situations. A more commonly used formulation consists of a one-phase flow model where it is assumed that the flow of gas is negligible, and the gas phase remains constantly at the ambient external atmospheric pressure through the partially saturated soil [14-17]. Therefore, the continuity equation of the gas flow is ignored. Another problem is that the porosity is often considered as a constant or a simple function of bulk strain [21, 22].

In the present paper, the above-mentioned simplifying assumptions are excluded from the numerical model, and a fully coupled formulation is presented to simulate the behaviour of the partially saturated clays. In the model, the pore-water and pore-air transfers are assumed to be governed by the generalized Darcy's law. The fully coupled, nonlinear, partial differential equations are established and then solved by using a Galerkin weighted residual approach in the space domain and an implicit integrating scheme in the time domain. The obtained model was finally validated by means of some case tests for the prediction of the thermo-hydro-mechanical behaviour of unsaturated swelling soils.

2 THEORETICAL FORMULATION

In this work a three-phase porous material consisting of solid, liquid and air requires is considered. A set of coupled governing differential equations are presented below to describe the coupled multiphase flow in the soil. The model is based on combinations of equations or derivations from conservation principles and the classical laws of known physical phenomena for coupled flow. The governing differential equations for pore water pore air and heat transfer in unsaturated soil are derived as follows:

2.1 HEAT TRANSFER

Considering heat transfer by means of conduction, convection and the latent heat of vaporisation effects, and applying the principle of the conservation of energy, the following equation is derived:

$$\frac{\partial \phi}{\partial t} = -\nabla \cdot Q \quad (1)$$

where ϕ is the heat content of the soil and Q is the total heat flux, defined as:

$$Q = -\lambda_T \nabla T - (v_v \rho_v + v_a \rho_a) L + (C_{pl} v_l \rho_l + C_{pv} v_v \rho_v + C_{pa} v_a \rho_a) (T - T_r) \quad (2)$$

$$\phi = H_c (T - T_r) + Ln S_a \rho_v \quad (3)$$

where H_c is the specific heat capacity of the soil, T is the temperature, T_r is the reference temperature, L is the latent heat of vaporization of the soil water, C_{pl} , C_{pv} and C_{pa} are the specific heat capacities of the soil water, the soil vapour and the soil dry air, respectively, and λ_T is the coefficient of the thermal conductivity of the soil.

Three modes of heat transfer are included: thermal conduction, sensible heat transfer associated with the liquid, vapour and air flow and latent heat flow with vapour.

2.2 MOISTURE TRANSFER

For the moisture transfer, the mass-transfer balance equation, accommodating both liquid and vapour, can be expressed as:

$$\frac{\partial(\rho_l n S_l)}{\partial t} + \frac{\partial(\rho_v n(S_l - 1))}{\partial t} = -\rho_l \nabla \cdot v_l - \rho_l \nabla \cdot v_v - \rho_v \nabla \cdot v_a \quad (4)$$

where n is the porosity, ρ is the density, S_l is the degree of saturation, t is the time and v is the velocity. The subscripts l , a and v refer to the liquid, air and water vapour, respectively.

In this simulation, a generalized Darcy's law is used to describe the velocities of the pore water and air:

$$v_l = -\frac{K_l}{\gamma_l} (\nabla u_l + \gamma_l \nabla z) \quad (5)$$

$$v_a = -K_a \nabla \left(\frac{u_a}{\gamma_a} \right) \quad (6)$$

where K_l and K_a are the hydraulic conductivities of the liquid and air, respectively, γ_l is the unit weight of the liquid, γ_a is the unit weight of the air, u_l is the pore water pressure, u_a is the pore air pressure, z is the elevation and ∇ is the gradient operator.

The hydraulic conductivities of the water and air through the soil may be expressed in terms of the saturation degree or water content, as follows:

$$K_l = K_l(S) \quad (7)$$

$$K_a = K_a(S_l, \eta_a) \quad (8)$$

where η_a is the dynamic viscosity of the air.

The water-vapour density ρ_v is evaluated from the thermodynamic assumptions, and when the liquid and vapour phases are in equilibrium, it can be evaluated with the following relationship [23]:

$$\rho_v = \rho_0 \cdot h_t \quad (9)$$

where h_t is the total relative humidity calculated by the following expression:

$$h_t = \exp\left(\frac{u_l - u_a}{\rho_l R_v T}\right) \quad (10)$$

and ρ_0 is the total saturated water vapour defined as [23]:

$$\rho_0 = \left[194.4 \exp(-0.06374(T - 273) + 0.1634 \cdot 10^3 (T - 273)^2)\right]^{-1} \quad (11)$$

where R_v is the gas constant for water vapour and T is the temperature.

2.3 PORE AIR MASS TRANSFER

Using Henry's law to take account of the dissolved air in the pore water, the following equation is derived for the dry air phase from the principle of mass conservation:

$$\frac{\partial [n\rho_a(S_a + HS_l)]}{\partial t} = -\nabla \cdot [\rho_a(v_a + Hv_l)] \quad (12)$$

where, H is Henry's volumetric coefficient of solubility and ρ_a is the dry air density.

The dry air density ρ_a can be evaluated from Dalton's law as:

$$\rho_a = \frac{u_a}{RT} - \frac{R_v}{R} \rho_v \quad (13)$$

R and R_v are the gas constants for the dry air and the water vapour respectively, and T is the temperature.

2.4 CONSTITUTIVE STRESS-STRAIN RELATIONSHIP

For problems in unsaturated swelling porous media the total strain ε is assumed to consist of components due to the suction, temperature and stress changes. This can be given in an incremental form as:

$$d\varepsilon = d\varepsilon_\sigma + d\varepsilon_s + d\varepsilon_T \quad (14)$$

where the subscripts σ , s and T refer to the net stress, suction and temperature contributions.

The stress-strain relationship can, therefore, be expressed as:

$$d\sigma'' = D(d\varepsilon - d\varepsilon_s - d\varepsilon_T) \quad (15)$$

where:

$$[\sigma''] = [\sigma_x \ \sigma_y \ \sigma_z \ \tau_{xy} \ \tau_{yz} \ \tau_{xz}] \quad (16)$$

where σ'' is the net stress and D is the elastic matrix. A number of constitutive relationships can be employed, for example, an elasto-plastic constitutive relationship [24].

2.5 COUPLED EQUATIONS

This leads to a set of coupled, non-linear differential equations, which can be expressed in terms of the primary variables T , u_l , u_a and u of the model as the energy balance:

$$C_{Tl} \frac{\partial u_l}{\partial t} + C_{TT} \frac{\partial T}{\partial t} + C_{Ta} \frac{\partial u_a}{\partial t} + C_{Tu} \frac{\partial u}{\partial t} = \nabla [K_{Tl} \nabla u_l] + [K_{TT} \nabla T] + [K_{Ta} \nabla u_a] + J_T \quad (17)$$

the mass balance:

$$C_{ul} \frac{\partial u_l}{\partial t} + C_{uT} \frac{\partial T}{\partial t} + C_{ua} \frac{\partial u_a}{\partial t} + C_{uu} \frac{\partial u}{\partial t} = \nabla [K_{ul} \nabla u_l] + [K_{uT} \nabla T] + [K_{ua} \nabla u_a] + J_l \quad (18)$$

$$C_{al} \frac{\partial u_l}{\partial t} + C_{aT} \frac{\partial T}{\partial t} + C_{aa} \frac{\partial u_a}{\partial t} + C_{au} \frac{\partial u}{\partial t} = \nabla [K_{al} \nabla u_l] + [K_{aa} \nabla u_a] + J_a \quad (19)$$

the stress equilibrium:

$$C_{ul} du_l + C_{uT} du_T + C_{ua} du_a + C_{uu} du + db = 0 \quad (20)$$

where K_{ij} and C_{ij} represent the corresponding terms of the governing equations ($i, j = l, T, a, u$)

3 DISCRETIZATION TECHNIQUES

The numerical solution of the theoretical models commonly used in geo-environmental problems is often achieved by a combination of numerical discretization techniques. For the example presented in this paper, the finite-element method was employed for the spatial discretization and a finite-difference time-stepping scheme for temporal discretization.

In particular, the Galerkin weighted residual method [25] is used to formulate the finite-element discretization. An implicit, mid-interval backward difference algorithm is implemented to achieve the temporal discretization, since it has been found to provide a stable solution for highly non-linear problems [26]. With the appropriate initial and boundary conditions, the set of typically non-linear coupled partial differential equations can be solved.

Applying a Galerkin formulation for the finite-element method we obtain a system of matrix equations, as follows:

$$[K]\{\varphi\} + [C]\{\dot{\varphi}\} + \{J\} = 0 \quad (21)$$

where:

$$[K] = \begin{bmatrix} K_{TT} & K_{TI} & K_{Ta} & 0 \\ K_{TI} & K_{II} & K_{Ia} & 0 \\ 0 & K_{aI} & K_{aa} & 0 \\ 0 & 0 & 0 & 0 \end{bmatrix}, [C] = \begin{bmatrix} C_{TT} & C_{TI} & C_{Ta} & C_{Tu} \\ C_{TI} & C_{II} & C_{Ia} & C_{Iu} \\ C_{aT} & C_{aI} & C_{aa} & C_{au} \\ C_{uT} & C_{uI} & C_{ua} & C_{uu} \end{bmatrix} \quad (22)$$

$$\begin{aligned} \{\varphi\} &= (T \quad u_I \quad u_a \quad u)^T, \\ \{\dot{\varphi}\} &= \left(\frac{dT}{dt} \quad \frac{du_I}{dt} \quad \frac{du_a}{dt} \quad \frac{du}{dt} \right)^T, \\ \{J\} &= (J_T \quad J_I \quad J_a \quad J_u)^T \end{aligned} \quad (23)$$

To solve equation (21), a general form of fully implicit, mid-interval, backward difference, time-stepping algorithm is used to discretise the governing equation temporally. Therefore, equation (21) can be rewritten as:

$$\begin{aligned} K(\varphi^n)[1-\theta]\{\varphi^{n+1}\} + \theta\{\varphi^n\} + \\ + C(\varphi^n) \left[\frac{\{\varphi^{n+1}\} - \{\varphi^n\}}{\Delta t} \right] + J(\varphi^n) = \{0\} \end{aligned} \quad (24)$$

where (φ^n) is the level of time at which the matrices K , C and J are to be evaluated and is given by:

$$(\varphi^n) = \omega\{\varphi^{n+1}\} + (1-\omega)\{\varphi^n\} \quad (25)$$

where ω is the integration factor, which defines the required time interval ($\omega \in [0,1]$) and $\theta = 0, 0.5, 1$ for the backward, central and forward difference schemes, respectively.

For a mid-interval backward difference scheme, $\omega = 0.5$ and $\theta = 0$. Therefore, equation (24) reduces to:

$$\begin{aligned} K \left(\frac{\{\varphi^{n+1}\} + \{\varphi^n\}}{2} \right) \{\varphi^{n+1}\} + \\ + C \left(\frac{\{\varphi^{n+1}\} + \{\varphi^n\}}{2} \right) \left[\frac{\{\varphi^{n+1}\} - \{\varphi^n\}}{\Delta t} \right] + J \left(\frac{\{\varphi^{n+1}\} + \{\varphi^n\}}{2} \right) = \{0\} \end{aligned} \quad (26)$$

Eq. (26) can be rewritten as:

$$K^{n+0.5} \{\varphi^{n+1}\} + C^{n+0.5} \left(\frac{\{\varphi^{n+1}\} - \{\varphi^n\}}{\Delta t} \right) + J^{n+0.5} = \{0\} \quad (27)$$

A solution for $\{\varphi^{n+1}\}$ can be obtained, provided the matrices K , C and J at the time interval $(n + 0.5)$ can be determined. This is achieved by the use of a predictor-corrector iterative solution procedure.

4 APPLICATIONS AND RESULTS

4.1 EXAMPLE 1

4.1.1 PROBLEM DEFINITION

The following example is investigated to demonstrate the swelling pressure calculation by using the back hydro-mechanical model. The simulation begins with an isothermal two-phase flow coupled with deformation. A free extension is allowed at the first stage to calculate the free-extension displacement on the boundary. The geometric set-up and boundary conditions are as shown in Fig. 1. The example is a compacted bentonite block, 0.025 m in length and 0.024 m in height. The element discretization is $\Delta x = 0.00125\text{ m}$ and $\Delta y = 0.00124\text{ m}$, eight noded composed elements. The initial conditions of the system are: atmospheric air pressure and liquid saturation $S_l = 0.357$. A water solution enters the sample from the bottom under a pressure described by the curve in Fig. 2. The corresponding part on the boundary is fully saturated.

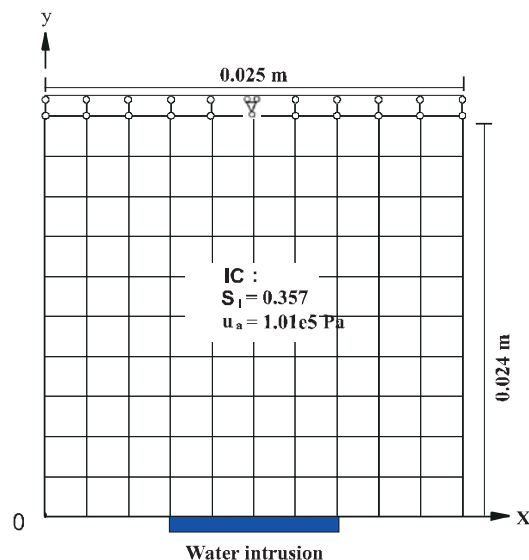


Figure 1. Model set-up of the example.

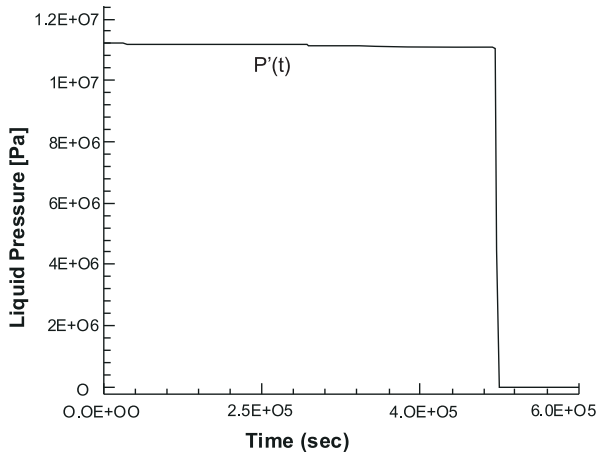


Figure 2. Curve of the liquid pressure on the boundary.

The material properties for this example are based on data in the literature [27, 28] and summarized in table 1. The deformation under free extension conditions is assumed to be non-linear elastic.

Table 1. Porous medium properties [27, 28].

Symbols	Functions and constants	Units
ρ_l	1000	kg/m ³
ρ_g	1.26	kg/m ³
ρ_s	1600	kg/m ³
S_t	$1 - 0.85[1 - \exp(-1.20 \times 10^{-7}(u_a - u_l))]$	
μ_l	1.20×10^{-3}	Pa s
μ_g	1.80×10^{-5}	Pa s
K_l	$\frac{1.2 \times 10^{-12}}{\mu_l[1 + 1.3 \times 10^{-10}(u_a - u_l)^{1.7}]}$	m/s
K_a	$1.3 \times 10^{-19} \frac{\gamma_a}{\mu_a} [e(1 - S_t)]^{3.0}$	m/s
n	0.37	
S_0	31.80	m ² /g
E	3.5	MPa
ν	0.3	
T_r	293	°K

4.1.2 RESULTS AND DISCUSSION

The simulation results of the free extension processes after 5.8×10^5 s (6.7 days) are shown in Fig. 3 and Fig. 4. With the intrusion of water from the bottom, the saturation process starts. This phenomenon can clearly be seen from the saturation evolution profile along the vertical symmetric axis (Fig. 3). At the early stage, the value of the

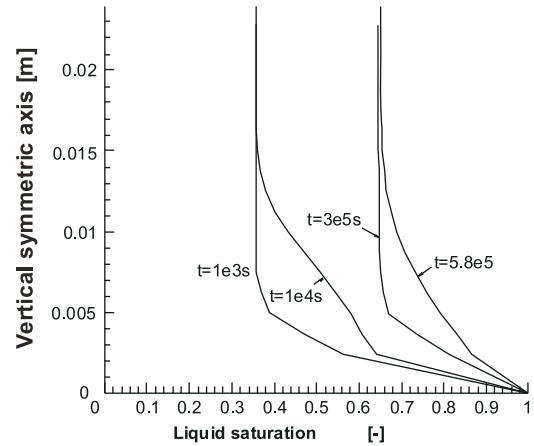


Figure 3. Computed profiles of liquid saturation along the vertical symmetric axis.

liquid saturation increases quite quickly. After 4.9×10^5 s (5.7 days) the liquid pressure on the bottom sinks at 5.0×10^5 s (5.8 days) and reaches zero. Because of the low permeability of the bentonite, the liquid pressure at the centre of the specimen sinks more slowly, which results in the higher-pressure region in the specimen after 6.7 days, as shown in Fig. 4 (a).

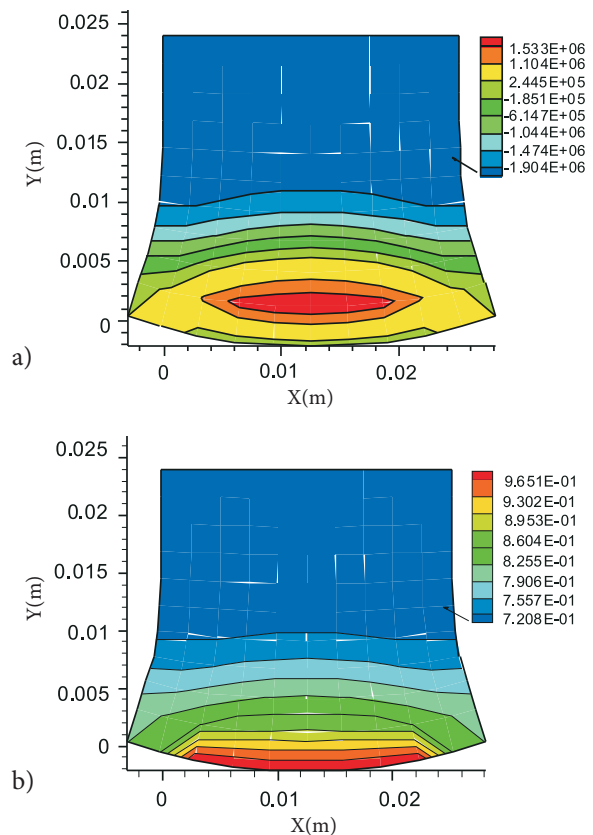


Figure 4. Simulation results of the free extension process a) Distribution of liquid pressure, b) Distribution of liquid saturation

With the intrusion of water, the sample begins to expand. After 6.7 days, the shape of the specimen should be as shown in fig. 5. The maximum width of the specimen increases by about 20% (Fig. 5). In this example, the experimental data from free swelling tests for compacted bentonites were used [27].

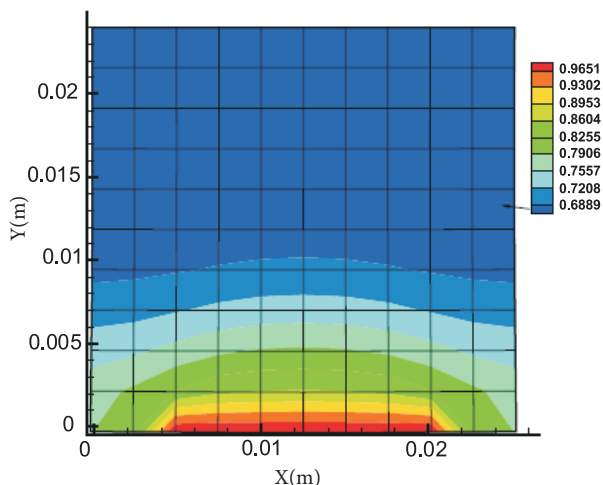


Figure 5. Simulated shape of the sample, and distribution of the liquid saturation for the material at $t = 5.8 \times 10^5$ s.

4.2 EXAMPLE 2

4.2.1 PROBLEM DEFINITION

The model was verified through simulating a test problem of bentonite tested in laboratory conditions [29]. The compacted bentonite is planned to be used to limit the flow velocity of groundwater in the near field of a geological repository for radioactive waste. The sample of bentonite has a height of 203 mm. To minimize the heat losses, the cell was insulated with a heat-proof envelope. Heat was applied at the bottom plate of the cylinder, while the temperature at the other end was kept constant and equal to 20 °C. A maximum temperature of 150 °C was applied. A constant water pressure was applied to the end opposite the end where the temperature variation was prescribed. Constant volume conditions were ensured in the test. The main variables that were measured during the test include the temperature, the relative humidity and the total axial stress. The model geometry is the same as the sample with a height equal to 203 mm. The temperature variation at the bottom end of the model is as specified during the test; it was raised in steps until it reached 150 °C. The temperature at the top end of the specimen was kept constant at 20 °C. The other surfaces are adiabatic.

According to the test procedure, the hydraulic boundary condition is impermeable for all surfaces of the model. The gas pressure is equal to the atmospheric pressure. The initial value of the porosity is 0.3242, the initial temperature is 20 °C, the initial gas pressure is 0.10132 MPa and the initial stress of the sample is 0.5 MPa. The initial values were obtained according to the measured data from experiments [28].

According to the measured data from the bentonite [29, 30, 31], the intrinsic permeability is $1.0 \times 10^{-21} \text{ m}^2$ and the specific heat capacity of the solids is 920 J/Kg.

4.2.2 RESULTS AND DISCUSSION

Fig. 6 shows a comparison between the measured temperatures as a function of time. At the bottom end of the sample, the measured and simulated temperatures agree well. At the top end of the sample, the simulation underestimates the temperature slightly at the initial heating stage, but trends generally agree well.

In this validation example, the calculated relative error percentage with respect to the temperature is 3%.

The good agreement between the simulated and measured temperature indicates that the model can simulate the thermal response of processes having high temperature gradients. The numerical simulation shows that the thermal conductivity of bentonite, treated as a multiphase material, plays an important role in the thermal response of the whole medium. The numerical results can be further improved if the effects of the material heterogeneity can be quantified during testing.

The simulated results of the vapour pressure are shown in Fig. 7. Although there are no measured results with which to compare, it shows that the variation of the vapour pressures is realistic.

The evolution of the axial stress was also reasonably well simulated (Fig. 8), in the trend, and the obtained relative error percentage is 7% for this validation. The numerical calculation shows that the results of stress strongly depend on the constitutive relationship between stress and strain. A more comprehensive development of the material properties is needed to further improve the numerical capability of the code. Complex boundary conditions for further work.

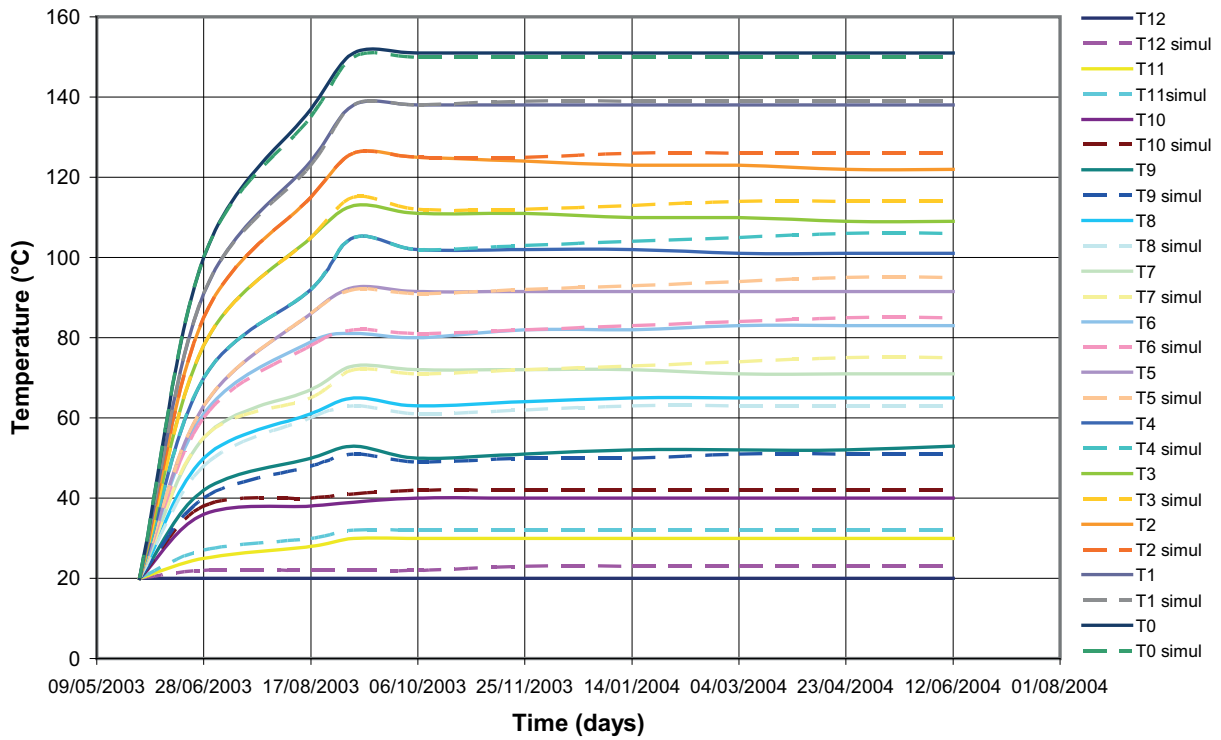


Figure 6. Comparison of results between the simulated and measured temperatures at different locations (heights) of the sample as a function of time.

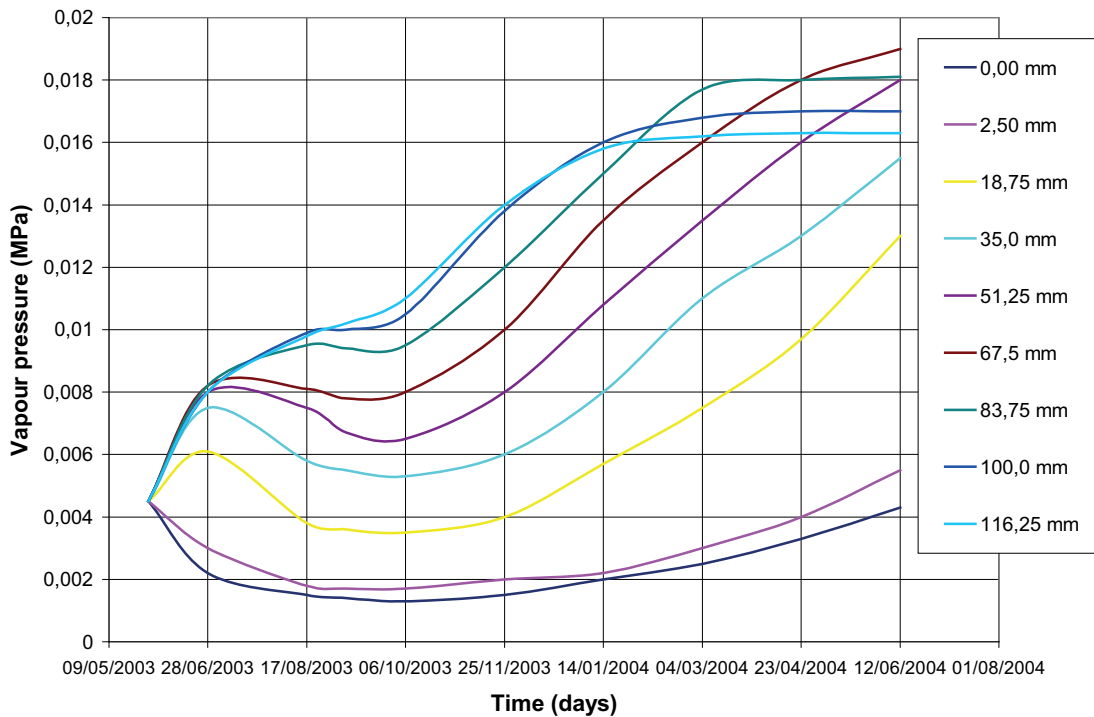


Figure 7. The simulated results of vapour pressure.

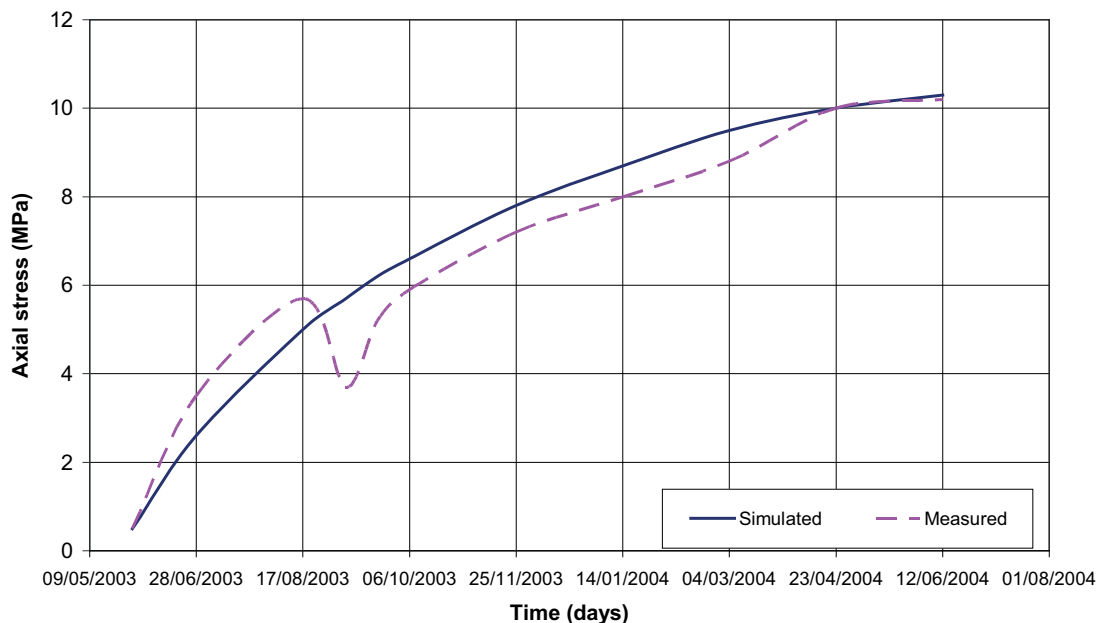


Figure 8. Comparison of the results between the simulated and measured axial stress.

5 CONCLUSION

A coupled thermo-hydro-mechanical model for a description of the behaviour of swelling porous media has been presented in this paper. A set of fully coupled, nonlinear, partial differential equations was established and then solved by using a Galerkin weighted residual approach in the space domain and using an implicit integrating scheme in the time domain. A range of simulation results was presented, detailing with the hydraulic and thermal behaviour of the expansive soil. The simulation results were compared with the experimentally measured results and it was shown that a good correlation was found in the hydraulic regime and a reasonable correlation in the thermal field. The results of the validations indicate that the model is general and suitable for the analyses of many different problems in unsaturated soils.

REFERENCES

- [1] Gens, A. and Olivella, S. (2001). Chemo-mechanical modelling of expansive materials. *6th International Workshop on Key Issues in Waste Isolation Research*. November, 2001. Paris (France). 463-495.
- [2] Andra (2005). Dossier argile. Evaluation de la faisabilité du stockage géologique en formation argileuse, *Rapport Andra C.RP.ADP.04.0002*.
- [3] Fredlund, D.G. and Morgenstern, N.R. (1977). Stress state variables for unsaturated soils. *J. Geotech. Engng. Div., ASCE* 103, N° 5, 447-466.
- [4] Alonso, E.E., Gens, A. and Josa, A. (1990). A constitutive model for partially saturated soils. *Geotechnique* 40, N° 3, 405-430.
- [5] Cui, J. and Delage, P. (1996). Yielding and plastic behaviour of an unsaturated compacted silt. *Geotechnique* 46, N° 2, 291-311.
- [6] Cui, Y.J., Yahia-Aissa, M. and Delage, P. (2002). A model for the volume change behaviour of heavily compacted swelling clays. *Engineering Geology* 64, N° 2, 233-250.
- [7] Fleureau, J.M., Verbrugge, J.C., Huergo, P.J., Correia, A.G. and Kheirbek Saoud, S. (2002). Aspects of the behaviour of compacted clayey soils on drying and wetting paths. *Can. Geotech. J.* 39, 1341-1357.
- [8] Saiyouri, N., Tessier D. and Hicher P.Y. (2004). Experimental study of swelling in unsaturated compacted clay, *Clay minerals*, 39, N° 4, 469-479.
- [9] Zienkiewicz, O.C., Chan, A.H.C., Pastor, M. and Paul, D.K. (1999). Static and dynamic behavior of soils: a rational approach to quantitative solution, I. Fully saturated problems, *Proc. Roy. Soc. London*; 429, 285-309.
- [10] Schrefler, B.A., Zhang, H.W., Pastor, M. and Zienkiewicz, O.C. (1998). Strain localization modeling and pore pressure in saturated and samples. *Compt. Mech.*, 22, 266-280.

- [11] Li, C., Borja, R.I. and Reguciro, R.A. (2004). Dynamic of porous media at finite strain. *Comput. Method Appl. Mech. Eng.*, 193, 3837-3870.
- [12] Zhang, H.W., Fu, Z.D. and Wu, J.K. (2009). Coupling multiscale finite element method for consolidation analysis of heterogeneous saturated porous media. *Adv. Water Resour.*, 32, 268-279.
- [13] Li, X., Thomas, H.R. and Fan, Y. (1999). Finite element method and constitutive modeling and computation for unsaturated soils. *Comput. Geotech.*, 196, 135-159.
- [14] Sheng, D., Sloan, S.W., Gens, A. and Smith, D.W. (2003). Finite element formulation and algorithms for unsaturated soils. *Int. J. Numer. Anal. Methods Geomech.*, 27, 745-765.
- [15] Stelzer, R. and Hofstetter, G. (2005). Adaptive finite element analysis of multi-phase problems in geotechnics. *Comput. Geotech.*, 32, 458-481.
- [16] Sheng, D., Gens, A., Fredlund, D.G. and Sloan, S.W. (2008). Unsaturated soils: from constitutive modeling to numerical algorithms. *Comput. Geotech.*, 35, 810-824.
- [17] Wang, W., Kosakowski, G. and Kolditz, O. (2009). A parallel finite element scheme for thermo-hydro-mechanical coupled problems in porous media. *Comput. Geotech.*, 35, 1631-1641.
- [18] Di Rado H.A., Beneyto, P.A., Mroginski, J.L. and Awruch, A.M. (2009). Influence of the saturation suction relationship in the formulation of non saturated soil consolidation models. *Math. Comput. Model.*, 49, 1058-1070.
- [19] Wu, Y.S. and Forsyth, P.A. (2001). On the selection of primary variables in numerical formulation for modeling multiphase flow in porous media. *J. Contam. Hydrol.*, 48, 277-304.
- [20] Callari, C. and Abati, A. (2009). Finite element methods for unsaturated porous solids and their application to dam engineering problems. *Comput. Struct.*, 87, 458-501.
- [21] Nuth, M. and Laloui, L. (2008). Advances in modeling hysteretic water retention curve in deformable soils. *Soil Tillage Res.*, 100, 7-72.
- [22] Thang, A.M., Cui, Y.J. and Le, T.T. (2008). A study on the thermal conductivity of compacted bentonites. *Appl. Clay Sci.*, 41, 179-181.
- [23] Edlefsen, N.E. and Anderson, A.B.C. (1943). The thermodynamics of soil moisture. *Hilgardia* 16, 31-299.
- [24] Thomas, H.R. and He, H. (1998). Modelling the behaviour of unsaturated soil using an elastoplastic constitutive relationship. *Geotechnique* 48, N° 5, 589-603.
- [25] Zienkiewicz, O.C. and Taylor, R.L. (2000). The finite element method. Butterworth-Heinemann, 5th ed., Oxford.
- [26] Thomas, H.R. and King, S.D. (1991). Simulation of fluid flow and energy processes associated with high level radioactive waste disposal in unsaturated alluvium. *Water Resour. Res.* 22, N° 5, 765-775.
- [27] Agus, S. and Schanz, T. (2005). Swelling pressures and wetting-drying curves of a highly compacted bentonite-sand mixture, in: Schanz, T. (2003), *Unsaturated Soils: Experimental Studies, Proceedings of the International Conference*. From Experimental Evidence Towards Numerical Modelling of Unsaturated Soils. Weimar, Germany, September 18-19, 2003, Volume 1 Series: *Springer Proceedings in Physics*, Vol. 93 Volume Package: Unsaturated Soils: *Experimental Studies* 2005, XIV, 533 p., Springer.
- [28] Poling, B. E., Prausnitz, J. M. and O'Connell, J. P. (2001). *The Properties of Gases and Liquids*, McGraw Hill, 5th ed., New York.
- [29] Gatabin, C. and Billaud, P. (2005). Bentonite THM mock up experiments. *Sensor data report. CEA, Report NT-DPC/SCCME 05-300-A*.
- [30] Lorete, B. and Khalili, N. (2000). A three phase model for unsaturated soils. *Int. J. Numer. Anal. Meth. Geomech.* 24, 893-927.
- [31] Marshall, T.J. and Holmes, J.W. (1988). *Soil physics*. Bristol. Cambridge University Press, 2nd ed., New York.

VPLIV GEOSINTETIČNEGA ARMIRANJA NA STRIŽNO TRDNOST DVOSLOJNIH TAL

MEHRAD KAMALZARE ĀN REZA ZIAIE-MOAYED

o avtorjih

vodilni avtor

Mehrad Kamalzare
Rensselaer Polytechnic Institute
2421, 21st street, apt5, Troy, NY, 12180, ZDA
E-pošta: mehrad_k@yahoo.com, kamalm@rpi.edu

Reza Ziaie-Moayed
Imam Khomeini International University
Block 10, Sina Complex, Iranzamin Street, Shahrake gharb, 1465896358 Teheran, Iran
E-pošta: reza_ziaie_moayed@yahoo.com

izvleček

Kljub slabi nosilnosti mehkih glinastih tal smo zaradi ekonomskih, vojaških ali geoloških pogojev prisiljeni graditi na takšnih tleh, zato za učvrstitev tal in izboljšanje nosilnosti uporabljamo geosintetiko. Za izboljšanje nosilnosti kompozitnih plasti na cestah namestimo geosintetiko na vmesno ploskev med zrnastim materialom in mehkiimi tlemi. V prejšnjih raziskavah smo s poskusnimi in analitičnimi metodami preučevali obnašanje ene plasti tal, ki je bila učvrščena z različnimi tipi geosintetike, ter razvili nekatere numerične modele. V tem prispevku podajamo rezultate raziskav odziva dveh plasti tal (zrnato osnovo in glineno plast), ki sta učvrščeni z geosintetiko.

Testi strižne trdnosti so izvedeni na nearmiranih in armiranih vzorcih z različnimi geosintetikami. Rezultati kažejo, da lahko vključevanje teh materialov poveča ali zmanjša parametre natezne trdnosti vmesne ploskve med dvema plastema tal, odvisno od značilnosti geosintetike. Iz tega vidimo, da so tla, učvrščena z geosintetiko v spodnjih osnovnih plasteh cest tako občutljiva na značilnosti geosintetike, da bodo delovala bolje kot neučvrščena in da se bo posledično izboljšala nosilnost temeljev samo, če uporabimo primerno geosintetiko. Geo-mreža je veliko bolj učinkovita za učvrstitev pri večjem vertikalnem pritisku. Tudi povečanje relativne gostote glinenih spodnjih plasti pozitivno učinkuje na geo-mrežo.

ključne besede

strižna trdnost, geosintetika, direktni strižni test, mehka glina, tamponska plast

INFLUENCE OF GEOSYNTHETIC REINFORCEMENT ON THE SHEAR STRENGTH CHARACTERISTICS OF TWO-LAYER SUB-GRADE

MEHRAD KAMALZARE and REZA ZIAIE-MOAYED

about the authors

corresponding author

Mehrad Kamalzare
Rensselaer Polytechnic Institute
2421, 21st street, apt5, Troy, NY, 12180, USA
E-mail: mehrad_k@yahoo.com, kamalm@rpi.edu

Reza Ziaie-Moayed
Imam Khomeini International University
Block 10, Sina Complex, Iranzamin Street, Shahrake gharb,
1465896358 Tehran, Iran
E-mail: reza_ziaie_moayed@yahoo.com

abstract

Due to the low bearing capacity of soft clayey soils in places that because of economic, military or geological conditions we are obliged to build a structure on, geosynthetics will be used to reinforce the soil and improve its bearing capacity. Particularly, a good example is roadways, where geosynthetics are placed between the interface of the granular materials and the soft-soil sub-grade to improve the bearing capacity of the composite layers. In previous research the behavior of one-layer soils that were reinforced with different kinds of geosynthetics were studied by experimental and analytical methods and some numerical models have been developed. In this paper the behavior of two-layer soils (granular base and clayey sub-grade) that were reinforced with some geosynthetics are investigated. Large-scale direct shear tests were performed on unreinforced and reinforced samples with different geosynthetics. The results show that depending on the characteristics of the geosynthetics, the inclusion of these materials may increase or decrease the shear strength parameters of the interface of two-layered soils. It implies that the geosynthetic-reinforced soils in the sub-base layer of roads are so sensitive to the characteristics of geosynthetics and will perform better than non-reinforced soils and consequently the load-carrying capacity of the basement will improve only if the appropriate geosynthetics are used. However, geogrid shows more reinforcement efficiency under higher vertical stresses. Increasing the relative density of the clayey sub-grade would also cause the geogrid reinforcement to be more effective.

keywords

shear strength, geosynthetic, large scale direct shear test, soft clay, subgrade

1 INTRODUCTION

In places which, because of the economic, military or geological conditions, building a structure on such soils is essential, geosynthetics will be used to reinforce the soil and improve the bearing capacity. Different investigations have been performed to study the interaction of soils/geosynthetics in recent years. Abu-Farsakh et al. (2007) studied the behavior of a large modeled foundation, placed on reinforced soil. Feng et al. (2008) calculated the ultimate strength of red clay, reinforced by geogrid, using a pull-out test. Williams and Okine (2007) used a CBR test to study the effects of some kinds of geogrids on granular base soil. However, an understanding of the soil/geosynthetic interface's shear strength is essential to the design and stability analysis of geosynthetically reinforced soil structures. For example, an interface with a stronger shearing resistance in a geosynthetically lined slope can reduce the tensile forces mobilized in the geosynthetics, as well as increase the slope inclination (Liu and Gilbert, 2003; Palmeira and Viana, 2003). The shear strength of the soil/geosynthetic interface is also essential for a numerical simulation of the behavior of the sub-grade and base layers of roads. Though the shear strength of the soil/geosynthetic interface has been investigated by conducting other tests, such as tilt-table tests (Wu et al., 2008), the direct shear test is still the most common testing method. For example, direct shear tests involving the interfaces between soil and a geotextile have been performed by Richards and Scott (1985), Lee and Manjunath (2000), Mahmood et al. (2000), and Bergado et al. (2006). Studies involving the interfaces between soil and geogrid include Jarret and Bathurst (1985), Cancelli et al. (1992), Bauer and Zhao (1993), Cazzuffi et al. (1993), Bakeer et al. (1998), Abu-Farsakh and Coronel (2006) and Mostafa A. El Sawwaf (2006).

However, the scale effect of the shear box has always been an important parameter in these investigations. Ingold (1982) conducts laboratory direct-shear tests of the soil/geotextile interface by using different sizes of shear boxes. He concluded that the friction angle obtained from a 60 mm × 60 mm shear area was 2–3° higher than that obtained from a 300 mm × 300 mm shear area. Liu et al. (2008) investigated the effect of a special kind of geogrid on some kinds of soils by using a large-scale direct-shear test. Abu-Farsakh et al. (2007) used a large-scale direct-shear test to study the effect of moisture and dry density on the interaction between the soil and the geosynthetics. Cindric et al. (2006) investigated the effects of a geogrid on the elastic and shear moduli of soils. O'Kelly and Naughton (2007) performed some large-scale direct-shear tests to investigate the behavior of a new kind of geogrid, which has the capability of drainage and presented some graphs. Liu et al. (2008) studied the behavior of soil/PET-yarn geogrid interfaces by using large-scale direct-shear tests. Jesmani et al. (2010) conducted some undrained direct-shear tests to study the effect of plasticity index and normal stress on the shear behavior and the shear modulus of remolded clays.

Almost all previous investigations have studied the behavior of geosynthetics in a one-layered soil. Although several investigations were performed in order to find the best depth for embedding the geosynthetics, there have been very limited investigations on the interactions of two-layered soils and geosynthetics. Zhou and Wen (2006) studied a model of sand soil, placed on soft clay that was reinforced by a geogrid, using a compression test. Kazimierowicz-Frankowska (2007) studied the effect of reinforcement on the load-settlement characteristics of a two-layer subgrade. Sireesh et al. (2008) investigated the bearing capacity of circular footing on a geocell-sand mattress overlying a clay bed. Anubhav and Basudhar (2010) conducted experiments in a direct-shear test apparatus to study the shear force-displacement behavior at the soil-geotextile interface using two differently textured woven geotextiles. A non-linear constitutive model was presented for predicting both the pre-peak and the post-peak interface behavior. The predictions made with the developed model were found to be in good agreement with the experimental data obtained from direct shear tests. Palmeira (2009) discussed some experimental, theoretical and numerical methods for the study and evaluation of the interaction between soils and geosynthetics, with particular reference to the applications of these materials in soil reinforcement. The main advantages and limitations of some traditional experimental and theoretical methods for the study of soil-geosynthetic interactions were presented

and new applications of these methods were addressed; and the need for improvements in the experimental and theoretical techniques for a better understanding of soil-geosynthetic interactions was highlighted.

In this paper, due to the importance of the shear-strength characteristics of reinforced soils, the effects of reinforcing a two-layer soil with geosynthetics on the shear-strength parameters of the interface of two soils were investigated by conducting a series of large-scale direct-shear tests.

2 TEST APPARATUS

The size of the shearing device can influence the direct-shear test results. Generally, the boundary effect and device friction are more significant for a smaller shear box. Ingold (1982) conducted laboratory direct-shear tests of the soil/geotextile interface by using different sizes of shear boxes. He concluded that the friction angle obtained from a 60 mm × 60 mm shear area was 2–3° higher than that obtained from a 300 mm × 300 mm shear area. The dimension of the shear box, as regulated by ASTM D5321 (ASTM 2002), with minimum dimensions of five times the maximum opening size (in plan) of the geosynthetic being tested, should be used in the direct shear test of the geosynthetic/soil interface. It also mentioned that the depth of each container that contains the soil must be a minimum of 50 mm or six times the maximum particle size of the coarser soil being tested, whichever is greater. In this study a large-scale direct-shear device was used, which has length, width, and thickness of 150mm × 150mm × 100mm. The movement of the upper shear box in the horizontal direction is controlled by a set of gears that are mobilized by an electric motor. The vertical loading applied by a hydraulic jack is transferred through the rigid reaction frame and adds on a rigid load plate that is placed on top of the soils in the upper shear box. The normal load is constant during the test, satisfying the requirement regulated by ASTM D5321 (ASTM 2002).

A rigid plate is conventionally used as the loading plate in direct-shear tests (for example, Bakeer et al., 1998; Lee and Manjunath, 2000). The system is capable of applying a vertical force and a shear force of up to 50 kN. Fig. 1 shows a frontal view of the large-scale direct-shear device used in this study. The vertical force applied on the rigid plate and its vertical displacement are measured during the tests. The horizontal movement of the upper shear box and the shear force exerted during the shearing testing are also recorded. These data are collected by using two load cells and two linear variable displacement

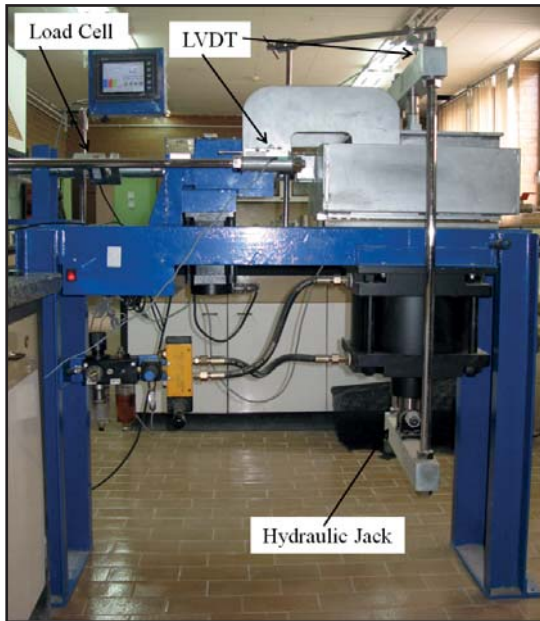


Figure 1. Large-scale direct-shear device (Imam Khomeini International University).

transformers (LVDT). The capacity for both load cells is 50kN. The capacities for the vertical and horizontal LVDT are 50 mm and 100 mm, respectively.

3 TEST MATERIAL

The tests herein use two soils, including a clay soil and a granular soil that has been grained in a manner that satisfies the suggestion of AASHTTO M147 for the sub-base soil of roads. In order to obtain comparable results with practical projects, the clay soil was chosen from Varamin region, Iran, where a railroad project was under construction. Table 1 lists the physical characteristics of each soil, while Fig. 2 shows their grain-size distribution curves. It should be noted that in this figure the upper and lower limit means the maximum and minimum grain size that the AASHTO M147 suggested. The granular soil is classified as SW according to the Unified Soil Classification System (USCS). The dry unit weight for the granular soil sample was 21.33 kN/m³. The clay soil is classified as CL according to Unified Soil Classification System (USCS)

Table 1. Soil Characteristics.

Property	D ₁₀ (mm)	D ₃₀ (mm)	D ₆₀ (mm)	Coefficient of uniformity	Coefficient of curvature	Liquid limit	Plastic limit	USCS symbol
Sand	0.12	1.20	5.15	42.92	2.33	-	-	SW
Clay	-	-	-	-	-	32	19	CL

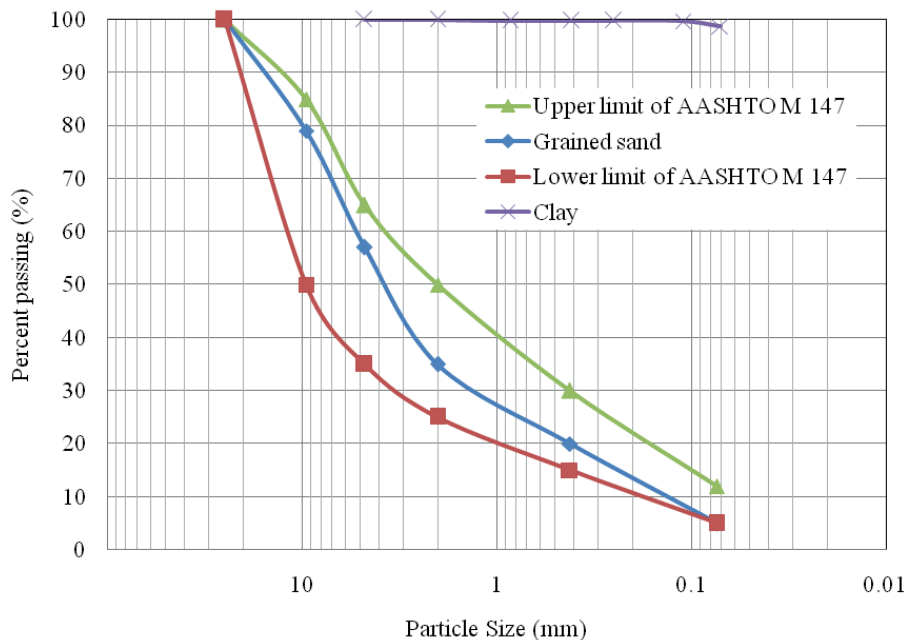


Figure 2. Grain-size distribution curves of soils.

Table 2. Geosynthetic characteristics.

Geosynthetic	Material	Aperture size (mm)	Weight (g/m ²)	Tensile strength-MD (kN/m)	Tensile strength-CD (kN/m)
GG	Polyethylene (HDPE)	10 × 10	700	7.6	7.6
GT-NW	Polyester	0.062	300	8	11.1
GT-W	Yarns polyester	-	2286	100	10

and its dry unit weight was 19.20 kN/m³. Both soils were prepared in a relative density (R) of 90% of the maximum density with the optimum water content (16.0% for clay and 9.0% for sand), which has been calculated according to B-method of AASHTO T180. The maximum sand sizes were smaller than 9.5 mm. This satisfies the general requirement that the ratio of the minimum size of the shear box to the maximum size of the soil particle is greater than 6. Research on the interface of geosynthetic and cohesive materials is becoming popular (for example, Fourie and Fabian, 1987; Abu-Farsakh and Coronel, 2006). The rationale behind the application of a cohesive material is that of an economic concern.

This study uses two geotextile and one geogrid, and they are denoted as GT-NW (Non-Woven Geotextiles), GT-W (Woven Geotextiles) and GG (Geogrids), respectively (Fig. 3). The woven geotextile has a tensile strength in one direction, but the non-woven one has in it two directions. Table 2 lists the physical characteristics of these geosynthetics.

4 TEST PROCEDURES

The soil used for the large-scale direct-shear testing program is dried in an oven and after wetting to the optimum water content, compacted to the target unit

weight within the shear box. Each soil is compacted in three layers. The compaction of the sand and clay is conducted by using a manual plastic hammer to hit the steel plate, which was placed on top of the soil until reaching the target unit weight. The geosynthetic is positioned on top of the lower shear box and at the interface of the sand and clay soils. These tests are conducted using normal stresses of 44, 96, and 192 kPa, which represent the normal stresses that different vehicles may apply to a sub-grade layer of roads. The normal loading is applied on the specimen and the vertical deformation of the test specimen is then monitored. Shear loading is not applied until the vertical deformation reaches its equilibrium. According to ASTM D5321, a shear rate of 1 mm/min is used in this test program in order to satisfy the undrained failure condition. However, it should be noted that undrained conditions cannot be guaranteed in direct shear tests. But for the purpose of this research, the suggestion of the ASTM standard would be precise enough.

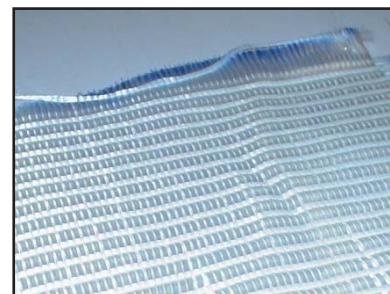
The test stops when the shear displacement reaches about 30 mm, i.e., about 20% of the shear strain. The maximum shear strength during the shear process is recorded as the peak shear strength. The direct-shear tests for the soil-soil interfaces and the soil-geosynthetic were conducted under the same normal loading and same testing procedures for the sake of the comparison.



a)



b)



c)

Figure 3. Geosynthetic specimens a) Geogrid, b) Non-Woven Geotextile, c) Woven Geotextile.

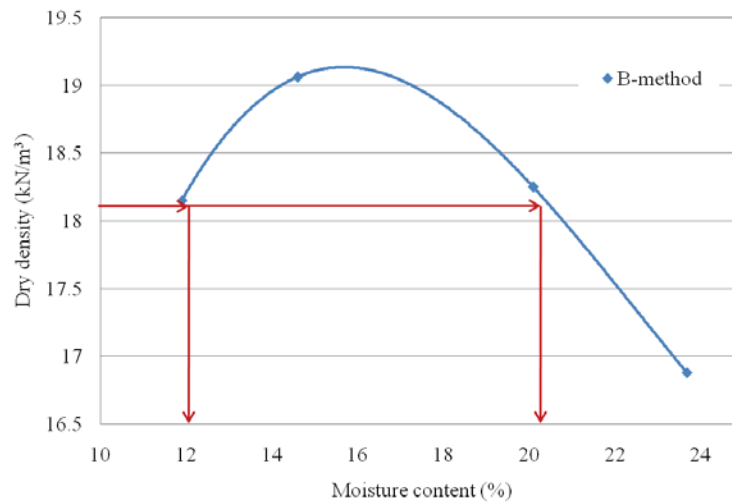


Figure 4. Choosing different water contents of the clay soil.

Tests with various clay relative densities (75%, 85% and 90%) and different clay moisture contents (12%, 16% and 20%) were also performed to investigate the effects of the sub-grade relative density and water content. To make the test results comparable, the moisture contents were chosen based on the compaction curve of the clay soil to obtain the same density in both 12% and 20% water contents (Fig. 4).

Richards and Scott (1985) concluded that the test using a large solid block as the lower shear box is the best at replicating the testing results of the soil/geotextile interface. Jewell (1996) stated that the geotextile and geomembrane can be tested with a solid block or soil in the lower part of the shear box, while the geogrid must be tested by a device in which both parts of the shear test device have to be filled with soil. The set-up of the direct shearing device is not strictly regulated by testing standards. For example, only the minimum size of the shearing box is stated explicitly in ASTM D5321 for the direct shear test of the soil-geosynthetic interface. Few

research studies focus on the appropriate setup of direct-shear testing device for the soil/geogrid interface. For example, the difference in the measured shear strength when using different sizes of a lower shear box has not been discussed. Liu et al. (2009) tested three different set-ups of a lower shearing box. The effects of different set-ups on the test results were evaluated by comparing the direct-shear test results using different set-ups of the lower shear box. The set-ups included: a box with the same size that was filled with soil, a box with a larger size filled with soil, and a larger lower shear box filled with a solid block (Liu et al., 2009). It was observed that among these set-ups, a box with the same size that was filled with soil produces the greatest interface shear strength. For conducting the direct shear test against the geosynthetic interface in the soil, the sizes of the upper and lower shear boxes should be same and they must be filled with the necessary soil. Therefore, in this study, all of the tests were performed in manner such that the sizes of the upper and lower shear boxes were the same and they were filled with the necessary soils (Fig. 5).

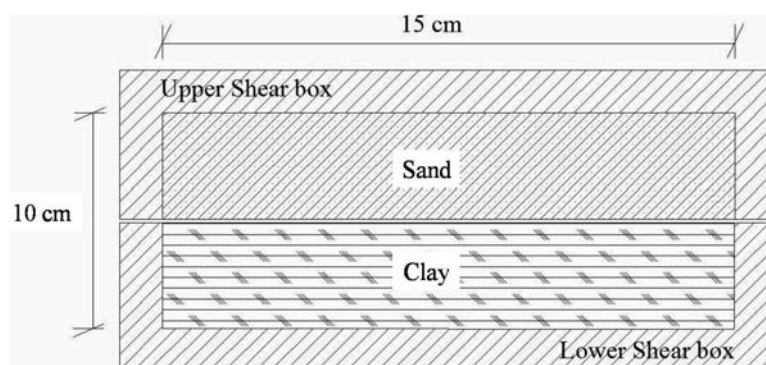


Figure 5. Set-up of upper and lower shear box.

5 RESULTS AND DISCUSSIONS

The results of the large direct-shear tests are presented in this section in terms of the shear behavior for different soil/geosynthetic interfaces.

5.1 SHEAR BEHAVIOR OF THE SOIL/GEOSYNTHETIC INTERFACE AT OPTIMUM WATER CONTENT AND $R=90\%$

To discuss the stress–strain behavior of the soil/geosynthetic interface, the results of the direct-shear tests for samples with a relative density of 90% and optimum water content are presented in Fig. 6. The results of the vertical deformation versus the shear displacement for these samples are shown in Fig. 7.

The results show that there is no well-defined peak shear strength observed for the soil/geosynthetic interface in higher normal stresses. In general, a yield shear stress is reached at a small shear displacement (usually less than 15 mm). The shear stress of the soil/geosynthetic interface became constant after a displacement of about 15 mm. It is clear that the geogrid causes the soils to show more shear strength than the two other geotextiles. However, these differences become smaller when increasing the normal stress. Calculating the values of the cohesion (c) and the internal friction angle (φ) for the geogrid-reinforced soil reveals that c would decrease by 22% and φ would increase by 13% relative to the non-reinforced two-layer soil. Similar calculations for woven and non-woven geotextiles show 31% and 81% decreases for the cohesion and a 5% decrease and a 3% increase for the internal friction angle, respectively.

As is clear from Fig. 7, during the initial stage, when the shear displacement is small, the geosynthetics-reinforced soil undergoes a vertical contraction. Following the contraction, the vertical deformation behavior then depends on the geosynthetic type. The contraction would become constant for soils reinforced by non-woven geotextile and would decrease for other reinforced soils, especially for geogrid-reinforced soils.

5.2 PEAK SHEAR STRENGTH OF SOILS AND SOIL/GEOSYNTHETIC INTERFACES AT THE OPTIMUM WATER CONTENT AND $R=90\%$

Fig. 8 shows the peak shear strength for soils and the soil/geosynthetic interface. The results show an apparent

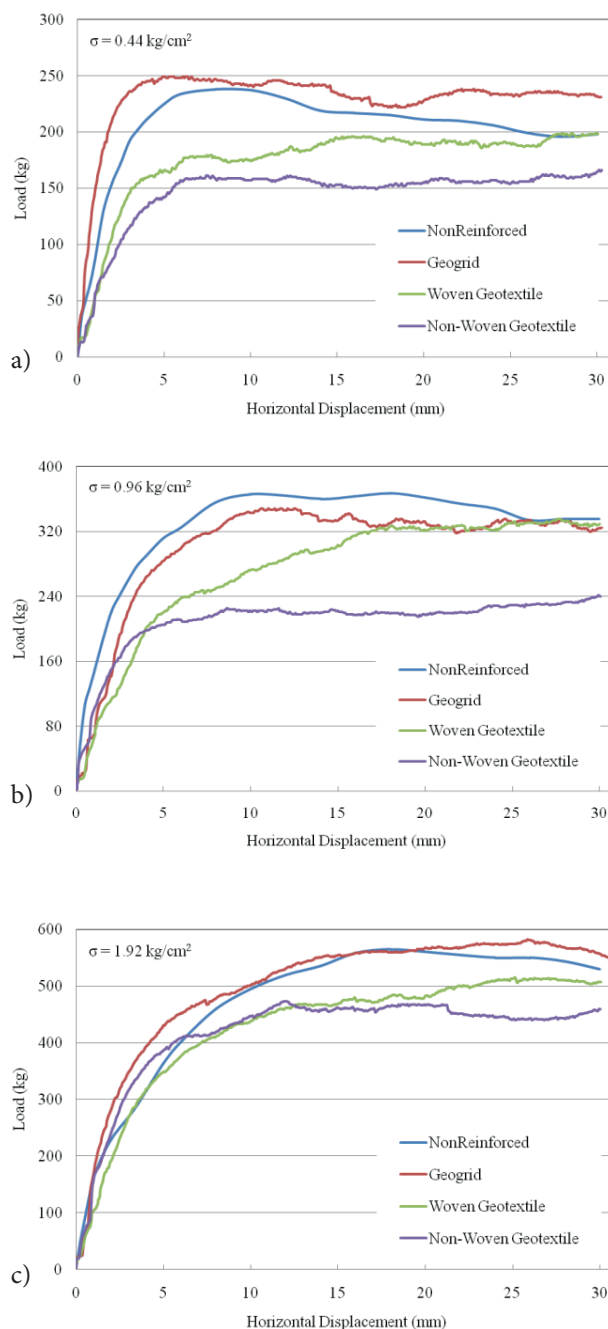


Figure 6. Stress–strain behavior of the soil/geosynthetic interface under different normal loading ($R=90\%$, $\omega=16\%$), a) $\sigma=44$ kPa, b) $\sigma=96$ kPa, c) $\sigma=192$ kPa.

cohesion in these peak shear strengths. Possible explanations are in the non-linear relationship of the shear stress and in the machine friction under this stress level. The interface shear strength of the soil against the geotextile is significantly lower than the internal shear strength of the corresponding soils.

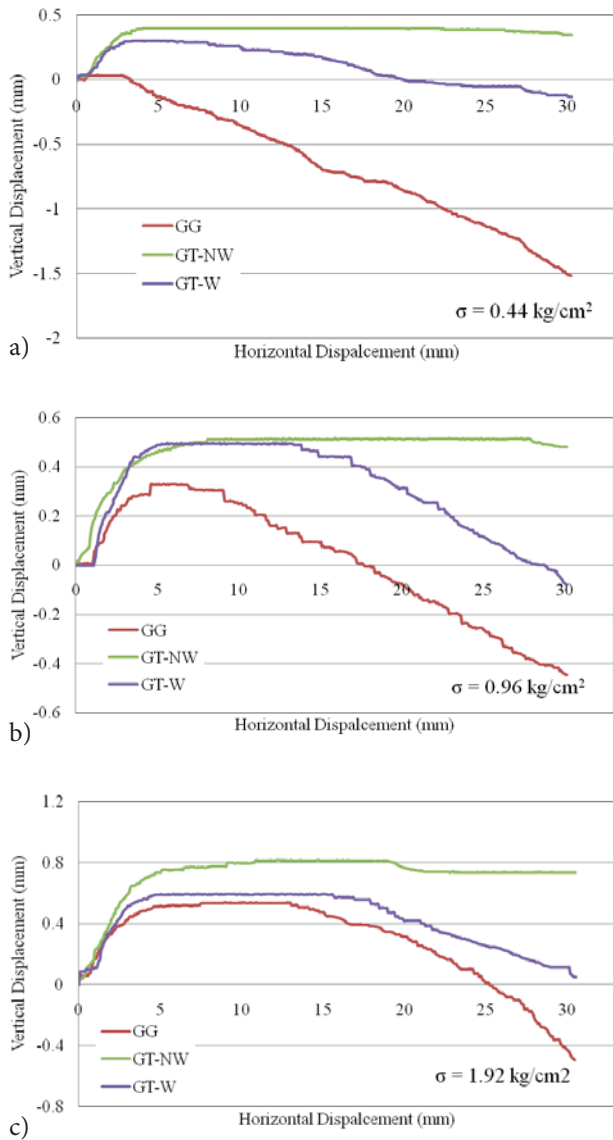


Figure 7. Vertical deformation versus horizontal displacement under different normal loading ($R=90\%$, $\omega=16\%$), a) $\sigma=44 \text{ kPa}$, b) $\sigma=96 \text{ kPa}$, c) $\sigma=192 \text{ kPa}$.

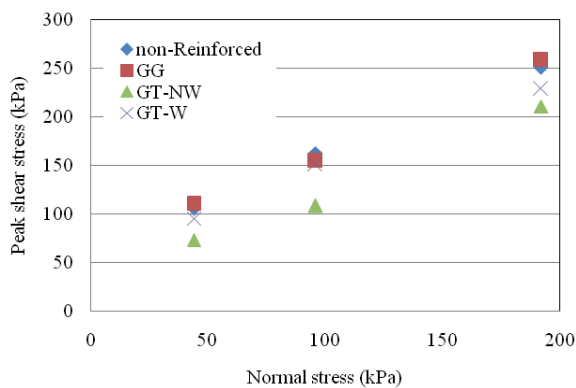


Figure 8. Peak shear strength versus normal stress for the soil/geosynthetic interface ($R=90\%$).

It is observed that under different normal stresses, the shear strength of the soil-geogrid interface is always higher than that of soil-geotextile interface. Alfaro et al. (1995) and Tatlisoz et al. (1998) stated that the direct-shear resistance of the soil/geogrid interface is composed of the soil-to-geosynthetic shear resistance and the soil-to-soil shear resistance within the geogrid openings. As presented in Fig. 8, the internal geogrid reinforced soil shear strength is higher than the interface shear strength of the soil against the geotextile, and therefore this increase in the shear strength is mainly attributed to the interlocking of soil particles that penetrate through the geogrid apertures. This conclusion is in agreement with the presented results of Liu et al. (2009).

5.3 EFFECT OF DENSITY ON THE SHEAR STRENGTH OF SOIL/GEOSYNTHETIC INTERFACES

To investigate the effect of sub-grade soil density, samples with different clay densities (75%, 85% and 90%) were prepared. However, in order to avoid clay settlement and consequently changing the shear plane due to placing a sand layer in upper box, in samples with a clay relative density other than 90%, clay soil was placed in upper box of the shear apparatus and sand with a relative density equal to 90% placed in the lower box. Fig. 9(a) shows the failure envelopes of non-reinforced and reinforced samples with $R=75\%$ for the clay layer, as an example. It is clear that the geogrid is the only geosynthetic that increases the shear strength of the samples. Similar envelopes in $R=90\%$ are presented in Fig. 9(b). Comparing these two figures reveals that the reinforcing effect of the geogrid is more significant in a lower relative density of the sub-grade soil. However, specimens with a higher relative density of clay soil show a higher shear strength.

5.4 EFFECT OF WATER CONTENT ON SHEAR STRENGTH OF SOIL/GEOSYNTHETIC INTERFACES

Samples with different water contents (12% and 20%) for the clay layer, in addition to the optimum water content (16%), were prepared and tested in order to study the effect of the moisture content of the sub-grade soil on the shear strength of reinforced roads at the interface of the sub-grade and base layers. Values of the water content chosen in a manner to let us investigate just the effect of the water content with all the other parameters, including the dry density (γ), kept constant (Fig. 4). The behavior of the non-reinforced and the reinforced samples at different water contents and a relative density of $R=90\%$ are shown in Fig. 10.

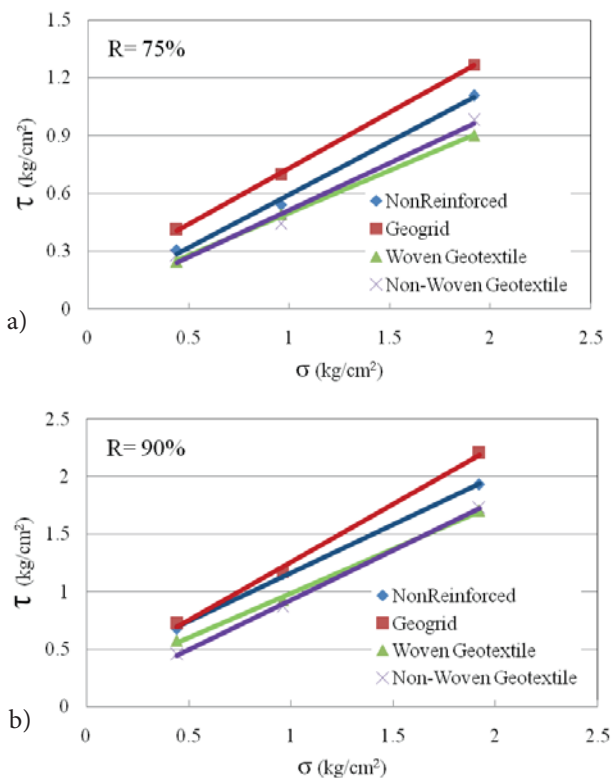


Figure 9. Failure envelopes of non-reinforced and reinforced soil samples with the optimum water content, a) R=75%, b) R=90%.

It is clear that the samples with $\omega=20\%$ for the clay layer show a higher shear strength at the interface of two layers; and the samples reinforced by the geogrid reveal a higher shear strength in comparison to the geotextiles, which could be up to a 9% increase in the internal friction angle relative to the non-reinforced two-layer soil. However, the reinforcing effect of the geosynthetics is negligible and has almost the same procedure in both water contents.

Figs. 9 and 10 reveal that the geogrid is the best geosynthetic that can be used to improve the shear-strength parameters of the two-layer soils. Both geotextiles decrease the shear-strength characteristics of the interface plane of two soils, which probably is because of the lack of apertures in the geotextile and consequently the lack of interlocking between the two soils.

5.5 EFFICIENCY OF REINFORCEMENT

The efficiency of all the geosynthetics for reinforcing the two-layer soils was evaluated using equation (1).

$$\eta = \tau_{reinforced} / \tau_{unreinforced} \quad (1)$$

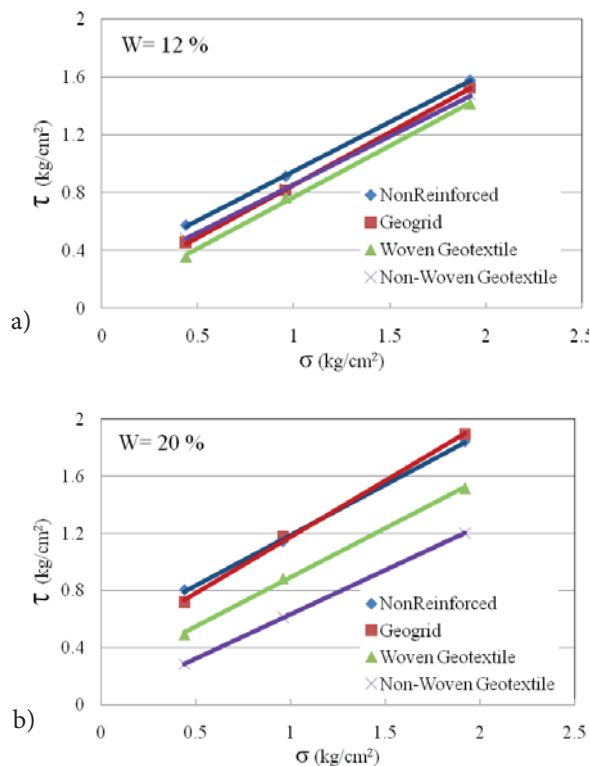


Figure 10. Failure envelopes of non-reinforced and reinforced soil samples with different water contents and R=90%, a) $\omega=12\%$, b) $\omega=20\%$.

Calculating the efficiency of the reinforcement (η) for all the geosynthetics in various water contents and different relative densities shows that in samples with a relative density equal to 90%, with respect to the amount of water content, by increasing the normal stress, the efficiency of the reinforcement would increase (Fig. 11). However, at R=75%, increasing the normal stress would cause a decrease in the efficiency of the reinforcement.

It is clear that the geogrid has the higher efficiency in all conditions.

5.6 COEFFICIENT OF INTERACTION

The frictional resistance obtained from the direct-shear test on soil-geogrid specimens is a combination of the soil-to-reinforcement interface friction and the soil-to-soil shear resistance at the geogrid openings (Abu-Farsakh et al., 2007). Bergado et al. (1993) suggested the following equation to calculate the frictional resistance force at the soil-geogrid interface:

$$P_s = A[\alpha_{ds} c_a + (1 - \alpha_{ds}) c] + A\sigma_n[\alpha_{ds} \tan \delta + (1 - \alpha_{ds}) \tan \varphi] \quad (2)$$

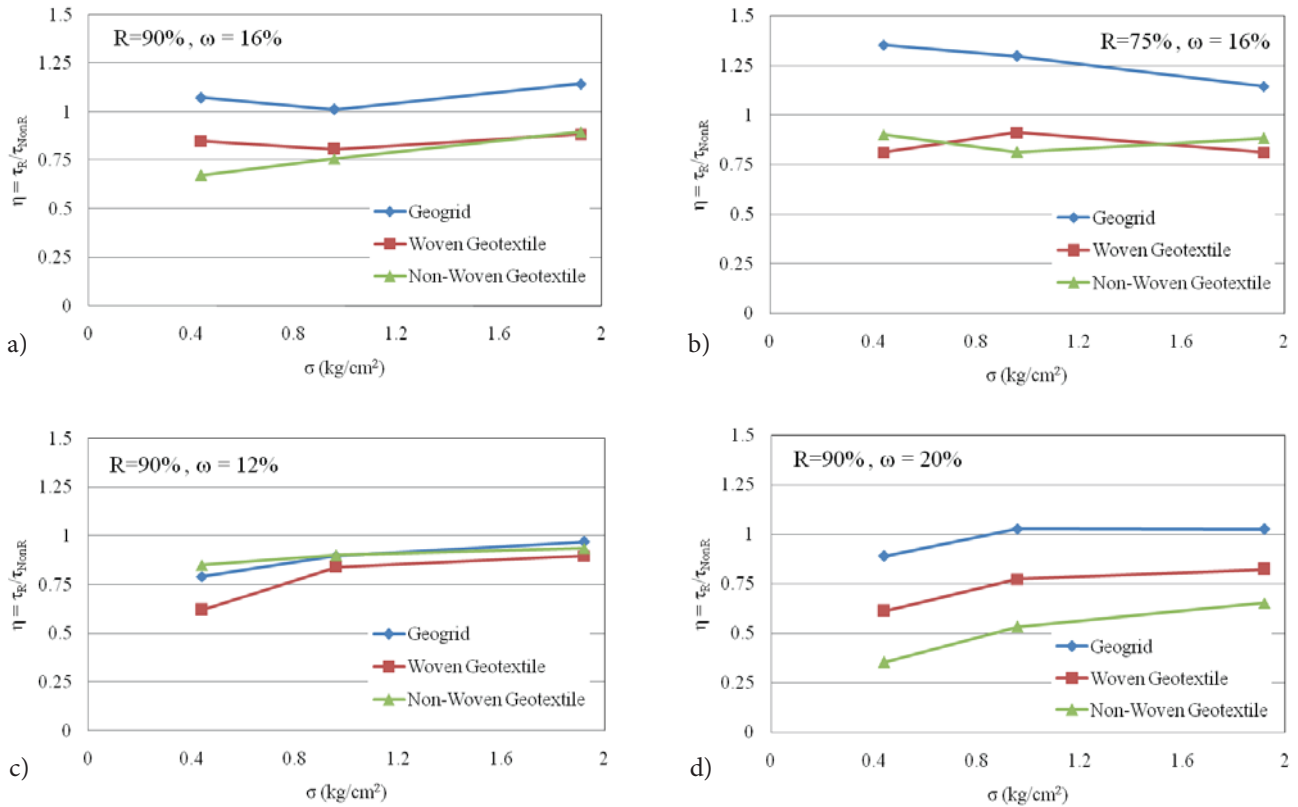


Figure 11. Efficiency of geosynthetic reinforcement in various water contents and different relative densities, a) $R=90\%$, $\omega=16\%$, b) $R=75\%$, $\omega=16\%$, c) $R=90\%$, $\omega=12\%$, d) $R=90\%$, $\omega=20\%$.

Where

- P_s = direct shear resistance;
- A = total shear area of the samples;
- α_{ds} = ratio of the reinforcement shear area to the total shear area;
- c_a = soil-geogrid adhesion;
- c = soil-soil cohesion;
- σ_n = normal stress at the shear plane;
- δ = soil-geosynthetic interface friction angle;
- φ = frictional angle of soil-to-soil from direct shear test.

Eq. (2) can be divided into two parts: the soil-to-geogrid frictional shear force, and the soil-to-soil direct frictional shear force. The soil-to-geogrid direct shear force can be formulated using the Mohr–Coulomb criterion as

$$F_{s-g} = (c_a + \sigma_n \tan \delta) A_{s-g} \quad (3)$$

Where

A_{s-g} = area between the soil and the geogrid. Similarly, the soil-to-soil direct shear force is given as

$$F_{s-s} = (c + \sigma_n \tan \varphi) A_{s-s} \quad (4)$$

Where

A_{s-s} = area of the soil-to-soil friction at the geogrid openings.

Eqs. (2)-(4) yield the following equation:

$$\tau_{s-g} = (P_s - A(1 - \alpha_{ds})(c + \sigma_n \tan \varphi)) / (A \alpha_{ds}) = c_a + \sigma_n \tan \delta \quad (5)$$

where

τ_{s-g} = shear stress along the soil-geosynthetic interface.

By plotting τ_{s-g} versus σ_n , c_a and δ were calculated ($c_a=0.44$ kg/cm² and $\delta=43^\circ$).

Many researchers have discussed the importance of using the “interface efficiency” or “Coefficient of interaction,” c_i (Abu-Farsakh et al., 2007). As a primary design parameter in the geosynthetically reinforced soil structures (Cowell and Sprague, 1993; Koutsourais et al., 1998; Tatlisoz et al., 1998), the interface efficiency is used to calculate the effective length of the reinforce-

ment required beyond the critical failure plane for MSE walls and reinforced slopes (Abu-Farsakh et al., 2007). The interface efficiency for cohesive soils is defined as the ratio of the shear strength at the soil-reinforcement interface to the shear strength of the soil at the same overburden condition (Cowell and Sprague, 1993).

$$c_i = (c_a + \sigma_n \tan \delta_a) / (c + \sigma_n \tan \varphi) \quad (6)$$

Calculating c_i for a two-layer soil reveals that the average Coefficient of interaction is equal to $c_i = 1.19$, which shows a considerable adhesion between the soil and the geogrid. However, the interface efficiency depends on the normal (confining) stress (i.e., the depth of the reinforcement layer) in addition to the material characteristics (Abu-Farsakh et al., 2007). Based on the value of c_i , the most appropriate geosynthetic could be chosen in a specific project with a specific soil and specific circumstances.

6 CONCLUSIONS

In this study we conducted a series of large-scale direct-shear tests on a two-layer soil that was reinforced by three kinds of geosynthetics. The geosynthetics were placed at the interface of the two soils, which was located between the upper and lower boxes of the direct shear device. The following specific conclusions can be drawn from the study:

1. The interface shear strength of the soil/geotextile is lower than the soil shear strength. It indicates that the geotextile placed within the soil usually acts as a weak interface in terms of direct sliding.
2. The direct-shear resistance of the soil/geogrid interface is higher than the soil/geotextile; and it usually increases the value of the shear resistance of the two-layer soil. This increment is due to the creation of the shear resistance between the soil and surface and the opening of the geogrid, and the bearing resistance provided by transverse ribs. These resistances would be created when a relative movement occurs in the soil and geogrid interface.
3. It is clear that the geogrid increases both the internal friction and the cohesion of the soil (it increases the cohesion by about 23% and the internal friction by about 3 degrees), but geotextiles just increase the cohesion of the two-layer soil (about 9%) and the internal friction would decrease by about 1 to 3 degrees.
4. The improvements of the shear strength for the geogrid-reinforced specimens are more in the higher normal stresses. In other words, the geogrid shows more reinforcement efficiency at higher vertical stresses.

5. Increasing the relative density of the clayey sub-grade would cause the geogrid reinforcement to be more effective. Also, the improvement of the shear strength by increasing the normal stress would be more at a denser sub-grade.
6. The internal friction angle (φ) and cohesion (c) of two-layer reinforced soil at a relative density of 90% could be up to 34% and 40% higher than samples at a relative density of 75%, respectively.
7. Increasing the water content of the clay soil in the geogrid-reinforced specimens increases the shear strength of the two-layer soil. This could be because of the increment of cohesion, while the internal friction would be produced by the geogrid.
8. Increasing the water content of the clay-geogrid-reinforced specimens from 12% to 20% could increase the internal friction angle and the cohesion by up to 5% and 200%, respectively.

REFERENCES

- Abu-Farsakh, M.Y., Coronel, J., 2006. Characterization of Cohesive Soil-Geosynthetic Interaction from Large Direct Shear Test. 85th Transportation Research Board Annual Meeting, Washington, D.C.
- Abu-Farsakh, M., Coronel, J., and Tao, M., 2007. Effect of Soil Moisture Content and Dry Density on Cohesive Soil-Geosynthetic Interactions Using Large Direct Shear Tests. *Journal of Materials in Civil Engineering*, 19 (7), 540-549.
- Alfaro, M.C., Miura, N., Bergado, D.T., 1995. Soil geogrid reinforcement interaction by pullout and direct shear tests. *Geotechnical Testing Journal* 18 (2), 157-167.
- Anubhav and P.K. Basudhar, 2010. Modeling of soil-woven geotextile interface behavior from direct shear test results. *Geotextiles and Geomembranes*, 28 (4), 403-408.
- ASTM D5321, 2002. Standard test method for determining the coefficient of soil and geosynthetic or geosynthetic and geosynthetic friction by the direct shear method. ASTM Designation: D5321-02. ASTM, USA.
- Bakeer, R.M., Sayed, M., Cates, P., Subramanian, R., 1998. Pullout and shear test on geogrid reinforced lightweight aggregate. *Geotextiles and Geomembranes* 16 (2), 119-133.
- Bauer, G.E., Zhao, Y., 1993. Evaluation of shear strength and dilatancy behavior of reinforced soil from direct shear tests. *ASTM Special Technical Publication* 1190, 138-157.
- Bergado, D.T., Chai, J.C., Abiera, H.O., Alfaro, M.C., Balasubramanian, A.S., 1993. Interaction between

- cohesive-frictional soil and various grid reinforcements. *Geotextiles and Geomembranes* 12 (4), 327–349.
- Bergado, D.T., Ramana, G.V., Sia, H.I., Varun, 2006. Evaluation of interface shear strength of composite liner system and stability analysis for a landfill lining system in Thailand. *Geotextiles and Geomembranes* 24, 371–393.
- Cancelli, A., Rimoldi, P., Togni, S., 1992. Frictional characteristics of geogrids by means of direct shear and pull-out tests. In: *Proceedings of the International Symposium on Earth Reinforcement Practice*, Kyushu, vol. 1, pp. 29–34.
- Cazzuffi, D., Picarelli, L., Ricciuti, A., Rimoldi, P., 1993. Laboratory investigations on the shear strength of geogrid reinforced soils. *ASTM Special Technical Publication* 1190, 119–137.
- Cowell, M. J., and Sprague, C. J., 1993. Comparison of pull-out performance of geogrids and geotextiles. *Geosynthetics*, 93, 579–592.
- El Sawwaf, M., 2006. Behavior of strip footing on geogrid-reinforced sand over a soft clay slope. *Geotextiles and Geomembranes* 25, 50–60.
- Fourie, A.B., Fabian, K.J., 1987. Laboratory determination of clay-geotextile interaction. *Geotextiles and Geomembranes* 6 (4), 275–294.
- Ingold, T.S., 1982. Some observations on the laboratory measurement of soil-geotextile bond. *Geotechnical Testing Journal* 5 (3), 57–67.
- Jarret, P.M., Bathurst, R.J., 1985. Frictional Development at a Gravel Geosynthetic Peat Interface. *Proceedings of the Second Canadian Symposium of Geotextiles and Geomembranes*, Edmonton. 1–6.
- Jesmani, M., Kashani, H. F., Kamalzare, M., 2010. Effect of Plasticity and Normal Stress on Undrained Shear Modulus of Clayey Soils. *Acta geotechnica slovenica*, (1), 47–59.
- Jewell, R.A., 1996. *Soil Reinforcement with Geotextiles*. Thomas Telford, London.
- Koutsourais, M., Sandri, D., and Swan, R., 1998. Soil interaction characteristics of geotextiles and geogrids. *Geosynthetics*, 98, 739–744.
- Liu, C.N., Ho, Y.H., Huang, J.W., 2008. Large scale direct shear tests of soil/PET-yarn geogrid interfaces. *Geotextiles and Geomembranes* 27 (1), 19–30.
- Liu, C.N., Gilbert, R.B., 2003. Simplified method for estimating geosynthetic loads in landfill liner side slopes during filling. *Geosynthetics International* 10 (1), 24–33.
- Mahmood, A., Zakaria, N., Ahmad, F., 2000. Studies on geotextile/soil interface shear behavior. *Electronic Journal of Geotechnical Engineering* 5.
- Palmeira, E.M., Viana, H.N.L., 2003. Effectiveness of geogrids as inclusions in cover soils of slopes of waste disposal areas. *Geotextiles and Geomembranes* 21 (5), 317–337.
- Palmeira, E. M., 2009. Soil-geosynthetic interaction: Modelling and analysis. *Geotextiles and Geomembranes* 27 (5) 368–390.
- Richards, E.A., Scott, J.D., 1985. *Soil Geotextile Frictional Properties*. Second Canadian Symposium on Geotextiles and Geomembranes, Edmonton. 13–24.
- Tatlisoz, N., Edil, T.B., Benson, C.H., 1998. Interaction between reinforcing geosynthetics and soil-tire chip mixtures. *Journal of Geotechnical and Geoenvironmental Engineering* 124 (11), 1109–1119.
- Wu, W., Wick, H., Ferstl, F., Aschauer, F., 2008. A tilt table device for testing geosynthetic interfaces in centrifuge. *Geotextiles and Geomembranes* 26 (1), 31–38.

SISTEM MEHKE MNOŽICE ZA ODLOČANJE PRI GEOTEHNIČNEM NAČRTOVANJU

DJAMALDDINE BOUMEZERANE, SMAÏN BELKACEMI IN BOJAN ŽLENDER

o avtorjih

Djamalddine Boumezerane
University of Bejaïa,
Civil Engineering Department
Route Targa Ouzemmour 06000 Bejaïa, Alžirija
E-pošta: dboumezerane@gmail.com

Smaïn Belkacemi
Ecole Nationale Polytechnique,
Civil Engineering Department
10 Avenue Pasteur, Hassan Badi – El-Harrach, Alžirija
E-pošta: smainbelkacemi@yahoo.com

Bojan Žlender
University of Maribor,
Faculty of Civil Engineering
Smetanova 17, 2000 Maribor, Slovenija
E-pošta: bojan.zlender@uni-mb.si

izvleček

Geotehnična terenska raziskava je pomembna in kompleksna naloga, ki se na splošno izvede v dveh korakih. Prvi korak, ki vsebuje preliminarne raziskave, vpliva na kasnejšo terensko raziskovanje. Glede na predhodne raziskave, se na podlagi inženirske presoje določi število raziskovalnih sond, potrebnih za ustrezen opis terena. Na to vplivajo geološke sovisnosti, topografija področja, vrsta projekta, ter poznavanje sosednjih površin.

Za odločanje je predlagan podporni sistem mehke množice (fuzzy sets decision support system). Sistem upošteva parametre, ki vplivajo na število raziskovalnih mest, potrebnih za ustrezen opis terena. Pri tem se upoštevajo tudi parametri negotovosti in pomanjkanja informacij. Predlagani sistem mehkega sklepanja (Fuzzy Inference System) omogoča, da se na podlagi razpoložljivih kvalitativnih in kvantitativnih informacij oceni število raziskovalnih točk, potrebnih za ustrezen opis terena. Iz predstavljenih primerov je razvidno, da se lahko sistem mehkega sklepanja uporablja kot sistematično orodje za pomoč pri odločanju, za inženirje, ki se ukvarjajo s terenskimi raziskavami.

ključne besede

geotehnično raziskovanje, število sond, mehke množice, mehko sklepanje, negotovosti

FUZZY-SETS DECISION-SUPPORT SYSTEM FOR GEOTECHNICAL SITE SOUNDINGS

DJAMALDDINE BOUMEZERANE, SMAÏN BELKACEMI and BOJAN ŽLENDER

about the authors

Djamalddine Boumezerane
University of Bejaïa,
Civil Engineering Department
Route Targa Ouzemmour 06000 Bejaïa, Algeria
E-mail: dboumezerane@gmail.com

Smaïn Belkacemi
Ecole Nationale Polytechnique,
Civil Engineering Department
10 Avenue Pasteur, Hassan Badi – El-Harrach, Algeria
E-mail: smainbelkacemi@yahoo.com

Bojan Žlender
University of Maribor,
Faculty of Civil Engineering
Smetanova 17, 2000 Maribor, Slovenia
E-mail: bojan.zlender@uni-mb.si

abstract

A geotechnical site investigation is an important and complex task that is generally carried out in two steps. The first step, consisting of preliminary soundings, guides the subsequent site characterization. The number of soundings required to adequately characterize a site is set on the basis of an engineering judgement following the preliminary investigation, this is affected by the geological context, the area topography, the project type, and the knowledge of the neighbouring areas.

A fuzzy-sets decision-support system, considering parameters that affect the number of soundings required to adequately characterize a site, is proposed. Parameter uncertainties and a lack of information are also considered. On the basis of the available qualitative and quantitative information, the proposed fuzzy system makes it possible to estimate, for a common project, the number of site soundings required to adequately characterize the site. The cases presented show that a Fuzzy Inference System can be used as a systematic decision-support tool for engineers dealing with site characterizations.

keywords

geotechnical investigation, soundings number, fuzzy sets, fuzzy inference, uncertainties

1 INTRODUCTION

The complexity of a geotechnical site characterization is a result of the various uncertainties that need to be considered. Tang (1993) used statistical methods and probabilities to detect anomalies in the soil volume. Huang and Siller (1997) used fuzzy logic to characterize the different layers of a soil profile with a limited number of site soundings. Baecher and Christian (2003) considered two steps in the geotechnical site characterization – a site inspection that allows the setting of appropriate hypotheses and a geotechnical investigation consisting of detailed measures to be used in predictive models.

Important construction projects require detailed information about the geometry and the properties of a soil profile. A geotechnical site characterization generally starts with a review of the local and regional geology; after which the soil and rock identifications are obtained through localized site soundings. Obviously, a complete geotechnical site characterization can only be achieved with a large number of site soundings. Testing procedures commonly used to characterize sites are of the destructive type. For economic reasons we cannot identify all the points of the soil mass, and if one is able to circumvent the economic constraints, the integrity of the site could be seriously altered. In many situations, the budget constraints restrict the geotechnical knowledge of the site. A good geotechnical investigation should take into consideration all the available site information and should minimize the sources of uncertainties, while following an in-situ and laboratory-exploration program.

The number, the depth, and the layout of the sampling at a site depend on the geometry of the project, on a preliminary knowledge of the soil profile and on the type of project. Parsons and Frost (2002), in their study on

the quality of a geotechnical investigation, indicate that the data collected from a site investigation represent less than 1/100 000 of the total soil volume. The determination of the number of soundings to undertake is still uncertain and fuzzy.

The sources of uncertainties associated with geotechnical analyses can be classified as: geometrical or model parameter uncertainty, model uncertainty, and human uncertainty. The type of uncertainty can be either quantifiable, random, related to the scatter of data or unquantifiable, epistemic, related to the lack of knowledge (Baecher and Christian, 2003; Christian, 2004; Tang, 1993).

Probabilities were widely used to deal with uncertainties in various geotechnical problems. Zadeh (1965) introduced the concept of the fuzzy set that has led to a new way to treat uncertainty and vagueness in all domains of engineering. In geotechnical engineering, fuzzy sets were used in various problems, like in soil and rock classifications (Huang and Siller, 1997), landslide analysis (Dodagoudar and Venkatachalam, 2000; Giasi et al., 2003), settlement calculations, and in the search for the characteristic values of a ground (Boissier, 2000; Chuang, 1995; Fetz et al., 1999; Hu et al., 2003; Nawari and Liang, 2000; Romo and Garcia, 2003; Santamarina and Chameau, 1989).

The objective of the present work is to outline, by using fuzzy sets, a systematic procedure to determine the appropriate number of site soundings required to achieve satisfactory geotechnical knowledge about the project site.

2 PROBLEM DESCRIPTION

A geotechnical site characterization is undertaken by either regular or random soundings, and the number of soundings is often based on the project engineer's evaluation. The objective of this study is to provide a systematic procedure that allows setting the required number of soundings to adequately identify the project site. Obviously, the greater the number of soundings, the better the knowledge of the site characterization; however, it is ineffective to go beyond a certain number of soundings that will not bring any more knowledge about the site.

The distribution of soundings to be made in a project area does not follow particular rules (Magnan, 2000); it depends on preliminary information, including:

- the geologic context of the project area,
- the topography of the project area,

- the project type,
- the knowledge of the neighbouring areas.

A geotechnical investigation is, generally, carried out in two stages. The first stage is a preliminary study leading to a rough site characterization that may guide a subsequent detailed site characterization. The second stage is a detailed site characterization based on the results of the preliminary study and on the project engineer's evaluation. Cambefort (1980) indicates that there is no precise rule about the number of soundings to be made on a site. He notes that the number of soundings to be made at a site depends on the results of the preliminary study. If an arbitrary loose mesh of soundings, used in the preliminary study, shows that the project area is relatively homogeneous then this number of soundings is satisfactory. However, if the results of the preliminary study show erratic information, the site characterization requires more soundings. The U.S. Corps of Engineers (1994) indicates that, for retaining-structures projects, the number of soundings to be made in the second stage varies from two to five times the number of soundings used in the preliminary stage.

The proposed approach, to determine the number of soundings to handle a geotechnical site characterization, consists of constructing an inference system based on fuzzy sets. Parameters, like the site's geologic nature, the site's topography and the project type, which may affect the number of soundings, are described. The theory of fuzzy sets makes it possible to treat parameters having vague or doubtful information as well as treating problems presented in linguistic or qualitative form. Each parameter entry (Input) of the system indicates if more or less soundings are required. The construction of the Fuzzy Inference System (FIS) allows us to implement the rules considered, by taking into account their weights, and to evaluate the final decision. The Fuzzy Inference System has the advantage of considering non-statistical uncertainties, such as inaccurate or vague variables.

3 FUZZY SETS AND INFERENCE SYSTEM

The concept of fuzzy sets consists of replacing standard sets (Crisp Sets) whose elements are discrete and carry only punctual values with sets whose elements are taken as belonging to a set with a degree of membership varying from zero to one [0,1]. Zadeh (1965) defines a fuzzy set as a class of objects with continuous degrees of membership. This set is characterized by a membership function that assigns to every object a degree of membership varying between zero and one.

3.1 FUZZY INFERENCE

A fuzzy inference model is generally based on the following three fundamental steps (Saboya et al., 2006):

- Selection of the Input and Output variables
- Description of the Input-Output fuzzy relation rules,
- Defuzzification, consisting of transforming the linguistic Output variables to values.

In the considered problem, various entry sets (Input) of the system are taken into account. These entry sets can be the geologic nature of the ground, the on-site slope, the project type, etc. The Output sets express themselves in terms of the density of the soundings on site (Important, Average, and Weak).

The fuzzy rules of the system are expressed as follows:

IF X IS A THEN Y IS B .

where A is the entry set and B the output set. These rules will be executed in parallel during the inference. An example of a fuzzy rule in our case can be as:

IF “*Relatively Known Geology*” THEN “*Moderate the number of soundings on the site*”.

The suitable selection of the elements for the entry sets is fundamental. Elements of the entry sets are of linguistic or qualitative form, such as the geology of the project area. For a “Known” geology, what will be the degree of knowledge that can be attributed to it? Collecting the knowledge is the difficult part in the development of the inference system. Santamarina and Chameau (1989) have noted that the information knowledge to be incorporated into a decision system is of most importance.

3.2 INFERENCE SYSTEM PARAMETERS

The proposed decision system is based on incomplete available information related to entry parameters, among which are:

- Site topography,
- Site geology,
- Site geotechnical conditions,
- Information on surrounding sites,
- Project type to be built.

The site topography is expressed in terms of the slopes in the project area; depending on the slope’s intensity, the site is classified as “Strongly tilted”, “Averagely tilted” and “Weakly tilted”. The slope of the site will affect our decision about the required number of soundings to be made. The more important the slope is the more soundings will be required to characterize the site. The fuzzy sets used are of triangular and trapezoidal shape, as indicated in Fig. 1.

The site geology is expressed in terms of “Known”, “Relatively Known” or “Unknown Geology”. The use of geologic maps is necessary to have an initial idea about the geologic formations constituting the site, their properties, as well as the possibilities of inadequate or adverse geologic details. Clayton et al (2005) recommend, for geotechnical studies, to use geologic maps with a scale of 1/2500. The fuzzy set “Geology” is classified as “Known Geology”, “Relatively Known Geology” and “Unknown Geology”.

The more we know the geology; the less will be the required number of soundings. If the maps indicate variability and erratic subsurface conditions, then more soundings will be required to better characterize the site (F.H.W.A, 2002). The degree of knowledge is scaled between 0 and 100%; it indicates the knowledge level of the site’s geological aspect. A map at a scale of 1/2500 provides a “Known Geology” at 80%, when a map scaled at 1/30000 does not furnish enough information. The set was constructed using the results of a questionnaire distributed to engineers and experts (Boumezerane, 2010). Fig. 2 illustrates the fuzzy set “Geology”.

If the geological maps show, for the site being considered, various soil horizons, it will be necessary to make more

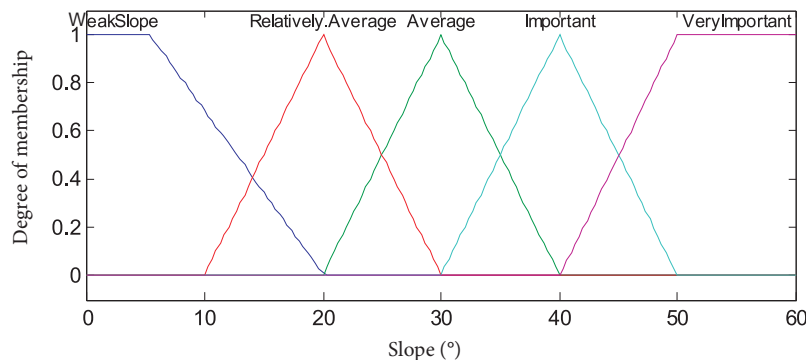


Figure 1. The fuzzy set “Topography-Slope of the site”.

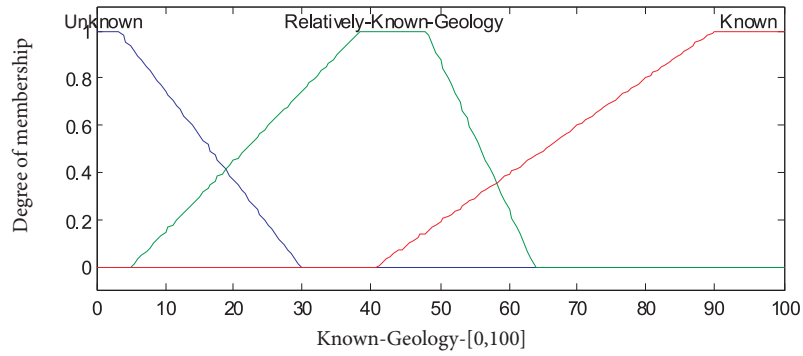


Figure 2. Fuzzy set “Known Geology” depending on the degree of information.

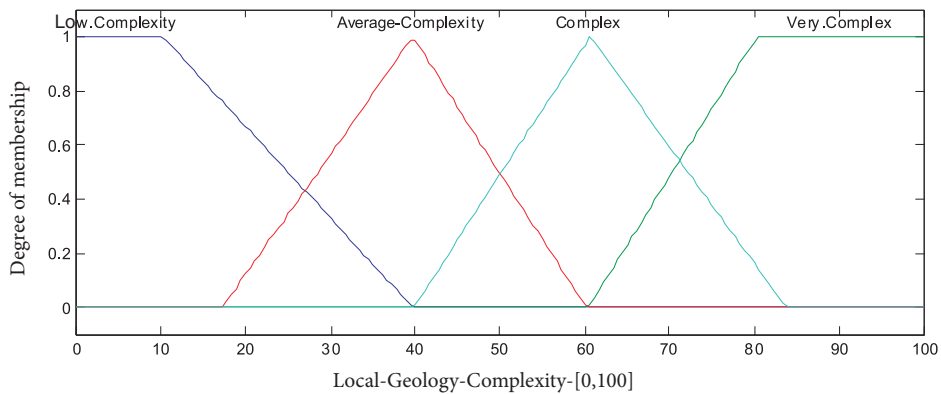


Figure 3. Fuzzy representation of “Local-Geology Complexity”.

soundings than if there was only a single soil horizon. The spacing of the borings depends on the geology of the area and may vary from one site to another. The fuzzy set “Local Geology Complexity” reflects the complexity of the site’s local geology. Expressed as a “Degree of complexity” of the local geology, it ranges between [0,100] with the linguistic attributes “Low-Complexity”, “Average Complexity”, “Complex” and “Very Complex”. The membership functions and limits of the set are given in the following Fig. 3.

Ground geotechnical conditions can be incorporated using “Good strength, Medium strength or Weak strength” according to the average soil profile; universally accepted literature results can be used for this purpose. The quality of the ground geotechnical conditions is an important factor in defining the soundings’ layout. When available, this information is generally given by the average trend of the soil (or rock) resistance. The weaker the quality of the geotechnical conditions, the more soundings are required. Fuzzy sets with elements based on the static modulus are used to set the

geotechnical conditions of the soil. We used results given by Bowles (1977) to construct these sets (Fig. 4).

A geotechnical survey is generally made in two steps. In the first, preliminary soundings are used to guide the subsequent site characterization. The number of borings in the second step should be greater than in the preliminary phase. No exact spacing is recommended, as the boring layout should be controlled by the geologic conditions, the geotechnical aspect and the project type.

Preliminary soundings indicate a trend about the ground variability. The horizontal variability of the soil parameters influences the number of boreholes to execute. The higher the variability, the more important is the number of boreholes to execute. Significant dispersions of the soil parameters necessitate planning more soundings; otherwise a moderate number of soundings will be sufficient. Available data on the neighbouring sites can be used as the parameters of entry. If the surrounding sites’ results are close to those obtained in the site’s preliminary investigation, then the number of soundings to be performed

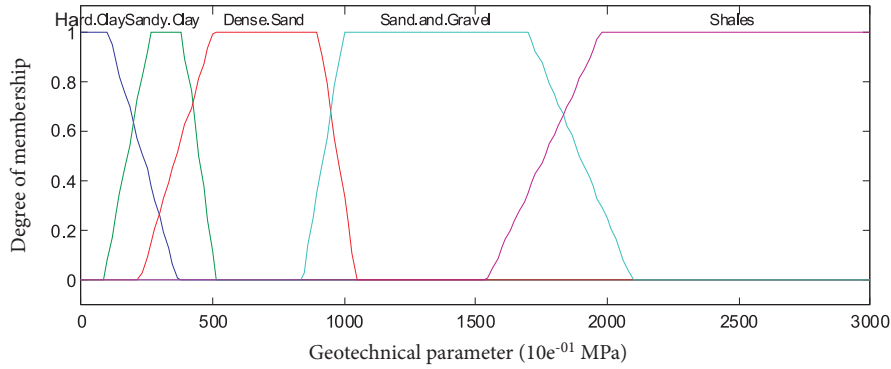


Figure 4. The fuzzy set “Geotechnical conditions” based on the Static Modulus of Soil.

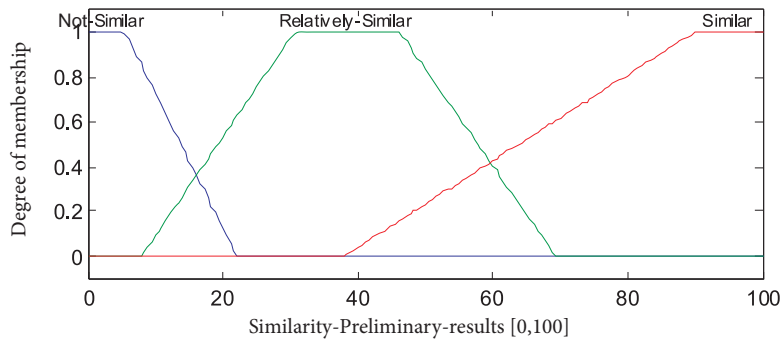


Figure 5. The fuzzy set “Similarity of preliminary results”.

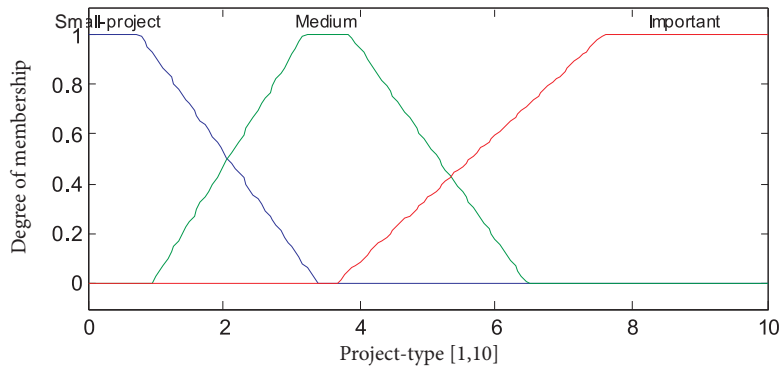


Figure 6. The fuzzy set “Type of project”.

can be moderate, and if they are highly dispersed, it will be necessary to increase this number of soundings. The fuzzy set expressing the engineer’s judgement on the results’ similarity is given in Fig. 5.

The project type indicates whether a dense layout of the soundings is required. For the same area, when different projects are expected, each one will necessitate a different number of soundings, depending on their loading importance; a multi-storey building needs more sound-

ings on site than a simple hall with the same area. The geometry of the project guides the spatial distribution of the soundings, which will be located according to the global shape of the building’s area and by considering specific areas of the project.

The elements of the fuzzy set are expressed as “Important”, “Medium” and “Small”, depending on the loading induced by the project size, as indicated by Fig. 6.

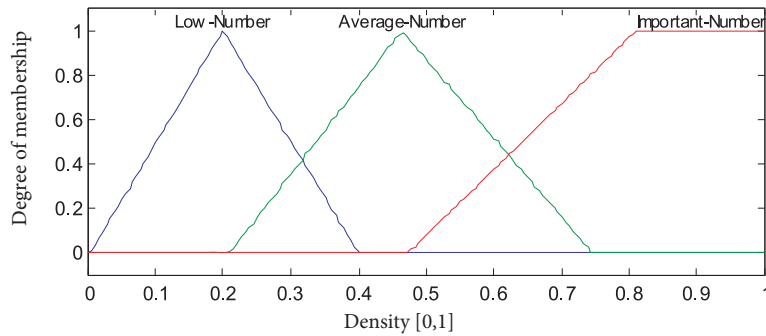


Figure 7. Output fuzzy set “Density of soundings”.

The quoted parameters have important effects on the site-characterization procedure. They are expressed under linguistic and qualitative forms. They are assumed to be the input parameters of the inference system.

The Output set of the fuzzy system to construct is represented by a density, from 0 to 1, which will be transformed into the number of soundings, depending on the site conditions, and the minimum number of soundings required by the codes of practice. The linguistic labels of the fuzzy set Output are “Low”, “Average” and “Important”. Their membership functions are illustrated in Fig. 7.

4 INFERENCE SYSTEM DESIGN

The parameters of entry (Input) are expressed as fuzzy sets (Geology, Topography, Type of project, and Information about neighbouring sites, etc). The Output parameter

is represented by a fuzzy set of the soundings’ density on site. Each of these Input parameters influences, in a certain way, the number of soundings to perform on the site. Fuzzy Rules are constructed based upon the parameters available; they relate the Input to the Output (Fig. 8).

These fuzzy rules are expressed, generally, in a linguistic form and consider various possibilities; their number depends on the parameters taken into account and on the form of those rules. We used rules in the form IF A THEN B; for example, IF “Geology” is “Unknown” THEN “Important” number of soundings, etc. The Mamdani scheme of inference is used (Saboya et al., 2006). After the aggregation and defuzzification a weight G of decision is calculated. The defuzzification result G is given in a weight form and considered as a density of soundings to perform on site and varying between zero (0) and one (1). For values of G close to 1, it will be necessary to carry out an important number of soundings on the site. On the other hand, if G is near 0, then the number of soundings will be low.

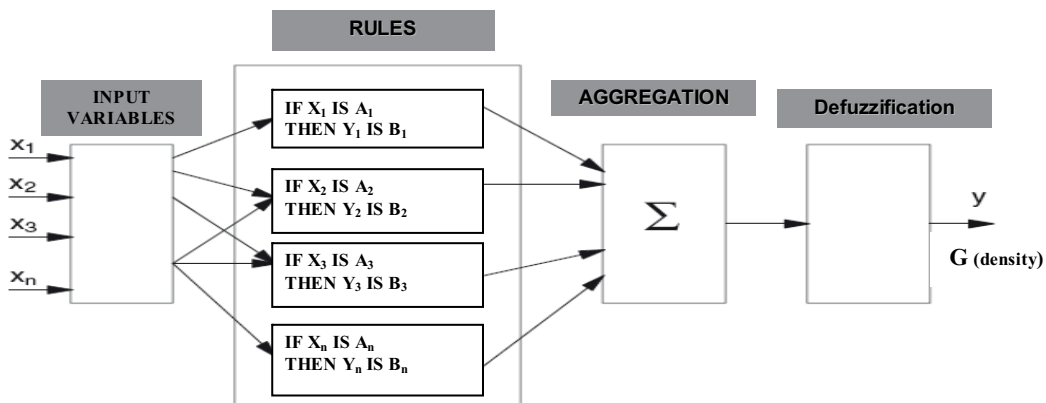


Figure 8. Scheme of the Fuzzy Inference System.

To translate this result into the number of soundings, it is necessary to calibrate the fuzzy model used to the guidelines that set the minimum soundings (Eurocode 7 1996, F.H.W.A 2002).

For this purpose, the Fuzzy Inference System is run with the following Input Parameters: Slope ($^{\circ}$), Geotechnical conditions (MPa, m/s), Project type, Known-Geology (%), Local Geology Complexity (%), Similarity of Preliminary Results (%) and Specifically Loaded Zones. The extreme defuzzification results in weight form were $G=0.201$ and $G=0.810$. The first result is obtained in the case of extremely favourable conditions (Topography (0°), Known-Geology (100%), etc.), and few soundings are necessary to characterise the site. The second result expresses the case of extremely unfavourable conditions (Unknown Geology, Important Variability, etc) and the necessity of making a large number of soundings.

4.1 TRANSFORMATION OF THE FUZZY INFERENCE SYSTEM (FIS) RESULT G INTO A NUMBER OF SOUNDINGS

The result G of the Fuzzy Inference System expresses the density of soundings on the site. To transform this density G into an optimum number of soundings N_{opt} we introduced N_{ref} , the reference number of soundings required by codes (Eurocode 7 1996, F.H.W.A 2002), and a weight G_{ref} corresponding to $N_{ref} \cdot G_{ref}$ is comprised in the interval of the possible results of the FIS.

For G corresponding to the “Optimum number of soundings N_{opt} ”

and

For G_{ref} corresponding to the “Reference number of soundings N_{ref} ”

we obtain

$$N_{opt} = (N_{ref} \cdot G) / G_{ref} \quad (1)$$

G_{ref} is set to correspond to the reference number N_{ref} of soundings given by the codes. N_{ref} depends only on the area of the project.

4.2 RECOMMENDATIONS FROM CODES ON THE NUMBER OF SOUNDINGS N_{REF}

Some technical documents recommend “guidelines” to set the required “minimum” sub-surface data to achieve a cost-effective, geotechnical design. The guidelines point out the dependency of the number of borings upon the type of project and its requirements. However,

there are no “rigid” rules that are established for this objective (F.H.W.A, 2002). The required “minimum” number of soundings (N_{ref}) can be set through these guidelines, and it is obvious that beyond a certain number of soundings there will be an information redundancy that will not lead to a better knowledge of the site. One of the objectives of this study is to provide a systematic procedure to check whether more than a minimum number of soundings are required to characterize the site.

The guideline (“minimum” boring, sampling and testing criteria) edited by F.H.W.A (2002) indicates, for the case of the Structure Foundation, a minimum number of borings of “one (1)” per substructure unit under 30m in width and “Two (2)” per substructure unit over 30m width. Additional borings are recommended in the case of erratic subsurface conditions. Eurocode 7 (1996) recommends, for large projects, one borehole for distances between 20m and 40m. According to Simons et al. (2002) the spacing for boreholes, for structures’ foundations, often lies in the range 20m to 40m. The borehole layout and frequency are partly controlled by the complexity of the geological conditions. If the ground conditions are relatively uniform, a wide spacing of boreholes may be satisfactory, but if the ground conditions are complex a closer spacing of boreholes will be required (Simons et al., 2002).

The number of soundings as set by F.H.W.A (2002) or by Simons et al. (2002) and Eurocode 7 (1996) depends only on the area of the project; other parameters that can influence the number of borings are not considered, such as soil variability, geotechnical and geological site conditions, the type of project, etc. The approach we propose permits taking into account those parameters whose information is generally qualitative and fuzzy sets are a suitable tool to use in this case.

4.3 CALIBRATION OF A REFERENCE G_{REF}

In order to apply the FIS to real sites, we calibrate a certain G_{ref} with codes (Eurocode 7 1996, F.H.W.A 2002) giving indications on the “minimum” number of soundings, noted here N_{ref} , depending only on the area of the project site.

The previously defined G_{ref} is set to correspond to the reference number N_{ref} of soundings given by the codes. The extreme defuzzification results of the Fuzzy Inference System are $G=0.201$ and $G=0.810$. As all the values of G are included in the interval $[0.201, 0.81]$ we can consider G_{ref} as the mean value of the results range, then:

$$G_{ref} = (0.201 + 0.81)/2 = 0.505$$

This G_{ref} is taken as corresponding to the reference number N_{ref} of soundings equal to the mean of the Eurocode 7 recommendations, one sounding between 20 to 40 m. In this case N_{ref} will be one boring every 30 m of the project area.

Using expression (1) we can then predict the optimum number of soundings N_{opt} for a site's geotechnical investigation using the fuzzy inference system.

The calibration of $G_{ref}=0.505$ makes it possible to predict the extreme values of N_{opt} for $G=0.201$ and $G=0.810$.

We obtain for the reference mean value from Eurocode 7, $N_{ref}=1/(30 \times 30 \text{m}^2)$;

$$N_{opt} = (N_{ref} \cdot G)/G_{ref} = \\ = N_{min} = 1/30 \times 30 \cdot 0.201/0.505 = 1/(48 \times 48) \text{m}^2,$$

one sounding for an area of $48 \times 48 \text{m}^2$ as a minimum number. This number is smaller than the minimum proposed by Eurocode 7, $N_{min}=1/40 \times 40 \text{m}^2$.

And

$$N_{max} = (1/(30 \times 30) \cdot 0.810 / 0.505 = 1/(24 \times 24) \text{m}^2,$$

one sounding for an area of $24 \times 24 \text{m}^2$, which is the maximum number, and in this case less important than the proposed one by Eurocode 7, one sounding for an area of $20 \times 20 \text{m}^2$.

In a second stage we standardize G_{ref} by using the minimum value of the interval $[0.201, 0.810]$, $G_{ref}=0.201$ and calibrate it with the minimum number of soundings N_{ref} recommended by Eurocode 7 (one boring every $40 \times 40 \text{m}^2$).

We obtain, in this case, the extreme values of N_{opt} for $G=0.201$ and $G=0.810$;

$$N_{opt} = (N_{ref} \cdot G)/G_{ref} = \\ = N_{min} = 1/(40 \times 40) \cdot 0.201/0.201 = 1/(40 \times 40) \text{m}^2,$$

one sounding every $40 \times 40 \text{m}^2$, as the minimum and

$$N_{max} = 1/40 \times 40 \cdot 0.810/0.201 = 1/(20 \times 20) \text{m}^2,$$

one sounding for an area of $20 \times 20 \text{m}^2$, representing the maximum number of borings.

The obtained numbers agree with those recommended by Eurocode 7, one boring every $40 \times 40 \text{m}^2$ as a minimum and one boring for $20 \times 20 \text{m}^2$ representing the maximum number.

Then, for a given site, for which an investigation is planned, we can use G_{ref} as a calibration from Eurocode 7; this allows us to have a range of values for N_{opt} .

The recommendations from F.H.W.A (2002) set a minimum number N_{ref} of soundings every 30m. We may use $G_{ref}=0.201$ as corresponding to this minimum number, and we can expect the maximum number of borings N_{max} by using $G=0.810$ as the upper limit of the FIS results range. Expression (1) gives in this case:

$$N_{opt} = (N_{ref} \cdot G)/G_{ref} = \\ = N_{max} = 1/(30 \times 30) \cdot 0.810/0.201 = 1/(15 \times 15) \text{m}^2,$$

one sounding for an area of $15 \times 15 \text{m}^2$.

The obtained N_{max} is greater than the maximum recommended by Eurocode 7 ($1/20 \times 20 \text{m}^2$).

5 APPLICATIONS

5.1 EXAMPLE 1

In this example the data is available and the number of performed soundings on site is known. The Fuzzy Inference System is run using the available parameters and the result is used as a comparison.

The site is described in "Adaptive Ground Modelling in geotechnical engineering" (Schönhardt and Witt, 2003). The main characteristics of the project are, as shown in Fig. 9.

- Surface area of study: $(100 \times 250) \text{m}^2$, Area of the project $(83 \times 205) \text{m}^2$, Type of the project: Industrial; Topography: Plane; Geology (Degree of information): Relatively unknown; Preliminary results show three geological formations (Silty Clay with soft consistency, Stiff Clay between 8-14m, Sandy clay until 70m depth); Specifically loaded zones (Machines): $(20 \times 60 + 2 \times (20 \times 25)) \text{m}^2$ approximately $(1200 + 1000) = 2200 \text{m}^2$, the specifically loaded area ratio is: $2200 / (83 \cdot 205) = 13\%$ of the total project area; No information available about neighbouring sites; The preliminary results show similarity (similarity around 60%); Number of preliminary soundings 8, performed at site corners, and at middle distance, and the total number of driven borings is 28 (considered here as optimum N_{opt}).

For this example, the Fuzzy Inference System parameters were set to: Slope is "Low" with a mean value around 3°, the Geologic knowledge of the site is taken as "fair"

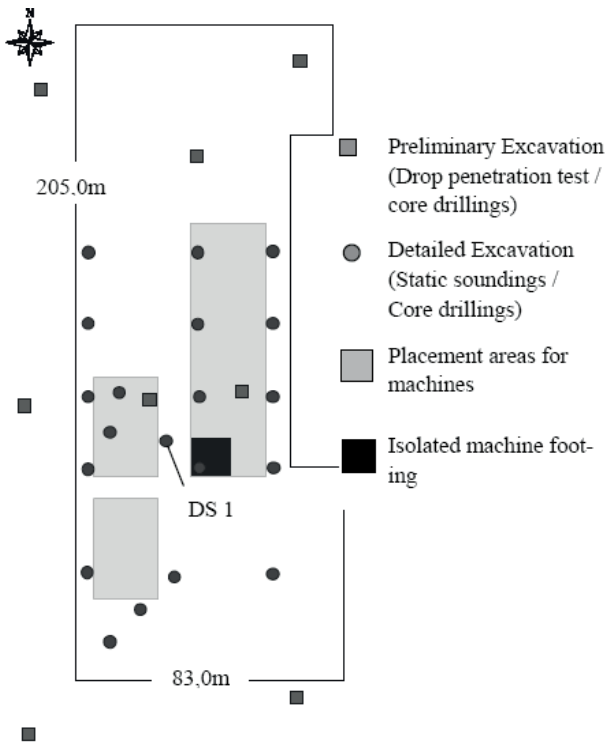


Figure 9. General view of the site of the study – performed soundings are mentioned (After Schönhardt and Witt, 2003).

around 15% (no geological maps are available) and the Geological complexity is “Average complexity”. The preliminary soundings indicate that three formations are quoted and they show a certain similarity between the results (around 60%). In this industrial project, the number of zones to be subjected to a specific loading (machines) is relatively important, as indicated in Fig. 9.

The number of soundings (28) given by Schönhardt and Witt (2003) was considered to be sufficient to obtain a good knowledge of the site.

The reference number of soundings N_{ref} deduced from the mean of the Eurocode 7 recommendations is 18 for the area of the project (one sounding every 30m).

We applied the Fuzzy Inference System given the site's conditions and the result was $G=0.565$, which reflects in a certain way the real site conditions, including the constraints associated with the complexity of the geology and the nature of the project.

Using (1) we calculate the optimum number of soundings N_{opt}

$$N_{opt} = N_{ref} \cdot G/G_{ref} = 18 \times 0.565 / 0.505 = 21 \text{ soundings}$$

The obtained number of borings is fewer than the 28 soundings used in the site.

In the second stage we use $G_{ref}=0.201$, the lower value of the interval of results $[0.201; 0.81]$, as corresponding to the minimum number of boreholes N_{ref} given by Eurocode 7, one borehole every 40m. For the surface of this project we obtain $N_{ref}=10$ soundings. Then using expression (1) again we can predict the optimum number of soundings N_{opt} for this site:

$$N_{opt} = 10 \cdot 0.565 / 0.201 = 29 \text{ soundings.}$$

The predicted number of soundings in the second stage is almost the same as the one given by Schönhardt and Witt (2003). Based on the results of the FIS, the proposed optimum number N_{opt} of soundings is between 21 and 29.

5.2 EXAMPLE 2

The site of the proposed building addition is located on the side of an existing High School. It consists of a two- and three-storey building with a footprint of approximately 6500m². It is assumed that the loads will be typical for a building of this size and type (Strater and McKown, 2002).

A preliminary investigation was carried out and this consisted of two test borings BHB-1 and BHB-2(OW). They were drilled, within the footprint of the proposed project, to depths of approximately 12.3m and 12m. Test pits were previously excavated in the vicinity of the existing buildings to determine the subsurface soil and groundwater conditions adjacent to the existing foundations.

The subsurface conditions observed indicate:

Topsoil: very thin layer of silt.

Fill: encountered in the vicinity of most of the proposed project location is around 1m thick and consists of medium-dense brown Silty Sand. In TP1 and TP2 it consists of brown Sandy Silt with Gravel and Sandy lean Clay.

Marine Deposits: encountered in borings BHB1 and BHB2 (OW) consisted of medium dense to dense poorly graded Sand with Silt and Silty Sand. The thickness ranges from 11.3m to 13.7m in the southern portion of the site. In the northern part the thickness varies from about 0m, up to 4.5m to 6m.

Glacial Till: Consisting of very dense Sand with Silt and Gravel. These soils were encountered below the marine deposits in BHB2 (OW) at a depth of about 11.30m.

Glacial Till was not encountered in the boring BHB1. It was anticipated by the engineers that a discontinuous layer of Glacial Till, ranging in thickness from about 0 to 1.5m, is present throughout most of the site.

Bedrock: Was encountered in Test Pits TP-3 and TP-6 at depths of around 1m. But it was not encountered with the conducted borings.

Engineers in charge of the preliminary investigation recommended a subsurface exploration program of three to five additional test borings and three to five test probes within the footprint of the proposed building.

5.2.1 THE USE OF THE FUZZY INFERENCE SYSTEM

To use the Fuzzy Inference System, some of the entry parameters from the site are defined as below:

- The slope is relatively average (25%), corresponding to a mean of 15°; The information about adjoining sites exists and could be exploited; The type of project to implant is a High School of three storeys; The geology is “Relatively Unknown” and it is suspected to have a great degree of soil variability, according to the soil layers encountered in the preliminary investigation; The results of preliminary tests (two boreholes) indicate important differences. The degree of similarity between them was taken as very low; According to the engineers the loads are typical for a building of this size and type; the modulus of the layer of Sand with Silt and Silty Sand ranges from 10 to 25MPa.

The defuzzification weight result obtained with the inference system is $G=0.546$.

In order to calculate the optimum number of soundings for this site, we first use $G_{ref}=0.505$, corresponding to the mean “reference” number of soundings from Eurocode 7 (1996). The required number of soundings for this surface (6500m²) is $N_{ref}=6$.

Using the result G of the Fuzzy Inference System on this site and expression (1) it is possible to expect an optimum number of boreholes;

$$N_{opt} = N_{ref} \cdot G/G_{ref} = 6 \cdot 0.546/0.505 = 7 \text{ soundings}$$

When using $G_{ref}=0.201$ corresponding to the “minimum” number of soundings N_{ref} recommended by Eurocode 7 (1996), and for an area of 6500m² ($N_{ref}=4$ soundings), we obtain:

$$N_{opt} = N_{ref} \cdot G/G_{ref} = 4 \cdot 0.546/0.201 = 12 \text{ soundings}$$

The result of the Fuzzy Inference System is in the same range as proposed by the engineers in charge of this geotechnical study. They have proposed a total number of soundings that ranges from 8 to 12.

If the engineer’s judgement, relative to the recommended number of borings, is considered to be reliable, then the Fuzzy Inference System used independently to evaluate the optimum number of soundings shows consistent results (from seven to twelve soundings).

6 EVOLUTION OF DENSITY G WITH REGARD TO THE INPUT PARAMETERS

The available input parameters are various and influence the density of soundings, each one in a certain way. Fig. 10 shows the variation of the Geological-complexity and Geotechnical parameters and their influence on the results when other parameters are taken constant. The surface presents a plateau of important values of G when the Geology is Complex and the geotechnical formations are relatively weak.

Another example illustrating the variation of G as a function of input parameters is given in Fig. 11 where the Known-Geology and Geological-Complexity vary and present a surface of an important density of boreholes when Geology is less known and more Complex. Those figures show the possibilities given to describe the variations of G depending on the different parameters. The fuzzy inference system is able to simulate different situations, and helps engineers to take decisions when dealing with a geotechnical investigation.

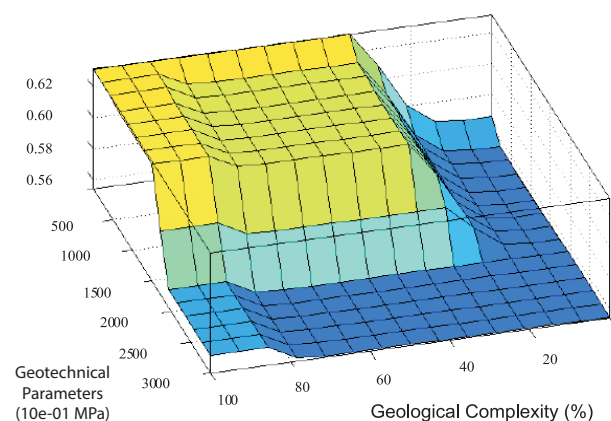


Figure 10. Influence of Geotechnical parameters and Geological Complexity on the density of the soundings (Known Geology 5%, Project Type 5, Similarity 50%).

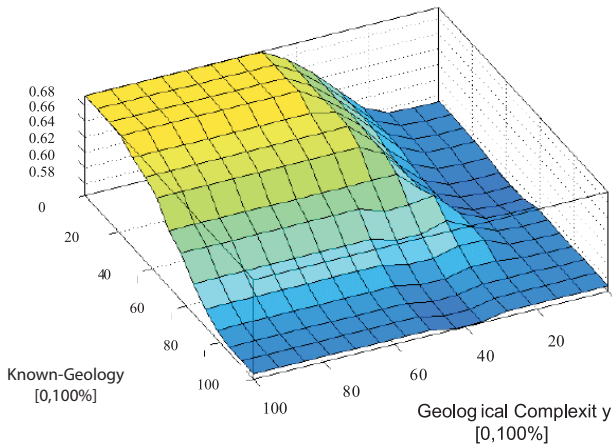


Figure 11. Influence of Known Geology and Geological Complexity on the density of the soundings (Geotechnical parameters 20MPa, Project Type 5, Similarity 5%).

6.1 COMPARISON OF FIS RESULTS WITH REGARD TO CODES (EUROCODE 7, F.H.W.A)

The following figures show the minimum number of soundings recommended by Eurocode 7 and the optimum number obtained using our approach with some parameters of entry (Known-Geology, Geology-Complexity). The project’s area is varying from small to important surfaces.

Figures 12 and 13 illustrate the ability of the FIS to work with available parameters of entry that can influence a geotechnical investigation. Two parameters (Known-Geology, Geology-Complexity) are used here for an illustration. The results show the differences between the recommendations of Eurocode 7 and the expected optimum number of soundings. The differences are increasing proportionally when the area of the project is becoming important. The FIS allows us to handle the available information and we note from Fig.12 and 13 the influence of local geology complexity when it decreases. We set those recommendations as the starting points for the Engineer when dealing with Geotechnical Investigations. The more information we have the easier and more precise will be the investigation.

7 CONCLUSION

A Fuzzy Inference System is developed to handle uncertainties occurring in a geotechnical site-characterization campaign. The main idea is to reproduce the site engineer’s reasoning to set the number of soundings to perform the site characterization. Various interfering parameters have to be considered in this case. Knowledge of Geology is an important part. The nature of the project to be built and the topography of the site affect the density of the soundings. Fuzzy sets are used to

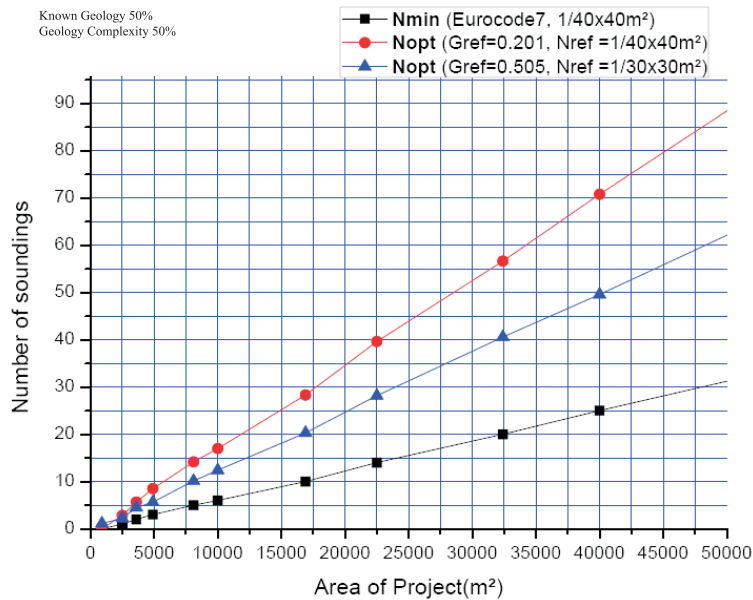


Figure 12. Optimum number N_{opt} of soundings using FIS compared to N_{ref} (Eurocode 7) (“Known-Geology” 50% and “Geology Complexity” 50%).

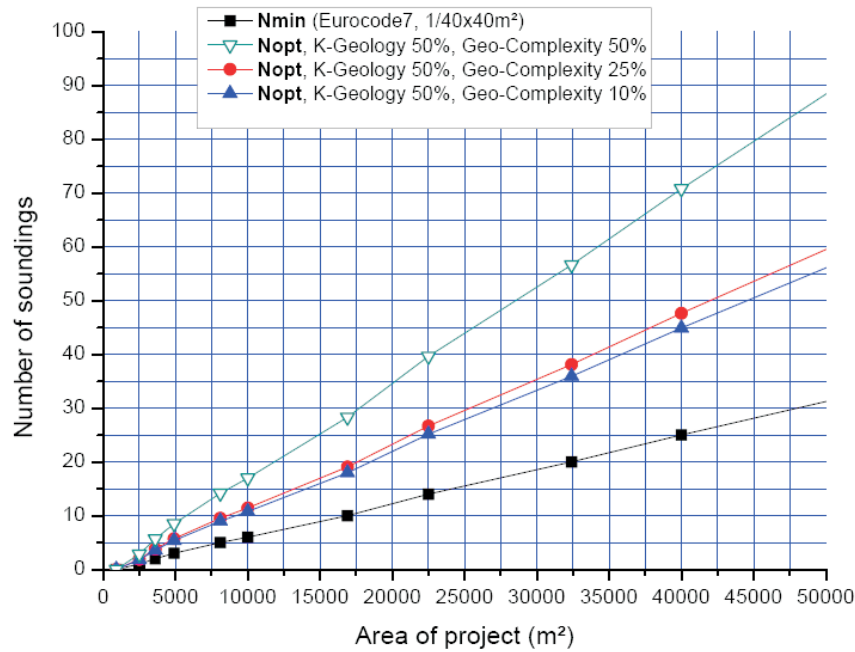


Figure 13. Optimum number of soundings compared to N_{min} (Eurocode 7) (Different cases of “Known-Geology” 50% and “Geology Complexity” 10%, 25%, 50%).

represent site-characterization parameters with possibilities to consider linguistic and qualitative information. They also make it possible to handle the uncertainties contained in the parameters. The fuzzy system consists of the Input Parameters (Geology, Topography, etc) and the Output parameters (Density of Soundings on the Site). Each entry parameter contributes to the weight of the decision. The fuzzy system assembles all the influences and aggregates them to obtain a fixed number, between 0 and 1, representing the optimum number of soundings to be performed on the site. The cases presented show the effect of the various parameters, and reveal the efficiency of the fuzzy sets used to represent the site-characterization parameters. The fuzzy inference system considers the influence of each individual entry parameter and computes the global, optimum density of the soundings relative to recommendation guidelines. The result is given in the form of a weight indicating the decision to be taken by the engineer. The available guidelines (F.H.W.A, 2002; Simons et al., 2002) give indications, depending on the project dimensions, on the number of borings required to characterize the site soil.

Confidence degree in the Fuzzy Inference System allow us to relate, for known cases, the weight G to the “optimum” number of soundings N_{opt} . The weight G_{ref} , corresponding to the “reference” number of soundings N_{ref} recommended by technical guidelines (Eurocode

7, FHWA), is then deduced and was set as a standard value, allowing us to calculate the “optimum” number of soundings for common sites.

The cases presented show that the Fuzzy Inference System can be used as a systematic decision-support tool for engineers dealing with the site’s characterization. The system is a step beyond the technical guidelines that set the required minimum number of soundings to characterize the site soil. The fuzzy inference system tells the engineer if more than the minimum number of soundings are needed to characterize the site.

REFERENCES

- Baecher, G.B. and Christian J.T. (2003). Reliability and Statistics in Geotechnical Engineering. Wiley Ed.
- Boumezerane D. (2010). Questionnaire about Geology and Soil Variability for Geotechnical Investigations. Department of Geotechnics, University of Maribor, Slovenia.
- Cambefort, H. (1980). Géotechnique de l’Ingénieur, reconnaissance des sols. Eyrolles Editeur – Paris.
- Christian, J.T. (2004). Geotechnical Engineering Reliability, How Well Do We Know What We Are Doing? Journal of Geotechnical and Geoenvironmental Engineering 130(10), 985-1003.

- Clayton, C.R.I., Matthews, M.C. and Simons, N.E. (2005). Site Investigation. Department of Civil Engineering, University of Surrey.
- Dodagoudar, G.R. and Venkatachalam, G. (2000). Reliability analysis of slopes using fuzzy sets theory. *Computers and Geotechnics* 27, 101-115.
- EUROCODE 7, (1996). Section 3. Données géotechniques, AFNOR.
- Fetz, J., Jäger, J., Köll, D., Krenn, G., Lessmann, H., Oberguggenberger M. And Stark, R.F. (1999). Fuzzy models in geotechnical engineering and construction management. *Computer-Aided Civil and Infrastructure Engineering* 14 (2), 93-106.
- F.H.W.A (2002). Sabatini, P.J, Bachus, R.C., Mayne, P.W., Schneider J.A. and Zettler T.E. Geotechnical Engineering Circular 5 (GEC5) - Evaluation of Soil and Rock Properties, Report No FHWA-IF-02-034. Federal Highway Administration, U.S. Department of Transportation.
- Giasi, C.I., Masi, P. and Cherubini, C. (2003). Probabilistic and fuzzy reliability analysis of a sample slope near Aliano. *Engineering Geology* 67, 391-402.
- Hu, Z., Chan. C.W. and Huang, G.H. (2003). A fuzzy expert system for site characterization. *Expert Systems with Applications* 24, 123-131.
- Huang, Y.T. and Siller, T.J. (1997). Fuzzy Representation and Reasoning in Geotechnical Site Characterization. *Computers and Geotechnics* 21(1), 65-86.
- Magnan, J.P. (2000). Quelques spécificités du problème des incertitudes en géotechnique. *Revue Française de Géotechnique* 93, 3-9.
- Nawari, N.O. and Liang, R. (2000). Fuzzy-based approach for determination of characteristic values of measured geotechnical parameters. *Canadian Geotechnical Journal* 37, 1131-1140.
- Parsons, R.L. and Frost, J.D. (2002). Evaluating Site Investigation Quality using GIS and Geostatistics. *Journal of Geotechnical and Geoenvironmental Engineering* 6, 451-461.
- Romo, M.P. and Garcia, S.R. (2003). Neurofuzzy mapping of CPT values into soil dynamic properties. *Soil Dynamics and Earthquake Engineering* 23, 473-482.
- Saboya, F.Jr., Alves, M.G. and Pinto, W.D. (2006). Assessment of failure susceptibility of soil slopes using fuzzy logic. *Engineering Geology* 86, 211-224.
- Santamarina, J.C. and Chameau, J.L. (1989). Limitations in decision making and system performance. *Journal of performance of Constructed Facilities* 3(2), 78-86.
- Schönhardt, M. and Witt, K.J. (2003). Adaptive Ground Modelling in geotechnical engineering. Proceedings of the International Symposium on Geotechnical measurements and Modelling, 23-25 September 2003, Balkema Publishers Karlsruhe (Germany), 297-305.
- Simons, N., Menzies, B. and Matthews, M. (2002). A Short course in Geotechnical Site Investigation. Thomas Telford Ed.
- Strater, N.H. and McKown, A.F. (2002). Draft Report on preliminary geotechnical studies, Proposed Beverly High School Building Addition, Beverly, Massachusetts. Haley & Aldrich Inc., Boston Massachusetts, June 2002, file N° 28022-001.
- Tang, W.H. (1993). Recent developments in geotechnical reliability, Probabilistic Methods in Geotechnical Engineering, pp.03-27. Li & Lo (Eds) Balkema.
- U.S. Corps of Engineers, 1994. Geotechnical Investigation, Report N° EM 1110-2-2504, March 1994.
- Zadeh, L.A. (1965). Fuzzy Sets. *Information and Control* 8, pp. 338-353.

GEO-INFORMACIJSKA TEHNOLOGIJA ZA OCENO TVEGANOSTI NESREČ

ĐORĐE ĆOSIĆ, SRĐAN POPOV, DUŠAN SAKULSKI I ANA PAVLOVIĆ

o avtorjih

Đorđe Ćosić
University of Novi Sad,
Faculty of Technical Sciences
Trg Dositeja Obradovića 6, 21000 Novi Sad, Srbija
E-pošta: djordjecosic@uns.ac.rs

Dušan Sakulski
United Nations University,
Institute for Environment and Human Security (UNU-EHS)
UN Campus, Hermann-Ehlers-Str.10, 53113 Bonn, Nemčija
E-pošta: dsakulski2@me.com

Srđan Popov
University of Novi Sad,
Faculty of Technical Sciences
Trg Dositeja Obradovića 6, 21000 Novi Sad, Srbija
E-pošta: boromir@uns.ac.rs

Ana Pavlović
University of Novi Sad,
Faculty of Technical Sciences
Trg Dositeja Obradovića 6, 21000 Novi Sad, Srbija
E-pošta: annaftn@uns.ac.rs

izvleček

Srbsko področje (skupaj s področjem bivše Jugoslavije) je nenehno izpostavljeno različnim tveganjem, ki imajo pogosto tragične posledice. Potresi in poplave, ki jim običajno sledijo plazovi, so najbolj pogosta tveganja v tej regiji. V Srbiji nimamo sistema zmanjševanja tveganja katastrof, preprečevanja in zgodnjega opozarjanja kot integralnega dela dolgoročnega razvoja. To je eden glavnih razlogov, zakaj je škoda ob nesrečah tako velika. V Srbiji nimamo znanstveno podprtih in standardiziranih postopkov za oceno tveganosti nesreč. Postopki obstajajo samo na področju tehničnih ocen tveganj.

Metoda ocenjevanja tveganja, ki jo predstavlja naša raziskava, vsebujejo poleg tveganj parametre kot so ranljivost, izpostavljenost in varnost. Vsebuje tudi okoljske in družbene komponente nevarnosti. Predlagano metodo, ki vključuje kombinirana matematična in 3D GIS orodja, smo uporabili za območje Donave, Petrovaradina (del Novega Sada), za katero smo imeli na razpolago podatke. Odnos med parametri tveganja smo izračunali in grafično predstavili. Metode kot je ta bi morale, v Srbiji in zahodno balkanski regiji, prispevati k premiku od pasivne obrambe v primeru nesreč do aktivnega delovanja, od zgolj nujne pomoči do preprečevanja nesreč, zagotavljanja pripravljenosti in ublažitve posledic.

ključne besede

tveganje, ogroženost, varnost, odpornost, ocena tveganja, upravljanje s tveganji, geografski informacijski sistemi, potres, plaz, poplava, skrajnost

GEO-INFORMATION TECHNOLOGY FOR DISASTER RISK ASSESSMENT

ĐORĐE ĆOSIĆ, SRĐAN POPOV, DUŠAN SAKULSKI AND ANA PAVLOVIĆ

about the authors

Đorđe Ćosić
University of Novi Sad,
Faculty of Technical Sciences
Trg Dositeja Obradovića 6, 21000 Novi Sad, Serbia
E-mail: djordjecosic@uns.ac.rs

Srđan Popov
University of Novi Sad,
Faculty of Technical Sciences
Trg Dositeja Obradovića 6, 21000 Novi Sad, Serbia
E-mail: boromir@uns.ac.rs

Dušan Sakulski
United Nations University,
Institute for Environment and Human Security (UNU-EHS)
UN Campus, Hermann-Ehlers-Str.10, 53113 Bonn, Germany
E-mail: dsakulski2@me.com

Ana Pavlović
University of Novi Sad,
Faculty of Technical Sciences
Trg Dositeja Obradovića 6, 21000 Novi Sad, Serbia
E-mail: annaftn@uns.ac.rs

abstract

The Serbian territory (including the territory of the former Yugoslavia) has been continuously exposed to different hazards, often with tragic consequences. Earthquakes and floods, usually followed by landslides, are the most dominant hazards in that region. Disaster risk reduction, prevention and early warning, as an integral part of sustainable development, do not exist in Serbia. That is one of the main reasons why the disaster-related damage is high. Despite very long experience in engineering and resources management in Serbia, there are no scientifically supported and standardized disaster risk-assessment procedures. Expertise only exists in the field of engineering-based hazard assessment.

The risk-assessment method proposed in this research includes, apart from hazards, parameters such as vulner-

ability, exposure and safety. It considers the environmental and social components of risk management. The proposed method, implementing combined mathematical and 3D GIS tools, was applied for the Danube River, Petrovaradin (the city of Novi Sad) area, for which data were available. The relationship between the risk parameters is calculated and graphically presented. Methods like this one should contribute to a shift from a passive disaster-related defense to a proactive disaster risk management, as well as from emergency management only, to disaster prevention, preparedness and mitigation activities, in Serbia and the Western Balkan Region.

keywords

hazard, vulnerability, safety, resilience, coping capacity, risk assessment, risk management, geographic information systems, earthquake, landslide, flooding, exceedance

1 INTRODUCTION

The number of natural disasters is ever increasing. According to the CRED EM-DAT, there were 6387 natural disasters between 1974 and 2008, worldwide, not counting epidemics. This resulted in the following consequences: more than 2 million people lost their lives; 1.5 billion people were affected; 182 million people were made homeless; and economic damage estimated was US\$ 1.38 trillion (Guha-Sapir et al., 2004).

An increasing trend in the number of natural disasters is evident over the past 50 years globally (CRED EM-DAT). As the global population is constantly increasing, so the number of people exposed to the same types of hazard has also increased.

The Western Balkan Region is experiencing the same trend. Its territory (including the territory of the former Yugoslavia) has been continuously exposed to different hazards, often having tragic consequences (Table 1).

Table 1. Natural disasters in the Western Balkan Region over the past 50 years (CRED EM-DAT).

Disaster	Date	No. Killed
Earthquake	07/1963	1100
Earthquake	04/1979	121
Flood	03/1981	70
Extreme temperature	07/1988	38
Epidemic	03/1972	35
Flood	11/1979	22
Earthquake	10/1969	15
Earthquake	02/1983	12

Table 2 shows number of people affected by natural disasters, for the past 50 years, in the Western Balkan region. It is obvious that earthquakes and floods are the most frequent hazards. Those two events have accumulatively affected close to one million people (CRED EM-DAT).

Table 2. People affected by natural disasters in the Western Balkan for the past 50 years (CRED EM-DAT).

Disaster	Date	People Affected
Earthquake	04/1979	310100
Earthquake	10/1969	286116
Flood	10/1964	240000
Flood	05/1965	95000
Earthquake	11/1967	21870
Earthquake	11/1968	15030
Flood	11/1979	12000

Earthquakes and floods, followed by landslides, were not the only natural disaster in the Western Balkan territory. Summer heat and extreme summer temperatures have been recorded for the past few years. Departures from the maximum annual temperatures were significant. The day and night maximum temperatures significantly exceeded those recorded in the past. It has also resulted in an increased number of dry spells and forest fires, especially in the summer of 2007 (Republic Hydrometeorological Services of Serbia).

The cost of those recorded disasters has an increasing trend. The reasons for this are twofold: the number of natural disasters has increased (Guha-Sapir et al, 2004) as has the value of the built infrastructure (as a result of the increased urbanization and industrialization).

Disaster response in Serbia has been chaotic and disorganized. Each time it is another disaster on its own. The

disaster-related legislation and regulations are, by their nature, “reactive”, based on the civil protection legislations, covering only the right-hand side of the Disaster Management Cycle. There is a continuous lack of horizontal and vertical coordination in the disaster risk management. One very fresh example is the disasters in Serbia in February and June 2010.

Why this research was conducted?

Disaster risk reduction, prevention and early warning do not exist in Serbia. That is one of the main reasons why the disaster-related damage is very high. Despite the very long experience in hazard engineering and resource management in Serbia, there are no scientifically supported and standardized disaster risk-assessment procedures. Expertise exists only in the field of engineering-based hazard assessment.

This paper presents the results of risk-assessment research involving vulnerability as one of the most important risk parameters (Turner et al., 2003; Birkmann and Bogardi, 2004; Cannon et al., 2005), with the main goal to address the risk accordingly. These results will be used to maximize the prevention and mitigation activities, based on the best possible interdisciplinary experience and knowledge, methods, models, as well as information technologies. The proposed geographical area is the Republic of Serbia, with the intention to expand the implementation of this model to the Western Balkan Region.

2 THEORETICAL BACKGROUND

Generally, risk can be represented as a temporal-spatial function of a series of complex parameters (Turner et al, 2003; Birkmann and Bogardi, 2004; Cannon et al, 2005):

$$R = f(H, V, E, CC, Re, etc.) \quad (1)$$

Where R is the Risk, H is the Hazard, V is the Vulnerability, E is the Exposure, CC is the Coping Capacity and Re is the Resilience.

The likelihood of hazardous events can hardly be affected. It increases year after year. To assess risk adequately, data about the underlying hazardous event should be collected first. For an accurate assessment of the probability of occurrence it is necessary to have the largest possible number of measurements (historical registry) for every hazardous event. According to the law of large numbers, with an increase of the sample, the deviation will decrease, which results in a more accurate frequency of an event.

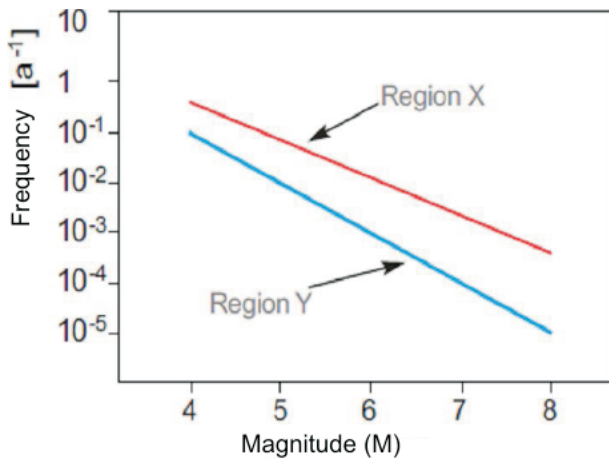


Figure 1. Frequency-Magnitude relation for a particular hazard.

To determine it quantitatively, every hazard magnitude is related to a certain frequency. The location or region is continuously characterized by the connection between the magnitude and the frequency of a certain hazard, as shown in Figure 1 (Thywissen, 2006).

The largest contribution to risk reduction could be achieved through four different types of vulnerability reduction: Infrastructural vulnerability, Environmental vulnerability, Economic vulnerability and Social vulnerability (Birkmann and Bogardi, 2004; Cannon et al., 2005).

The vulnerability component, along with the exposure analysis, is related to the possible damage caused by the effects of hazardous events on certain systems and their operation. Vulnerability is a dynamic and characteristic property of any community (or household, region, nation, infrastructure or of any other risk element), itself consisting of a multitude of components. It is a continuous and dynamic feature, revealed to the certain extent during the event, depending on the intensity of the harmful event.

Understanding the damage pattern of a certain society, without knowing the event's magnitude, prevents us from making accurate conclusions regarding the vulnerability of society. Hence, the threatened element's (community, household, nation, infrastructure, etc.) vulnerability is reflected in the damage-intensity relation (Thywissen, 2006; Figure 2).

A vulnerability assessment starts with a historical analysis of events with disastrous effects, identifying and systematizing the conditions of vulnerability from data about the damage and loss of the entity (household or community). It is very important to obtain the largest

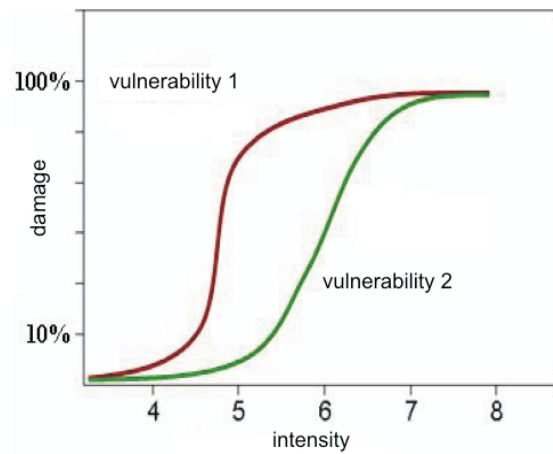


Figure 2. Vulnerability damage-intensity relation.

possible number of damage data, since the function of vulnerability on specific hazard levels can be expressed according to those data.

Along with hazard and vulnerability, exposure is another prerequisite of risk and disaster. Exposure implies the number of people and/or other elements under risk, which may be affected by a certain event. While the level of events effecting the elements under risk is determined by vulnerability, the final level of damage or harm is determined by exposure.

In everyday life, the damage does not depend only on the hazard, vulnerability and exposure, but also on the safety of the elements exposed to the hazard. Safety is seen as a function of resilience and resistance. Resilience consists of strategies and measures that directly help to mitigate the damage during an event. The degree of a system's resilience depends on what has been done to cope with the hazard.

2.1 EQUATION REVIEW

There are many variations of the generic risk equation (1). For example, ISDR (2004) proposed the most simple risk equation:

$$\text{Risk} = \text{Hazard} \cdot \text{Vulnerability} \quad (2)$$

Alexander (2000) defined risk as "the likelihood, or more formally the probability, that a particular level of loss will be sustained by a given series of elements as a result of a given level of hazard". Total risk would then consist of the sum of the predictable casualties, damages and losses, represented by the equation:

$$Total\ Risk = \sum element\ at\ risk \cdot Hazard \cdot Vulnerability \quad (3)$$

Recent publications have incorporated Coping Capacity, Exposure and Susceptibility in calculating risk. For example, one typical equation, implemented by many authors (such as Birkmann, 2006; Thywissen, 2006) is:

$$Risk = Hazard \cdot Vulnerability / Coping\ Capacity \quad (4)$$

Coping Capacity refers to the means by which people and/or institutions use the available capacities and resources to face adverse consequences related to a disaster.

Dilley et al. (2005) represents Risk as the combination of Hazard, Exposure and Vulnerability:

$$Risk = Hazard \cdot Exposure \cdot Vulnerability \quad (5)$$

Hahn (2003), using Hazard, Exposure, Coping Capacity and Vulnerability, has developed the following equation to calculate risk:

$$Risk = Hazard + Exposure + Vulnerability - Coping\ Capacity \quad (6)$$

An interesting formulation concerning vulnerability was proposed by White et al. (2005). Vulnerability itself is a combination of Exposure, Coping Capacity and Susceptibility:

$$Vulnerability = Exposure \cdot Susceptibility / Coping\ Capacity \quad (7)$$

Theoretically, a risk assessment would be more accurate if it involved more parameters. On the other hand, it makes the assessment more complex and more difficult to implement, very often having a nonlinear relation between those parameters. There is always one more practical difficulty: the availability of the input data for

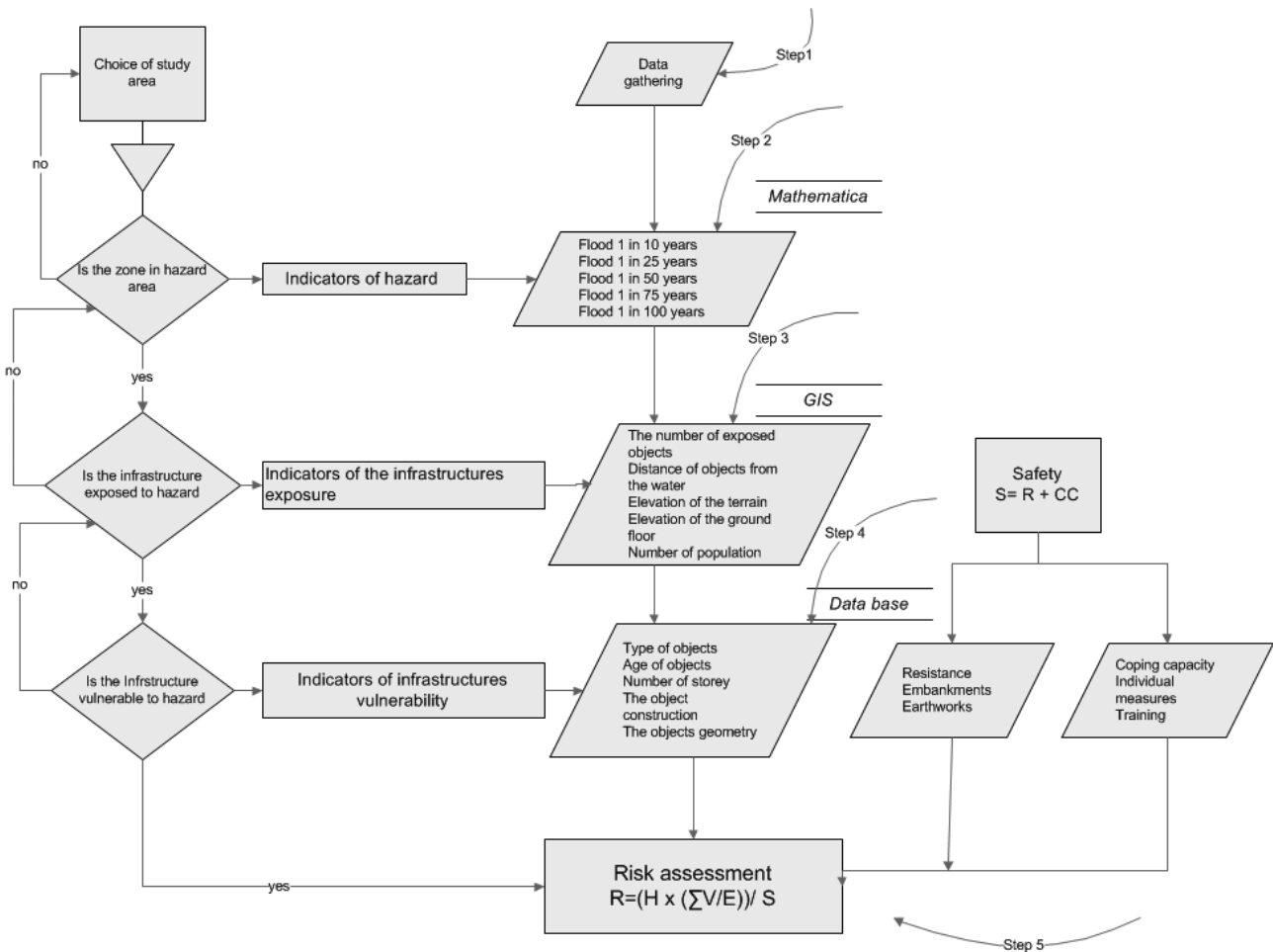


Figure 3. Risk-assessment model implemented in this research.

the calculation of the selected parameters. It was an obstacle in our research, forcing us to modify the risk equation we wanted to select.

3 METHOD AND MODEL

After a detailed analysis of the various risk equations, and being realistic regarding the data availability for Serbia and the Western Balkans, we decided to implement the following risk parameters: Hazard, Vulnerability, Exposure and Safety, implemented using the following formula:

$$Risk = \frac{Hazard \times \left(\frac{\sum Vulnerability}{Number\ of\ exposed\ objects} \right)}{Safety} \quad (8)$$

Expression $\sum Vulnerability / Number\ of\ exposed\ objects$ represents an average vulnerability.

As per equations (2), (3), (4) and (5), hazard and vulnerability are the factors contributing risk. On the other hand, safety (incorporating coping capacity) is inversely proportional to risk. This approach was the most practical for implementation in the selected pilot area of Petrovaradin.

The risk-assessment procedure is given by the flowchart (Figure 3) and consists of the following 5 steps:

1. Select study area
2. Select indicators to assess hazard
3. Determine exposure indicators
4. Determine vulnerability indicators
5. Perform risk assessment.

To enable a spatial dimension of the risk assessment proposed, a Geographic Information System (GIS) was implemented, with components of the architecture required for a 3D spatial view (Figure 4). The focus was on the following requirements:

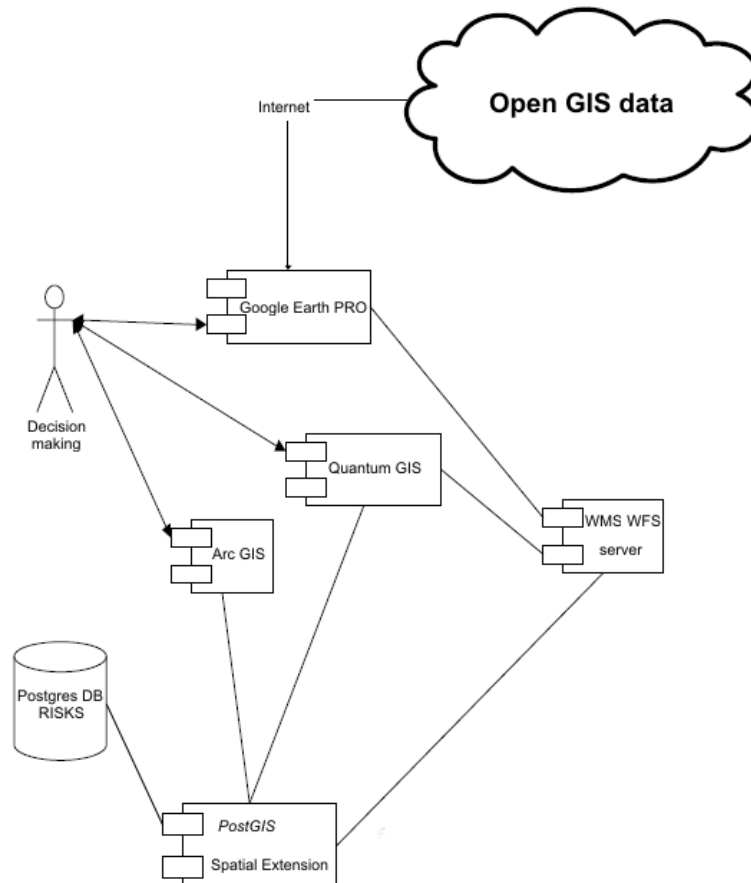


Figure 4. GIS system architecture applied in this research.

- Representation of different types of GIS-related geographical data;
- Representation of the map or chart containing the elements and explaining their relation according to the geographic position;
- Representation of the model resulting from the application of specific analytical functions on well-known data;
- Representation of the full 3D model.

4 RESULTS

The study area was defined first. It is a part of the Petrovaradin settlement (City of Novi Sad, Figure 5), on the bank of the Danube River, a place with considerable exposure to flooding. Here, both residential and industrial objects, traffic, arable and forest land, orchards and vineyards are threatened by flooding, making the area increasingly interesting.

Data were collected for the investigated area regarding the water level measured at the "Novi Sad" gauging

station. The maximum water level of 778 cm was recorded in 1965. The terrain "0" height above which the water level is measured at the "Novi Sad" gauging station, the closest to the Petrovaradin area, is 71.73 m above sea level (a.s.l.). The maximum or absolute height of the Danube near Novi Sad was 79.51 m.a.s.l., which occurs once in 88 measurements. The flood is considered a 100-year flood if the absolute height is 80 m above sea level. The flood hazard indicators were determined according to this data. Data on the water-level height, based on which the charts on return periods and the exceedance probability were calculated (MATHEMATICA software, Figures 6 and 7):

To determine what was exposed to flooding regarding the above-mentioned water levels of the Danube, GIS software was used as a tool to construct the Digital Elevation Model (DEM). The terrain's digital model was covered by aerial orthophoto snapshots of the studied area. These orthophoto snapshots were in the geoTiff format in a scale of 1:5000 with coordinates in the Gauss-Krüger system. The geo referencing was carried out manually (Figures 8 and 9):

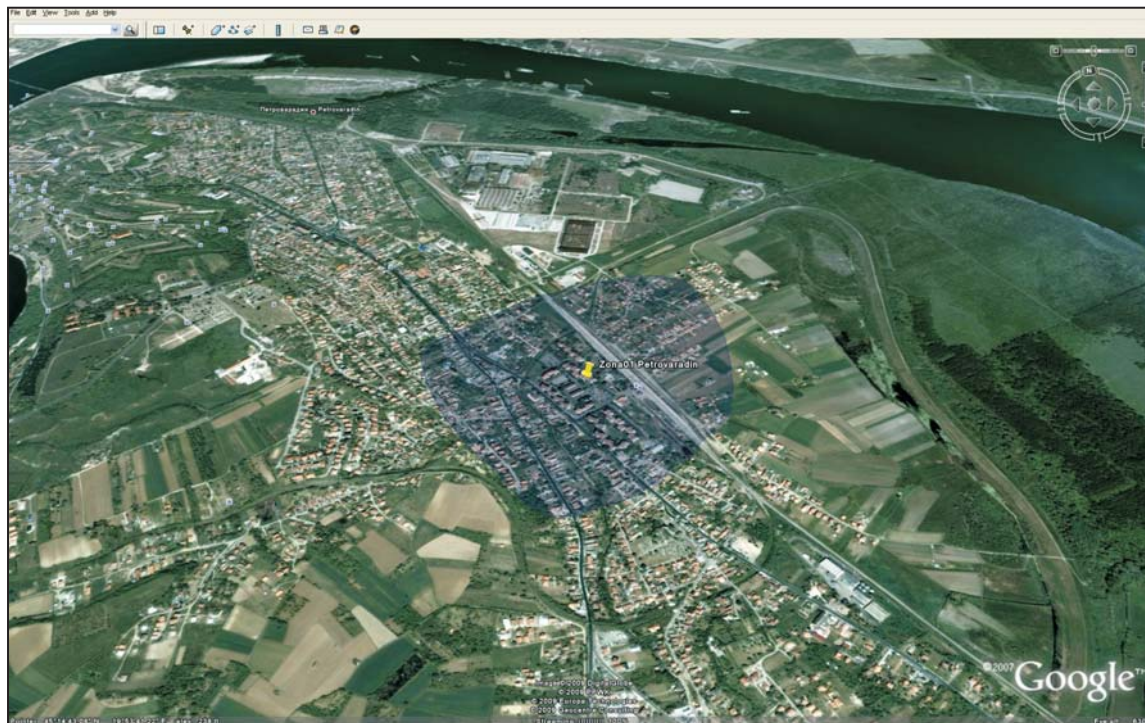


Figure 5. Petrovaradin area (by Google Earth).

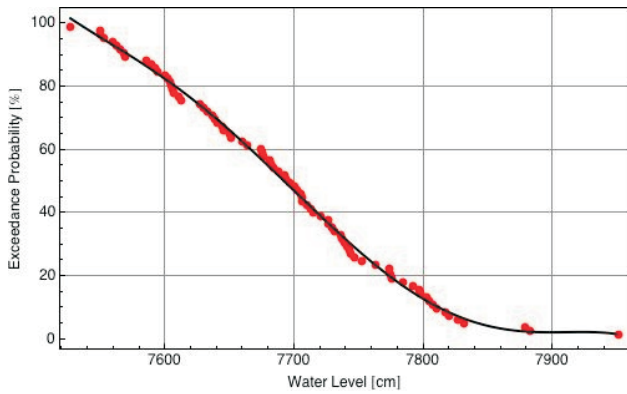


Figure 6. Exceedance probability for the Novi Sad gauging station.

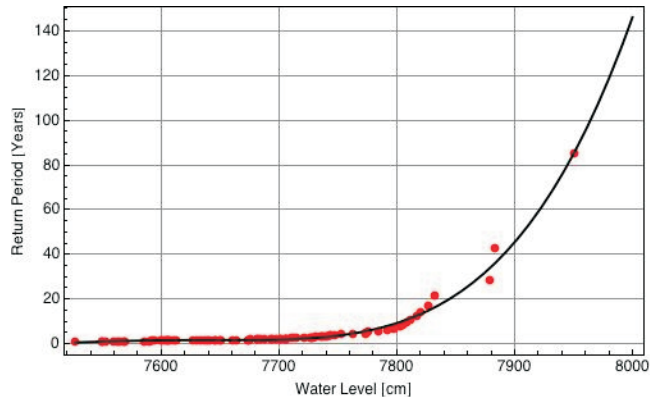


Figure 7. Return period for the Novi Sad gauging station.

Unfortunately, whenever there was a flood on Serbian territory, a systematic damage assessment was never conducted. Here and there some damage data exists, but there was no possibility to structure them and do a correlation analysis. The damage-magnitude (Figure 10) was obtained by comparing the most similar

hydrological conditions for the Danube River, near the City of Novi Sad, and the Rheine River in Germany, near the City of Cologne, for the same infrastructure object types. The German Federal Ministry have been continuously recording the damage whenever a flood occurred.

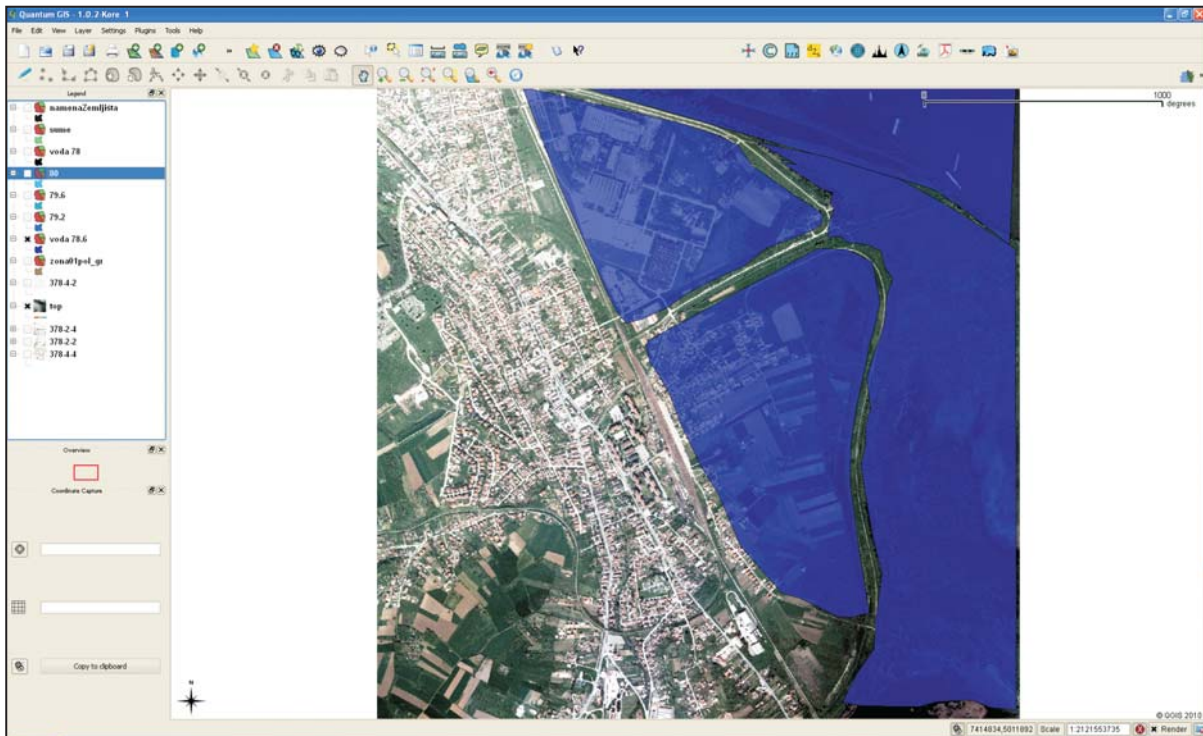


Figure 8. Exposed object at 78 m.a.s.l. for Petrovaradin.

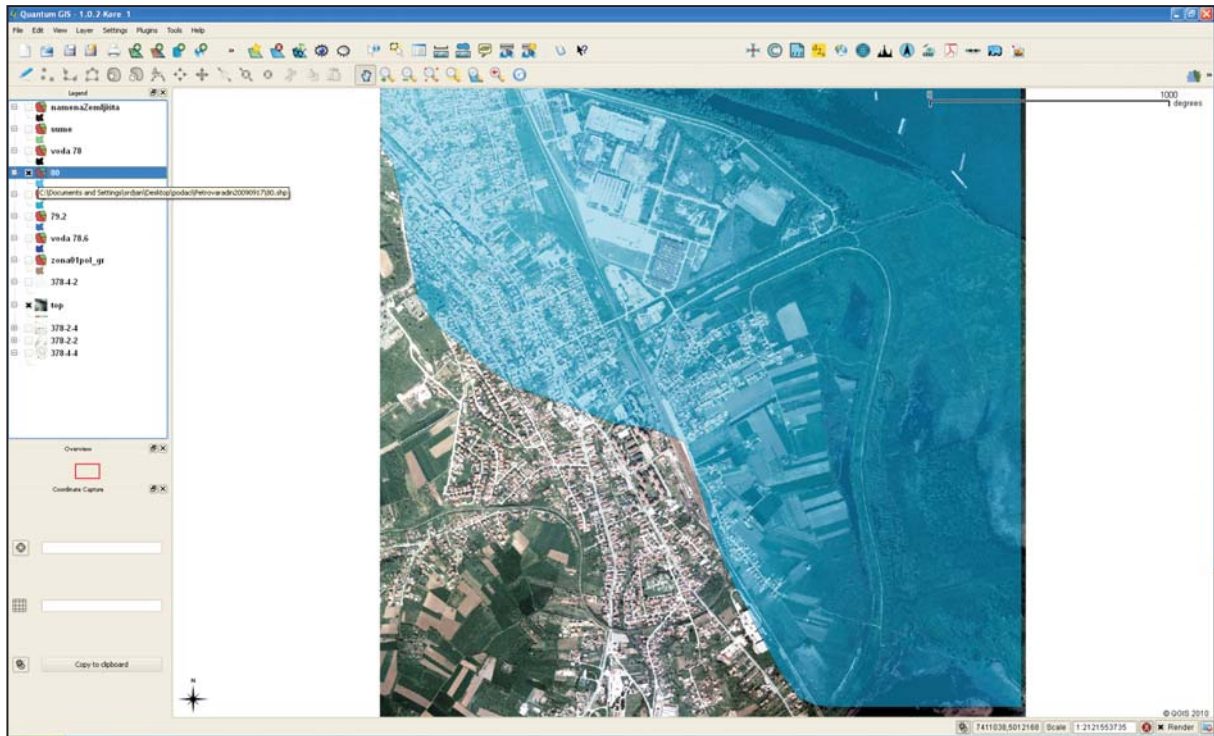


Figure 9. Exposed object at 80 m.a.s.l. for Petrovaradin.

To determine the vulnerability of objects to a flood, this model uses data that were collected through the GIS and through field inquiries. The most important indicators of the infrastructural vulnerability assessment were the following: the Depth of flooding; the Duration of flooding; the Object's surface area; the Elevation of the terrain; the Elevation of the object's ground floor; the Object type; the Type of material; the Number of floors; and the Construction elements.

The degree of vulnerability was expressed through a coefficient that ranges from 0 to 1, after the normalization. This means that the coefficient of vulnerability for a specific depth was read from the depth-damage relation. Based on data from the infrastructural objects' attribution table, as well as on the vulnerability graph (Figure 10), the damage to objects at a particular flooding depth was estimated and the coefficient of vulnerability was determined.

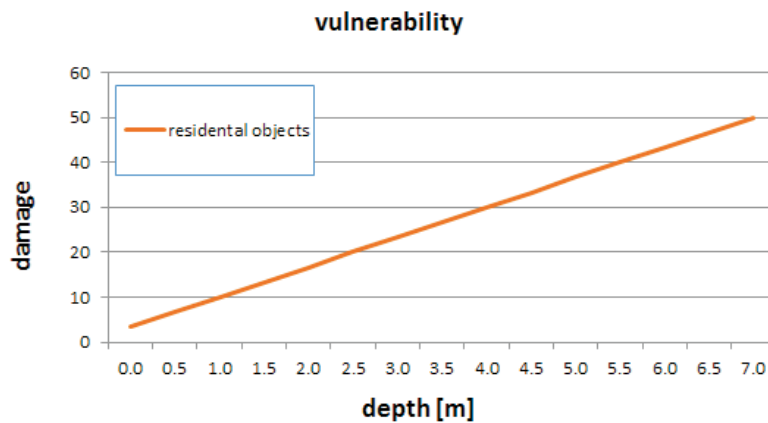


Figure 10. Historical vulnerability expressed by a damage-magnitude (depth) relation.

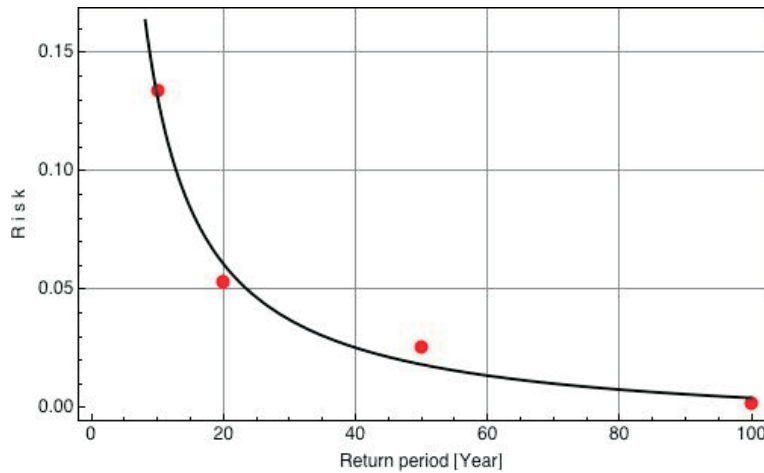


Figure 11. Relation between risk and return period for the Petrovaradin area.

Finally, risk, in relation with vulnerability, exposure and safety, and expressed in terms of the return period (10, 20, 50 and 100 Years) were calculated according to equation (8), and the following relation (9) was obtained (Figure 11).

$$R = (1.42/x) - 0.01 \quad (9)$$

where: x = Return Period [Years]

5 CONCLUSIONS AND RECOMMENDATIONS

For decades, disaster risk assessments in Serbia were based on a hazard assessment only. It was mostly done by engineers, following basic engineering principles. No attention was paid to the environmental or social components of a particular hazard, such as earthquake, flood or landslide. Parameters, such as vulnerability, exposure, coping capacity, resistance or resilience were never considered. Still today, official institutions and related legislations are in the sphere of hazard-related defense and civil protection.

The main purpose of this research was to show the significance of those risk parameters, other than hazard, and their contribution to the overall risk assessment. Highlighting the importance of vulnerability, exposure, and safety, and confirming it in this, and similar research, proof needs to shift from hazard-related defense to disaster-risk management, as well as from emergency management only, to disaster prevention, preparedness and mitigation activities.

The proposed equation (8) has those parameters included. Considering the relation between risk and flood the return period was calculated and graphically presented for the Petrovaradin area. This enables a graphical and analytical determination of the risk value for a particular return period.

ADVANTAGE

Disaster risk assessment is a much more complex event than just an engineering analysis of, for example, slope stability, or flood wave and flood routing, or return period. The method proposed in this paper involves different dimensions of risk assessment, involving vulnerability, exposure and safety. It certainly gives a better multidimensional risk assessment. The results should be the input parameters for a proactive disaster risk management in Serbia.

DISADVANTAGE

Involving more risk parameters requires more and more input data for the calculation. This type of data has not been systematically collected in Serbia. To enable this type of data collection will require a modification to the existing national and local disaster risk management structure.

RECOMMENDATIONS

To make an implementation of the proposed disaster risk-assessment method sustainable, we recommend the following:

- To systematize disaster risk-assessment models in a multi-hazard framework: The common practice, from many countries, is to perform a risk assessment for most frequent hazards, one by one. It is more costly, requires repetition of data relations and database design, and field data collection. The optimum way is to do a multi-hazard risk assessment.
- To adopt those most suitable for Serbia and its environment: There are no recipes for disaster risk assessment. Every natural surrounding is unique, and requires modification of the generally accepted methodologies.
- To structure basic input-data measurements and collection: Disaster risk assessment, especially a vulnerability assessment, requires interdisciplinary skills. Different disciplines (i.e., social science and engineering) have their own terminology, methods and indicators. To avoid misunderstanding and duplication, some framework in the field of data collection is required.
- To officially task governmental institution to continuously manage a multi-hazard risk assessment: The proposed disaster risk assessment is a result of academic research. The practical implementation of such a method will require a custodian institution. The most appropriate will be an existing national disaster risk-management institution.

REFERENCES

- Alexander, D. (2000). *Confronting Catastrophe*. Terra, Hertfordshire.
- Birkmann, J. (Ed) (2006). *Measuring Vulnerability to natural Hazards*. UNU-EHS.
- Birkmann, J., Bogardi, J.J. (2004) *Vulnerability assessment: the first step towards sustainable risk reduction*. In: *Disasters and society – From hazard assessment to risk reduction* (D. Malzahn and T. Plapp, eds). Logos Verlag Berlin, Berlin, 75-82.
- Cannon, T., J. Twigg, et al. (2005). *Social Vulnerability, Sustainable Livelihoods and Disasters*, Report to DFID Conflict and Humanitarian Assistance Department (CHAD) and Sustainable Livelihoods Support Office. London, DFID: 63.
- CRED-EMDAT, *The International Disaster Database*. (<http://www.emdat.be/>).
- Dilley, M., Chen, R.S., Deichmann, U., Lerner-Lam, A.R., Arnold, M. (2005). *Natural Disaster Hotspots. A Global Risk Analysis*. World Bank.
- Guha-Sapir, D., Hargitt, D., Hoyois, P. (2004). *Thirty-years of natural disasters 1974-2003: The Numbers*. Centre for Research on the Epidemiology of Disasters. UCL Presses.
- Hahn, H. (2003). *Indicators and Other Instruments for Local Risk Management for Communities and Local Governments*. GTZ.
- International Strategy for Disaster Reduction ISDR (2004). *Living with Risk. A Global Review of Disaster Reduction Initiatives*. (<http://www.unisdr.org/>).
- Programmable mathematical language Mathematica. Wolfram Research. <http://www.wolfram.com/>.
- Mid-term weather report for Serbia. Republic Hydrometeorological Services of Serbia (HMZ). Belgrade, Serbia (<http://www.hidmet.gov.rs/>).
- Thywissen, K. (2006). *Components of Risk: A Comparative Glossary*, UNU-EHS, Bonn.
- Turner, B.L., Kasperson, R.E., Matson, P., McCarthy, J.J., Corell, R.W., Christensen, Eckley, L., N, Kasperson, J.X., Luers, A., Martello, M.L., Polsky, C., Pulsipher, A., Schiller, A. (2003). *A Framework For, Vulnerability Analysis In Sustainability Science*. Proceedings, National Academy of Sciences 100 (14),8074-8079.
- White, P., Pelling, M., Sen, K., Seddon, D., Russel, S., Few, R. (2005). *Disaster Risk Reduction. A Development Concern*. DFID.

NAVODILA AVTORJEM

Članki so objavljeni v angleškem jeziku s prevodom izvlečka v slovenski jezik.

VSEBINA ČLANKA

Članek naj bo napisan v naslednji obliki:

- Naslov, ki primerno opisuje vsebino članka in ne presega 80 znakov.
- Izvleček, ki naj bo skrajšana oblika članka in naj ne presega 250 besed. Izvleček mora vsebovati osnove, jedro in cilje raziskave, uporabljeno metodologijo dela, povzetek izidov in osnovne sklepe.
- Uvod, v katerem naj bo pregled novejšega stanja in zadostne informacije za razumevanje ter pregled izidov dela, predstavljenih v članku.
- Teorija.
- Eksperimentalni del, ki naj vsebuje podatke o postavitvi preiskusa in metode, uporabljene pri pridobitvi izidov.
- Izidi, ki naj bodo jasno prikazani, po potrebi v obliki slik in preglednic.
- Razprava, v kateri naj bodo prikazane povezave in posplošitve, uporabljene za pridobitev izidov. Prikazana naj bo tudi pomembnost izidov in primerjava s poprej objavljenimi deli.
- Sklepi, v katerih naj bo prikazan en ali več sklepov, ki izhajajo iz izidov in razprave.
- Literatura, ki mora biti v besedilu oštevilčena zaporedno in označena z oglatimi oklepaji [1] ter na koncu članka zbrana v seznamu literature.

OBLIKA ČLANKA

Besedilo naj bo pisano na listih formata A4, z dvojnimi presledki med vrstami in s 3.0 cm širokim robom, da je dovolj prostora za popravke lektorjev. Najbolje je, da pripravite besedilo v urejevalniku Microsoft Word. Hkrati dostavite odtis članka na papirju, vključno z vsemi slikami in preglednicami ter identično kopijo v elektronski obliki.

Enačbe naj bodo v besedilu postavljene v ločene vrstice in na desnem robu označene s tekočo številko v okroglih oklepajih.

ENOTE IN OKRAJŠAVE

V besedilu, preglednicah in slikah uporabljajte le standardne označbe in okrajšave SI. Simbole fizikalnih

veličin v besedilu pišite poševno (npr. v , T itn.). Simbole enot, ki sestojijo iz črk, pa pokončno (npr. Pa, m itn.).

Vse okrajšave naj bodo, ko se prvič pojavijo, izpisane v celoti.

SLIKE

Slike morajo biti zaporedno oštevilčene in označene, v besedilu in podnaslovu, kot sl. 1, sl. 2 itn. Posnete naj bodo v kateremkoli od razširjenih formatov, npr. BMP, JPG, GIF. Za pripravo diagramov in risb priporočamo CDR format (CorelDraw), saj so slike v njem vektorske in jih lahko pri končni obdelavi preprosto povečujemo ali pomanjšujemo.

Pri označevanju osi v diagramih, kadar je le mogoče, uporabite označbe veličin (npr. v , T). V diagramih z več krivuljami mora biti vsaka krivulja označena. Pomen oznake mora biti razložen v podnapisu slike.

Za vse slike po fotografskih posnetkih je treba priložiti izvorne fotografije ali kakovostno narejen posnetek.

PREGLEDNICE

Preglednice morajo biti zaporedno oštevilčene in označene, v besedilu in podnaslovu, kot preglednica 1, preglednica 2 itn. V preglednicah ne uporabljajte izpisanih imen veličin, ampak samo ustrezne simbole. K fizikalnim količinam, npr. t (pisano poševno), pripišite enote (pisano pokončno) v novo vrsto brez oklepajev.

Vse opombe naj bodo označene z uporabo dvignjene številke¹.

SEZNAM LITERATURE

Vsa literatura mora biti navedena v seznamu na koncu članka v prikazani obliki po vrsti za revije, zbornike in knjige:

- [1] Feng, T. W. (2000). Fall-cone penetration and water content relationship of clays. *Geotechnique* 50, No. 2, 181-187.
- [2] Ortolan, Ž. and Mihalinec, Z. (1998). Plasticity index-Indicator of shear strength and a major axis of geotechnical modelling. *Proceedings of the*

Eleventh Danube-European conference on soil mechanics and geotechnical engineering, Poreč, 25–29 May 1998.

- [3] Toporišič, J. (1994). Slovenski pravopis. 2nd.ed., DZS, Ljubljana.

PODATKI O AVTORJIH

Članku priložite tudi podatke o avtorjih: imena, nazive, popolne poštno naslove, številke telefona in faksa, naslove elektronske pošte. Navedite kontaktno osebo.

SPREJEM ČLANKOV IN AVTORSKE PRAVICE

Uredništvo si pridržuje pravico do odločanja o sprejemu članka za objavo, strokovno oceno mednarodnih recenzentov in morebitnem predlogu za krajšanje ali izpopolnitev ter terminološke in jezikovne korekture.

Avtor mora predložiti pisno izjavo, da je besedilo njegovo izvirno delo in ni bilo v dani obliki še nikjer objavljeno. Z objavo preidejo avtorske pravice na revijo ACTA GEOTECHNICA SLOVENICA. Pri morebitnih kasnejših objavah mora biti AGS navedena kot vir.

Rokopisi člankov ostanejo v arhivu AGS.

Vsa nadaljnja pojasnila daje:

Uredništvo
ACTA GEOTECHNICA SLOVENICA
Univerza v Mariboru
Fakulteta za gradbeništvo
Smetanova ulica 17
2000 Maribor
Slovenija
E-pošta: ags@uni-mb.si

INSTRUCTIONS FOR AUTHORS

The papers are published in English with a translation of the abstract into Slovene.

FORMAT OF THE PAPER

The paper should have the following structure:

- A Title that adequately describes the content of the paper and should not exceed 80 characters;
- An Abstract, which should be viewed as a mini version of the paper and should not exceed 250 words. The Abstract should state the principal objectives and the scope of the investigation and the methodology employed, it should also summarise the results and state the principal conclusions;
- An Introduction, which should provide a review of recent literature and sufficient background information to allow the results of the paper to be understood and evaluated;
- A Theoretical section;
- An Experimental section, which should provide details of the experimental set-up and the methods used for obtaining the results;
- A Results section, which should clearly and concisely present the data using figures and tables where appropriate;
- A Discussion section, which should describe the relationships shown and the generalisations made

possible by the results and discuss the significance of the results, making comparisons with previously published work;

- Conclusions, which should present one or more conclusions that have been drawn from the results and subsequent discussion;
- References, which must be numbered consecutively in the text using square brackets [1] and collected together in a reference list at the end of the paper.

LAYOUT OF THE TEXT

The text should be written in A4 format, with double spacing and margins of 3 cm, to provide editors with space to write in their corrections. Microsoft Word for Windows is the preferred format for submission. One hard copy, including all figures, tables and illustrations and an identical electronic version of the manuscript must be submitted simultaneously.

Equations should be on a separate line in the main body of the text and marked on the right-hand side of the page with numbers in round brackets.

UNITS AND ABBREVIATIONS

Only standard SI symbols and abbreviations should be used in the text, tables and figures. Symbols for physical

quantities in the text should be written in *Italics* (e.g. *v*, *T*, etc.). Symbols for units that consist of letters should be in plain text (e.g. Pa, m, etc.).

All abbreviations should be spelt out in full on first appearance.

FIGURES

Figures must be cited in consecutive numerical order in the text and referred to in both the text and the caption as Fig. 1, Fig. 2, etc. Figures may be saved in any common format, e.g. BMP, JPG, GIF. However, the use of CDR format (CorelDraw) is recommended for graphs and line drawings, since vector images can be easily reduced or enlarged during final processing of the paper.

When labelling axes, physical quantities (e.g. *v*, *T*) should be used whenever possible. Multi-curve graphs should have individual curves marked with a symbol; the meaning of the symbol should be explained in the figure caption.

Good quality black-and-white photographs or scanned images should be supplied for illustrations.

TABLES

Tables must be cited in consecutive numerical order in the text and referred to in both the text and the caption as Table 1, Table 2, etc. The use of names for quantities in tables should be avoided if possible: corresponding symbols are preferred. In addition to the physical quantity, e.g. *t* (in *Italics*), units (normal text), should be added on a new line without brackets.

Any footnotes should be indicated by the use of the superscript¹.

LIST OF REFERENCES

References should be collected at the end of the paper in the following styles for journals, proceedings and books, respectively:

- [1] Feng, T. W. (2000). Fall-cone penetration and water content relationship of clays. *Geotechnique* 50, No. 2, 181-187.
- [2] Ortolan, Ž. and Mihalinec, Z. (1998). Plasticity index-Indicator of shear strength and a major axis of geotechnical modelling. Proceedings of the Eleventh Danube-European conference on soil mechanics and geotechnical engineering, Poreč, 25–29 May 1998.

- [3] Toporišič, J. (1994). *Slovenski pravopis*. 2nd.ed., DZS, Ljubljana.

AUTHOR INFORMATION

The following information about the authors should be enclosed with the paper: names, complete postal addresses, telephone and fax numbers and E-mail addresses. Indicate the corresponding person.

ACCEPTANCE OF PAPERS AND COPYRIGHT

The Editorial Committee of the Slovenian Geotechnical Review reserves the right to decide whether a paper is acceptable for publication, to obtain peer reviews for submitted papers, and if necessary, to require changes in the content, length or language.

Authors must also enclose a written statement that the paper is original unpublished work, and not under consideration for publication elsewhere. On publication, copyright for the paper shall pass to the ACTA GEOTECHNICA SLOVENICA. The AGS must be stated as a source in all later publication.

Papers will be kept in the archives of the AGS.

For further information contact:

Editorial Board
 ACTA GEOTECHNICA SLOVENICA
 University of Maribor
 Faculty of Civil Engineering
 Smetanova ulica 17
 2000 Maribor
 Slovenia
 E-mail: ags@uni-mb.si

NAMEN REVIJE

Namen revije ACTA GEOTECHNICA SLOVENICA je objavljane kakovostnih teoretičnih člankov z novih pomembnih področij geomehanike in geotehnike, ki bodo dolgoročno vplivali na temeljne in praktične vidike teh področij.

ACTA GEOTECHNICA SLOVENICA objavlja članke s področij: mehanika zemljin in kamnin, inženirska geologija, okoljska geotehnika, geosintetika, geotehnične konstrukcije, numerične in analitične metode, računalniško modeliranje, optimizacija geotehničnih konstrukcij, terenske in laboratorijske preiskave.

Revija redno izhaja dvakrat letno.

AVTORSKE PRAVICE

Ko uredništvo prejme članek v objavo, prosi avtorja(je), da prenese(jo) avtorske pravice za članek na izdajatelja, da bi zagotovili kar se da obsežno razširjanje informacij. Naša revija in posamezni prispevki so zaščiteni z avtorskimi pravicami izdajatelja in zanje veljajo naslednji pogoji:

fotokopiranje

V skladu z našimi zakoni o zaščiti avtorskih pravic je dovoljeno narediti eno kopijo posameznega članka za osebno uporabo. Za naslednje fotokopije, vključno z večkratnim fotokopiranjem, sistematičnim fotokopiranjem, kopiranjem za reklamne ali predstavitvene namene, nadaljnjo prodajo in vsemi oblikami nedobičkonosne uporabe je treba pridobiti dovoljenje izdajatelja in plačati določen znesek.

Naročniki revije smejo kopirati kazalo z vsebino revije ali pripraviti seznam člankov z izvlečki za rabo v svojih ustanovah.

elektronsko shranjevanje

Za elektronsko shranjevanje vsakršnega gradiva iz revije, vključno z vsemi članki ali deli članka, je potrebno dovoljenje izdajatelja.

ODGOVORNOST

Revija ne prevzame nobene odgovornosti za poškodbe in/ali škodo na osebah in na lastnini na podlagi odgovornosti za izdelke, zaradi malomarnosti ali drugače, ali zaradi uporabe kakršnekoli metode, izdelka, navodil ali zamisli, ki so opisani v njej.

AIMS AND SCOPE

ACTA GEOTECHNICA SLOVENICA aims to play an important role in publishing high-quality, theoretical papers from important and emerging areas that will have a lasting impact on fundamental and practical aspects of geomechanics and geotechnical engineering.

ACTA GEOTECHNICA SLOVENICA publishes papers from the following areas: soil and rock mechanics, engineering geology, environmental geotechnics, geosynthetic, geotechnical structures, numerical and analytical methods, computer modelling, optimization of geotechnical structures, field and laboratory testing.

The journal is published twice a year.

COPYRIGHT

Upon acceptance of an article by the Editorial Board, the author(s) will be asked to transfer copyright for the article to the publisher. This transfer will ensure the widest possible dissemination of information. This review and the individual contributions contained in it are protected by publisher's copyright, and the following terms and conditions apply to their use:

photocopying

Single photocopies of single articles may be made for personal use, as allowed by national copyright laws. Permission of the publisher and payment of a fee are required for all other photocopying, including multiple or systematic copying, copying for advertising or promotional purposes, resale, and all forms of document delivery.

Subscribers may reproduce tables of contents or prepare lists of papers, including abstracts for internal circulation, within their institutions.

electronic storage

Permission of the publisher is required to store electronically any material contained in this review, including any paper or part of the paper.

RESPONSIBILITY

No responsibility is assumed by the publisher for any injury and/or damage to persons or property as a matter of product liability, negligence or otherwise, or from any use or operation of any methods, products, instructions or ideas contained in the material herein.